Performance predictions for oil contaminated supercritical carbon dioxide gas cooling

L Kleyn

orcid.org/0000-0002-9133-7375

Dissertation submitted in partial fulfilment of the requirements for the degree *Master of Engineering in Mechanical Engineering* at the North-West University

Supervisor: Dr P.v.Z Venter

Co-supervisor: Prof M van Eldik

Graduation ceremony: May 2019

Student number: 24186465

ABSTRACT

The international movement towards using natural refrigerants has resulted in the reinvestigation of trans-critical heat pump cycles using carbon dioxide. Subsequently, a need to predict the heat transfer of oil-contaminated supercritical carbon dioxide inside the gas cooler was identified.

A literature survey revealed that numerous correlations exist for the calculation of the Nusselt number of supercritical carbon dioxide during cooling, but only a limited number of correlations that take the effects of oil contamination into consideration were found. The complexity of the heat transfer prediction was increased by the large variations in the physical and transport properties at the pseudocritical temperature, which became even more complex with the introduction of oil to the fluid.

In this study, a correlation for calculating the Nusselt number of oil-contaminated supercritical carbon dioxide during cooling, was evaluated by comparing it to an independent published data set as well as to the results obtained by the authors' using their own data. It predicted 90% of the convection coefficients of the authors' data with an absolute error less than 20%, whilst only 39.7% of the coefficients were predicted for the independent data within this range. The oil concentrations in the independent data set was much higher than the oil percentages used to develop the correlation and might be the cause for the lower accuracy. It was concluded that this correlation's accuracy was not consistent between the two data sets. Based on this, a new correlation to improve on the performance consistency to predict the heat transfer in the gas cooler, whilst having a less complex form and not foregoing on accuracy, should then be investigated.

Due to a limited number of existing correlations found for the cooling of oil-contaminated supercritical carbon dioxide, different correlations for oil-free conditions were then firstly investigated. Dittus & Boelter (1930) was the most accurate among the correlations and improved on the performance consistency of the published correlation for oil-contaminated conditions. It predicted 59.5% of the data from the published correlation' authors with an error less than 20% and 44.4% for the independent data. It was then decided to investigate the enhancement of Dittus & Boelter (1930) to take the effect of oil into account and further improving on the accuracy consistency.

A new correlation was developed based on Dittus & Boelter and enhanced to take the effect of oil contamination into account. This correlation was developed using the independent data set, whilst keeping the data from the authors of the published correlation for oil contaminated supercritical carbon dioxide in cooling as a set for verification. Compared to Dittus & Boelter, the new correlation's accuracy was reported to be more consistent between the data sets. On the

data from the published correlation's authors, it predicted 49.4% of the results with an error less than 20% and 47.1% for the independent data set. It was noted that Dittus & Boelter was more accurate at lower oil concentrations, such as in the data from the published correlation's authors, compared to the new correlations. However, when the oil increases to higher values (as in the independent data) Dittus & Boelter became inaccurate, whilst the new correlation was consistently accurate. In addition, this new correlation is less complex than the published correlation for oil-contaminated supercritical carbon dioxide in cooling. A more simplified correlation eases the calculation process and typically reduces the calculation times of large simulations. A less complex correlation is often also more applicable to a wider range of applications.

Keywords: natural refrigerants, heat transfer, oil contaminated, supercritical, carbon dioxide, gas cooler, Nusselt number

ACKNOWLEDGEMENTS

The author of this study is very grateful and want to express a special thanks to the following people:

- my supervisor, Dr. Philip Venter, for his valuable time, insight and guidance throughout this study;
- my co-supervisor, Prof. Martin van Eldik, for his support, advice and thoughtful suggestions during this study;
- my family, my father Dirk Kleyn for his motivation and prayers, my mother Lettie Kleyn for her love and wisdom, my brother and sister, Morné, and Melanie, for their support and motivation.
- my financial sponsors, THRIP and Prof. Martin van Eldik, who made it possible for me to study fulltime.

Above all, I am grateful to my Heavenly Father, to Whom I give praise for my talents, perseverance and opportunities. All glory is His.

Soli Deo Gloria

TABLE OF CONTENTS

LIST OF TABLES

LIST OF FIGURES

NOMENCLATURE

A	Cross-sectional area	m^2
A_{ff}	Free flow area	m^2
$A_{heat\ transfer}$	Heat transfer wall area	m^2
α	Thermal diffusivity	m^2/s
B	Body force	N/m^3
c_p	Specific heat at a constant pressure	J/kg-K
$\overline{c_p}$	Integrated specific heat	J/kg-K
c_{p_b}	Specific heat at bulk temperature	J/kg-K
$c_{p_{pc}}$	Specific heat at pseudocritical temperature	J/kg-K
c_{p_w}	Specific heat at wall temperature	J/kg-K
$\overline{c_{p_t}}$	Mean specific heat value for Zhao & Jiang (2011)	J/kg-K
C_{vp}	Property variation coefficient for Zhao & Jiang (2011)	-
D_H	Hydraulic diameter	m
d_{in}	Inner diameter	m
Δp_{0L}	Total pressure change	Pa
E	Relative error	- or %
$\lvert\bar{E}\rvert$	Average absolute error	- or %
$\sum\lvert E\rvert$	Sum of absolute errors	- or %
η_o	Overall surface efficiency	-
f_{fil}	Filonenko friction factor	-
$f_{fil,f}$	Filonenko friction factor at film	-
g	Gravity	m/s^2
G	Mass flux	kg/m^2s
h	Static enthalpy	J/kg
h_b	Static enthalpy at bulk	J/kg
h_w	Static enthalpy at wall	J/kg
h_e	Static enthalpy at outlet	J/kg
h_i	Static enthalpy at inlet	J/kg
h_{0e}	Total enthalpy at exit	J/kg
h_{0i}	Total enthalpy at inlet	J/kg
h_c	Convection heat transfer coefficient	W/m^2-K
$h_{c,exp}$	Experimental convection coefficient	W/m^2-K
h_{c,CO_2}	Convection coefficient for oil-free carbon dioxide	W/m^2-K
h_{c,CO_2oil}	Convection coefficient: oil-contaminated carbon dioxide	W/m^2-K
$h_{c,Z}$	Convection heat transfer coefficient Zhao et al. (2011)	W/m^2-K
$h_{c,D\&B}$	Convection coefficient from Dittus & Boelter (1930)	W/m^2-K
$h_{c,G}$	Convection coefficient from Gnielinski (1976)	W/m^2-K
$h_{c,G,M}$	Convection coefficient from Gnielinski (1976)	W/m^2-K
$h_{c,Y}$	Convection coefficient from Yoon et al. (2003)	W/m^2-K

$h_{c,P}$	Convection coefficient from Pitla et al. (2002)	W/m^2-K
$h_{c,D\&H}$	Convection coefficient from Dang & Hihara (2004)	W/m^2-K
$h_{c,Z\&J}$	Convection coefficient from Zhao & Jiang (2011)	W/m^2-K
k	Thermal conductivity	W/m-K
k_b	Thermal conductivity at bulk	W/m-K
k_w	Thermal conductivity at wall	W/m-K
k_f	Thermal conductivity at film	W/m-K
L	Length of control volume	m
L_{ch}	Characteristic length	m
$\dot{m}$	Mass flow rate	kg/s
$\dot{m}_e$	Mass flow rate out of control volume	kg/s
$\dot{m}_i$	Mass flow rate into control volume	kg/s
$\dot{m}_{oil}$	Mass flow rate of oil	kg/s
$\dot{m}_{CO2}$	Mass flow rate of carbon dioxide	kg/s
μ	Dynamic viscosity	Ns/m^2
μ_b	Dynamic viscosity at bulk	Ns/m^2
μ_f	Dynamic viscosity at film	Ns/m^2
μ_{oil}	Dynamic viscosity of oil	Ns/m^2
μ_{CO_2}	Dynamic viscosity of carbon dioxide	Ns/m^2
μ_{PAG100}	Dynamic viscosity of PAG100 range	Ns/m^2
$\mu_{POE_{solest68}}$	Dynamic viscosity of POE solest 68 range	Ns/m^2
Nu	Nusselt number	-
$Nu_{D\&B}$	Nusselt number from Dittus & Boelter	-
Nu_G	Nusselt number from Gnielinski	-
$Nu_{G,M}$	Nusselt number from Gnielinski (modified)	-
$Nu_{G,w}$	Nusselt number from Gnielinski at wall	-
$Nu_{G,b}$	Nusselt number from Gnielinski at bulk	-
Nu_Y	Nusselt number from Yoon et al.	-
Nu_P	Nusselt number from Pitla et al.	-
$Nu_{D\&H}$	Nusselt number from Dang & Hihara	-
$Nu_{Z\&J}$	Nusselt number from Zhao & Jiang	-
ω	Oil concentration	-
p	Static pressure	Pa or MPa
p_c	Critical pressure	Pa or MPa
p_{0e}	Total pressure at outlet	Pa or MPa
p_{0i}	Total pressure at inlet	Pa or MPa
p_i	Static pressure at inlet	Pa or MPa
Pr	Prandtl number	-
Pr_b	Prandtl number at bulk	-
Pr_w	Prandtl number at wall	-
$Pr_{D\&H}$	Prandtl number for Dang & Hihara	-
P_w	Wetted perimeter	m

$\dot{Q}$	Rate of heat transfer	W
$\dot{Q}_{flux}$	Heat flux	W/m^2
Re	Reynolds number	-
Re_b	Reynolds number at bulk temperature	-
Re_f	Reynolds number at film temperature	-
ρ	Density	kg/m^3
ρ_b	Density at bulk	kg/m^3
ρ_w	Density at wall	kg/m^3
$\rho_{oil,ref}$	Density of oil at reference temperature	kg/m^3
ρ_{pc}	Density at pseudocritical temperature	kg/m^3
ρ_{oil}	Density of oil	kg/m^3
ρ_{CO_2}	Density of carbon dioxide	kg/m^3
R_{tot}	Total resistance between bulk and wall	K/W
R_{foul}	Fouling factor	m^{2}K/W
r	Radius	m
T	Temperature	K
T_{ave}	Average temperature of test section	K
T_c	Critical temperature	K
T_e	Temperature at outlet	K
T_i	Temperature at inlet	K
T_{0e}	Stagnation temperature at outlet	K
T_{0i}	Stagnation temperature at inlet	K
T_{pc}	Pseudocritical temperature	K
T_{ref}	Reference temperature	K
T_f	Film temperature	K
T_b	Bulk temperature	K
T_w	Wall temperature	K
τ	Shear stress	N/m^2
u	Internal energy	J/kg
V	Volume	m^3
V	Velocity	m/s
ν	Momentum diffusivity	m^2/s
$\dot{W}$	Work	W
$\bar{x}$	Mean/average	Varies
z_e	Elevation at outlet	m
z_i	Elevation at inlet	m

CHAPTER 1 INTRODUCTION

In this chapter, an introduction to refrigeration and heat pump cycles are given with a brief history that led to the development thereof. Different refrigerants used in these cycles are discussed and their environmental impact is stated. The main objectives and deliverables for this study are also described, including the contributions of this research.

1.1 History and background

From as early as the 1600s the basic characteristics of thermodynamics and heat transfer were researched and established. The scientists of the time believed that heat had an association with the movement of the constituents of matter. In the 1700s this believe changed as scientists speculated that heat was a form of fluid moving about. James Joule proved this theory wrong in the 1850s. He showed that heat was indeed a form of energy. With the discovery of the association between heat and energy the first steam engines were developed. Further studies resulted in the fundamental laws of thermodynamics, as we know it today (Wolfram, 2002).

An understanding of the laws of thermodynamics allowed for the development of refrigeration and heating methods. Applications thereof can be found in manufacturing processes, cold treatment of metals, food preservation, chemical and process industries, manufacturing of ice, manufacturing of drugs and industrial and residential air conditioning (Arora, 2010).

Refrigeration cycles can be classified in to the following main groups, namely absorption, gas cycle, mechanical vapour compression, thermo-electric, magnetic, steam jet and vortex tube refrigeration (Arora, 2010). Mechanical vapour compression technology is used in most household refrigerators and industrial refrigeration systems. The main components of a typical mechanical vapour compression cycle include the compressor, condenser/gas cooler (depending on the state of the refrigerant), expansion valve and an evaporator (Pearson, 2005). A refrigerant (such as Freon) is used as a working fluid within this cycle. The refrigerant is compressed in the compressor, cooled in the condenser/gas cooler, expanded in the expansion valve and heated in the evaporator. Mechanical vapour compression cycles can be used as either a refrigeration or a heat pump cycle depending on whether an environment must be cooled or heated. Conceptually, both cycles are equivalent: heat is withdrawn from one environment and then moved into another (Atlanta, 2004). Work performed on the refrigerant is required to sustain these cycles as the

second law of thermodynamics states that heat does not spontaneously move towards a positive temperature gradient (Borgnakke & Sonntag, 2014).

In recent years studies have shown that some refrigerants negatively affect the environment due to their global warming potential (GWP) and their ozone depletion potential (ODP). The GWP can be defined as the amount of heat being trapped by a certain mass of gas to the amount of heat trapped in the same mass of carbon dioxide. The ODP of a substance on the other hand refers to the relative amount that it degrades the ozone layer when compared to trichlorofluoromethane (R11). These negative findings are of great concern to the future of the earth (Austin & Sumathy, 2011).

Table 1 provides an overview of different refrigerants with a measurement of its potential impact on the environment. In 1989 the Montreal Protocol was implemented which regulates the use of certain substances, including refrigerants such as hydro-chlorofluorocarbons (HCFCs) and chlorofluorocarbons (CFCs). In 2010, a worldwide ban was implemented on all CFCs. Furthermore, since 2010 the use of HCFCs are illegal in most developed countries and must be phased out by 2030 in developing countries (Calm, 2008).

Table 1 Ozone depletion potential, global warming potential and atmospheric lifetime of different existing refrigerants (Calm, 2008).

Substance group	Abbreviation	ODP (ozone depletion potential)	GWP_{100} (global warming potential)	Atmospheric lifetime (years)
Saturated chlorofluorocarbons (R11, R12)	CFC	0.6-1	4,750-14,400	45-1,700
Saturated hydro-chlorofluorocarbons (R22, R141b)	HCFC	0.02-0.11	77-2,310	1.3-17.9
Saturated hydro-fluorocarbon (R32, R134a)	HFC	-	124-14,800	1.4-270
Unsaturated hydro-fluorocarbons (R1234yf, R1234ze, R1234yz)	u-HFC	-	<1-12	Days
Natural refrigerants (R744 (carbon dioxide), R717 (ammonia), R290 (propane))		-	0-20	

HFCs are listed under the Kyoto Protocol of the United Nations Framework Convention on Climate Change (UNFCCC) since 2005. This call requires that the use of HFCs must be reduced and emissions be limited. A typical domestic used refrigerant such as R134a is included. HFCs are not regulated by the Montreal Protocol and comprise of zero ODP, however a number of countries have already banned the use of any type of HFC. Adhering to the fulfilment of limiting HFC usage, synthetic refrigerants are produced. These are unsaturated HFCs (u-HFCs), consisting of low GWPs and a zero ODP (Calm, 2008).

Parallel to the production of synthetic refrigerants, the use of natural refrigerants in refrigeration and heat pump cycles are being researched. These includes ammonia (NH_3), carbon dioxide (CO_2) and hydrocarbons (which comprise of propene (C_3H_6), propane (C_3H_8) and isobutene (C_4H_{12})), (Pearson, 2005). These natural refrigerants are found in the biogeochemical cycles on earth and have no ODP and little GWP. A further advantage is that hazardous chemical compositions are not formed when in contact with water (Calm, 2008).

A potential natural replacement for conventional refrigerants in heat pumps is carbon dioxide. Carbon dioxide has a negligible GWP compared to HFCs, no impact on the ozone layer and is not flammable or corrosive. It is also readily available and inexpensive (Austin & Sumathy, 2011). Furthermore, it can be noted that using carbon dioxide as a refrigerant in heat pump cycles delivers a performance that is competitive with the refrigerants already used (Nekså, 2002).

Carbon dioxide can either be used within a conventional (subcritical) or trans-critical heat pump cycle. In a conventional heat pump cycle (Figure 1a), the refrigerant does not become a supercritical fluid (defined as when the temperature and pressure of a substance are greater than its critical temperature (T_c) and critical pressure (p_c)) throughout the whole cycle.

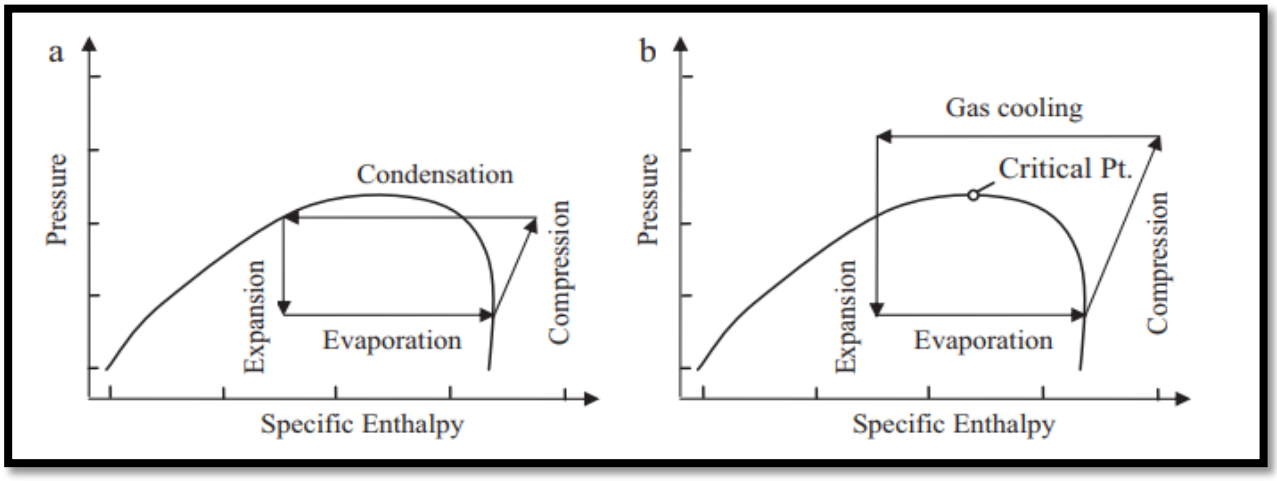

Figure 1 Pressure versus enthalpy state diagram of carbon dioxide: a) Conventional heat pump cycle (refrigerant stays below critical point), b) Trans-critical heat pump cycle (refrigerant moves in to supercritical region), (Austin & Sumathy, 2011).

Heat is absorbed through evaporation (in the evaporator) on the low-pressure side and rejected by first cooling the gas (sensible cooling) and then further rejecting heat through condensation (latent cooling) on the high-pressure side (in the condenser). In a trans-critical heat pump cycle however (Figure 1b), the refrigerant enters the supercritical region for a part of the cycle. On the low-pressure side, heat is still absorbed through evaporation. However, the compressor now increases the refrigerant's pressure into the supercritical region and single phase gas cooling takes place in a gas cooler (Austin & Sumathy, 2011). This means that carbon dioxide operates at supercritical conditions at the high-pressure side of the trans-critical heat pump cycle (Dang, et al., 2007). A heat pump cycle can be used for water heating applications. Nekså et al. (1999) and White et al. (2002) reported that a trans-critical heat pump cycle using carbon dioxide as a refrigerant can be used to heat water to a temperature of 90℃. According to the authors, a conventional heat pump cycle limits the heating of water to about 60℃ and electrical heating is needed to increase the temperature further. If a trans-critical heat pump cycle can be used to heat water to above 60℃, rather than electrical heating, then the electrical consumption will be greatly reduced. *Note: on the high-pressure side of a heat pump cycle a condenser is used when a condensation process is present while a gas cooler is used when a gas is cooled with no condensation process present, with both still classified as heat exchangers.*

As previously stated, a supercritical fluid is present when its temperature and pressure are greater than its critical temperature (T_c) and critical pressure (p_c). The critical point is defined by the intersection of the critical temperature and critical pressure of a substance as seen in Figure 2.

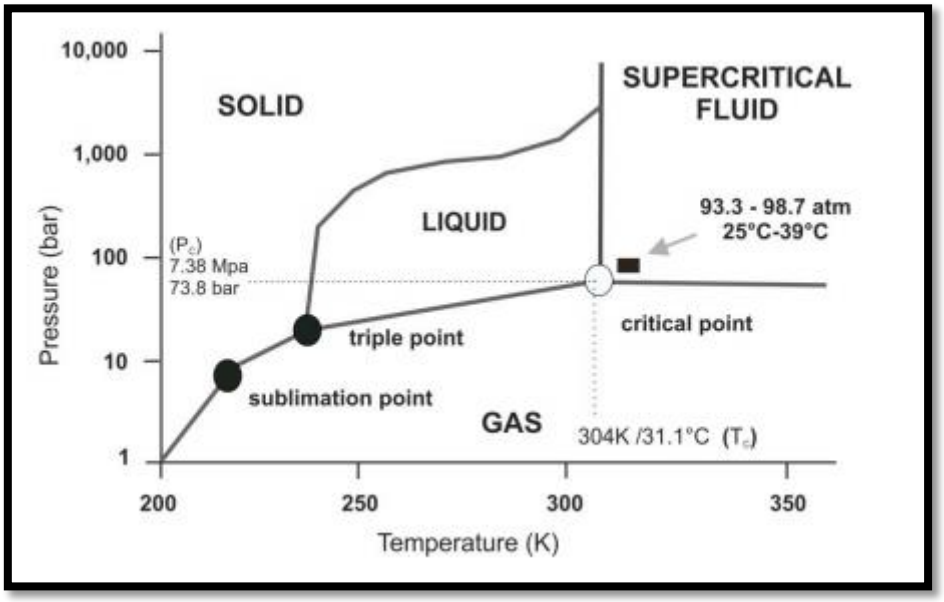

Figure 2 Pressure versus temperature state diagram for carbon dioxide showing the critical point and supercritical region (Budisa & Schulze-Makuch, 2014).

For carbon dioxide, the critical point is present at 31.06℃ and 7.38MPa (Budisa & Schulze-Makuch, 2014). The critical temperature of carbon dioxide is much lower than for most other refrigerants, consequently allowing it to enter the supercritical region in a heat pump cycle (Cavallini, 2004). On the boiling line (the line existing between the triple point and critical point in Figure 2), the liquid and gas phase co-exist. As the conditions move towards the critical point on this line, the density of the liquid reduces while the density of the gas increases until they are equal and no distinct gas or liquid phase exists. A supercritical fluid is formed at conditions greater than the critical point. Therefore, above the critical temperature, no substance can be liquefied by pressure alone.

The thermodynamic transport properties such as thermal conductivity (k), density (ρ), specific heat (c_p) and viscosity (μ) of a substance differ with pressure and temperature. These changes are much more significant at the pseudocritical temperature of a supercritical fluid (to be discussed in Section 2.2). These large changes in thermodynamic transport properties increase the complexity of the heat transfer and flow associated with supercritical fluids and has attracted numerous research studies in recent years (Dang & Hihara, 2004).

1.2 Problem statement

In a carbon dioxide trans-critical heat pump cycle, a compressor is used to apply work on the refrigerant. Oil is utilised in the compressor for cooling and lubrication purposes. An oil separator prevents the oil from mixing with the refrigerant. However, leakages are possible. The refrigerant may therefore be contaminated with a small quantity of lubricating oil, so that a carbon dioxide and oil mixture serves as the refrigerant (Dang, et al., 2007).

As reported in numerous studies (to be discussed in Chapter 2) oil entrainment has an adverse effect on the heat exchange of a refrigerant at the gas cooler. In the study of Dang et al. (2007), it was reported that the convection heat transfer coefficient decreased with oil entrainment when compared to oil-free conditions. The decrease was reported to be a maximum in the vicinity of the pseudocritical temperature. The highest reduction was reported to be about 75% for 3% oil contaminated supercritical carbon dioxide in a 1mm diameter pipe. Note that the 75% reduction does not refer to the average reduction of the convection coefficients over a temperature range, but only to the reduction at the pseudocritical temperature.

The large variations of the physical and transport properties of supercritical carbon dioxide at the pseudocritical temperature increases the complexity and uncertainty of the heat transfer that takes place in the gas cooler. Adding to the complexity of the heat transfer is the effects of oil contamination.

1.3 Focus of study

When designing the gas cooler of a trans-critical heat pump cycle using carbon dioxide as a refrigerant, a thermal-fluid simulation process is typically required. For such a simulation, accurate convection heat transfer coefficients (h_c) need to be predicted to obtain the heat transfer. The addition of oil in the cycle creates numerous uncertainties concerning the heat transfer. It is therefore necessary to evaluate the effects of oil entrainment on the convection coefficients of supercritical carbon dioxide in cooling. The focus of this study is to evaluate the performance consistency of existing correlations published for oil contaminated supercritical carbon dioxide in cooling and identify the shortcomings. Subsequently, a new correlation to improve on the consistency to predict the heat transfer process in the gas cooler must be investigated. Furthermore, it will be investigated whether the new correlation can deliver results that are more consistent but also be a simpler correlation than the existing complex correlations, which are not always applicable to a wide range of conditions. A more simplified correlation eases the calculation process and typically reduces the calculation times of large simulations.

1.4 Research objectives

In this section, the main objectives for this study are stated. These are to:

I. Research current literature available on:
    - The effects of oil entrainment in supercritical carbon dioxide on the heat transfer performance of the gas cooler in a trans-critical heat pump cycle.
    - The effects of different thermodynamic parameters (such as mass flow, temperature, pressure and heat flux) on the heat transfer.
    - Availability of published data.
    - The existing correlations published with a focus on obtaining the Nusselt number for this type of flow.

II. Calculate the predicted convection heat transfer coefficients of oil-contaminated supercritical carbon dioxide in cooling, by using relevant prediction correlations found in literature.

III. Compare the convection coefficients from published data to the values predicted.

IV. Evaluate the performance consistency of each correlation to predict the convection coefficients.

V. Based on the results, develop a new Nusselt number correlation to predict the convection coefficients with an improved consistency on a wide range of conditions.

VI. Develop a new Nusselt number correlation, comprising a less complex format, without foregoing on accuracy.

1.5 Research methodology

In this section, the research methodology that will be followed for this study is discussed. Firstly, current literature available on the cooling of supercritical carbon dioxide (especially with oil entrainment) will be investigated. An evaluation will be done of published data and prediction correlations as well as the characteristics of oil-contaminated supercritical carbon dioxide during cooling.

Theoretical calculations using the fundamental laws of thermodynamics and heat transfer will be used to predict the heat transfer process. The mathematical calculations will be coded in EES (Engineering Equation Solver), which is a software package comprising various thermodynamic property functions and uses iterative methods to solve simultaneous equations. The prediction correlations obtained from literature will be used in the calculations to compute the convection coefficients and then compared with the published data obtained in literature.

Constructing a test bench and generating experimental data are not within the scope of this study. An evaluation on the performance consistency of these correlations will be done and based on the results a new correlation will be developed. This proposed new correlation should be an improvement of performance consistency as well as simplicity when compared to the current published correlations.

1.6 Contributions of this study

In this section, the contributions of this study are presented. These are:

I. Understanding how oil contamination affects the heat transfer process of supercritical carbon dioxide during cooling.
II. An evaluation of the published correlations' performance consistency to predict the convection coefficients over a wide range of conditions.
III. The formulation of a more consistent prediction correlation for this flow.

CHAPTER 2 LITERATURE SURVEY

In Chapter 1, the focus of this study was stated. This included the performance consistency evaluation of existing correlations published for oil-contaminated supercritical carbon dioxide in cooling. Based on this, a new correlation to improve on the consistency and simplicity must be investigated. In this chapter an overview of the literature on carbon dioxide as a refrigerant and the effects of oil entrainment on its heat transfer performance are given. In addition, numerous studies done on the cooling of supercritical carbon dioxide are presented

2.1 Carbon dioxide as a refrigerant

At the end of the 19th century, the first mechanical heat pump and refrigeration cycles were developed, as we know it today. One of the first refrigerants used in these vapour compression cycles were carbon dioxide. At that time, the high operating pressures (above the critical pressure of 7.38MPa at the high-pressure side) in a trans-critical cycle were too great for the components. Today however, the manufacturing capabilities allow the components to be produced so that they are able to work under these conditions. These early carbon dioxide vapour compression cycles were mostly used in refrigeration ships, but also had other commercial applications, (Cavallini, 2004). There are numerous properties of carbon dioxide, which makes it favourable above other refrigerants, (Lorentzen, 1994):

I. Carbon dioxide is compatible with all plastics, elastomers and metals. It does not react with any material used in a vapour compression cycle.
II. It holds no safety concerns: it is non-toxic and not flammable which makes it a safe substance to work with.
III. It has no ODP and a negligible GWP compared to CFCs.

The pressure versus enthalpy state diagram of carbon dioxide is shown in Figure 3, indicating the critical temperature and pressure. As stated previously, when carbon dioxide is used above the critical point it will be in the supercritical fluid region (where no distinct gas or liquid phase are present).

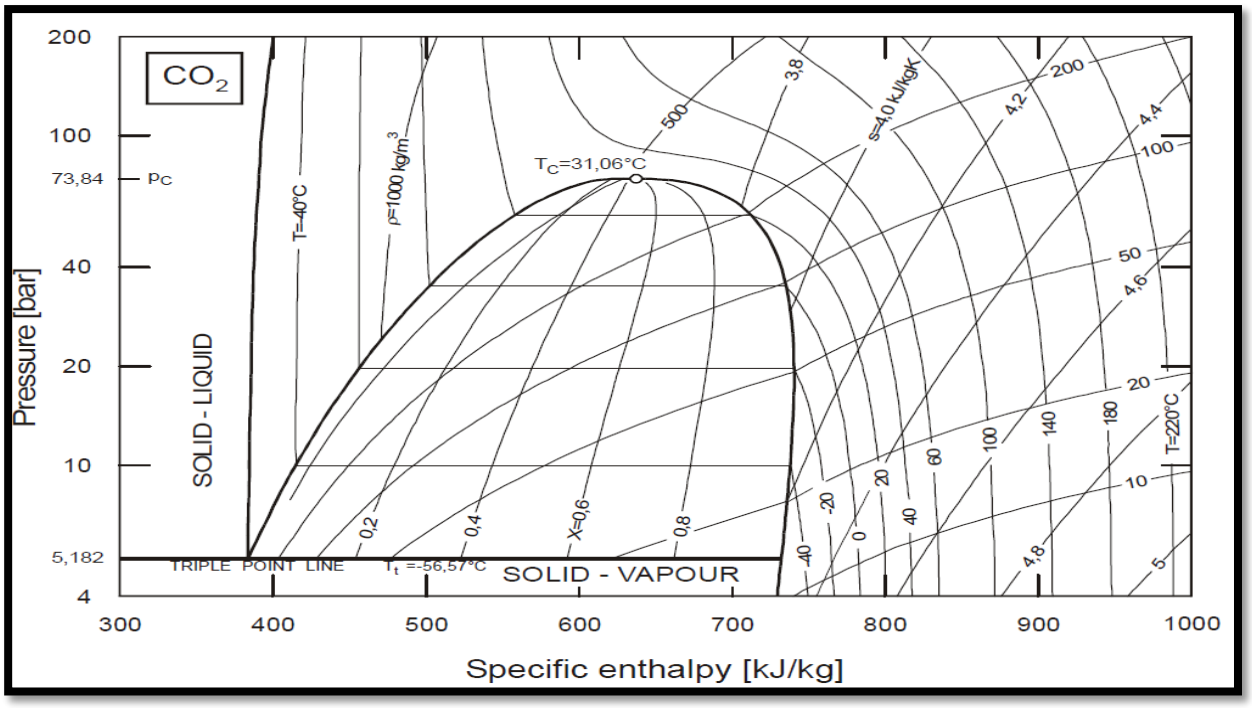

Figure 3 Pressure versus specific enthalpy state diagram for carbon dioxide (Cavallini, 2004).

A comparison of the thermodynamic characteristics of carbon dioxide and other common refrigerants are reported in Table 2. Here it is noted that the critical temperature of carbon dioxide is 31.06℃, which is much lower than the other refrigerants. The critical pressure is 7.38 MPa, which is higher than most of the refrigerants' critical pressures.

Table 2 Thermodynamic characteristics of carbon dioxide and other common refrigerants **(Cavallini, 2004)**.

Refrigerant	**Critical Pressure [bar]**	**Critical Temperature [°C]**	**Saturation pressure At -20°C at +30°C [bar]**		**Volumetric Latent Heat at -20°C [kJ/m³]**	**Molecular Mass [kg/kmol]**
Carbon Dioxide (CO_2)	73.84	31.06	19.67	72.05	14592	44.01
Chlorodifluoromethane (R-22)	49.90	96.15	2.453	11.92	2371	86.47
Tetrafluoroethane (R-134a)	40.59	101.06	1.327	7.702	1444	102.03
A Hydro-fluorocarbon (R-410A)	49.03	71.36	4.007	18.89	3756	72.59
Ammonia (NH_3)	113.33	132.25	1.901	11.672	2131	17.03

Numerous researchers developed heat pump cycles using carbon dioxide as a refrigerant. A heat pump cycle using carbon dioxide, with a coefficient of performance (COP) of 4.3, was obtained when water was heated from 9℃ to 60℃, (Nekså, et al., 1998). Water heated to 90℃ with a COP of three, was achieved by White et al. (2002) who furthermore predicted that water could potentially be heated up to 120℃ at a reduced COP of 2.46. The coefficient of performance (COP) of a heat pump cycle refers to the ratio of useful heating provided by the cycle to the work required, (Nekså, et al., 1998). Using trans-critical heat pump cycles, water can be heated above 60℃, which is usually the limit for conventional Freon based heat pump cycles.

2.2 Characteristics of supercritical carbon dioxide in cooling

Carbon dioxide at the high-pressure side of a trans-critical heat pump cycle operates under supercritical conditions. At this side the heat transfer does not take place through a condensation process, but a supercritical gas cooling process is observed. Fluids in a supercritical state possess large changes in transport and physical properties at or near the pseudocritical temperature, (Cheng, et al., 2008). In Figure 4, characteristics of supercritical carbon dioxide with respect to temperature are shown, (REFPROP, 2002).

The pseudocritical point can be described as the position where the specific heat extends to a maximum for a constant pressure above the critical pressure. This can be seen in Figure 4 (c) where the intersection of the dashed line and the line described by '3' indicates the pseudocritical point of carbon dioxide at 9MPa. The corresponding temperature for the pseudocritical point of a certain pressure above the critical pressure is identified as the pseudocritical temperature (T_{pc}). For pressures close to the critical pressure of carbon dioxide (7.38MPa), the thermal conductivity shows a sharp increase with a decrease in temperature at the pseudocritical temperature. This can be seen in Figure 4 (d) at the lines described as '1' and '2', (Cheng, et al., 2008).

In an isobaric heat transfer process, using supercritical fluids, it is observed that the transport and physical properties change significantly when the temperature is neighbouring the pseudocritical temperature. This is particularly true when the supercritical fluid's pressure is near the critical pressure, (Cheng, et al., 2008). The changes of the properties near the pseudocritical region become less drastic for when the supercritical fluid is at a pressure further away from its critical pressure. The maximum values for the supercritical fluid's specific heat, thermal conductivity and Prandtl number can be seen in Figure 4 (c), (d) and (f) at the pseudocritical temperature of line '1' which are for a pressure near the critical pressure. These maximums drop rapidly for operating pressures further away from the critical pressure.

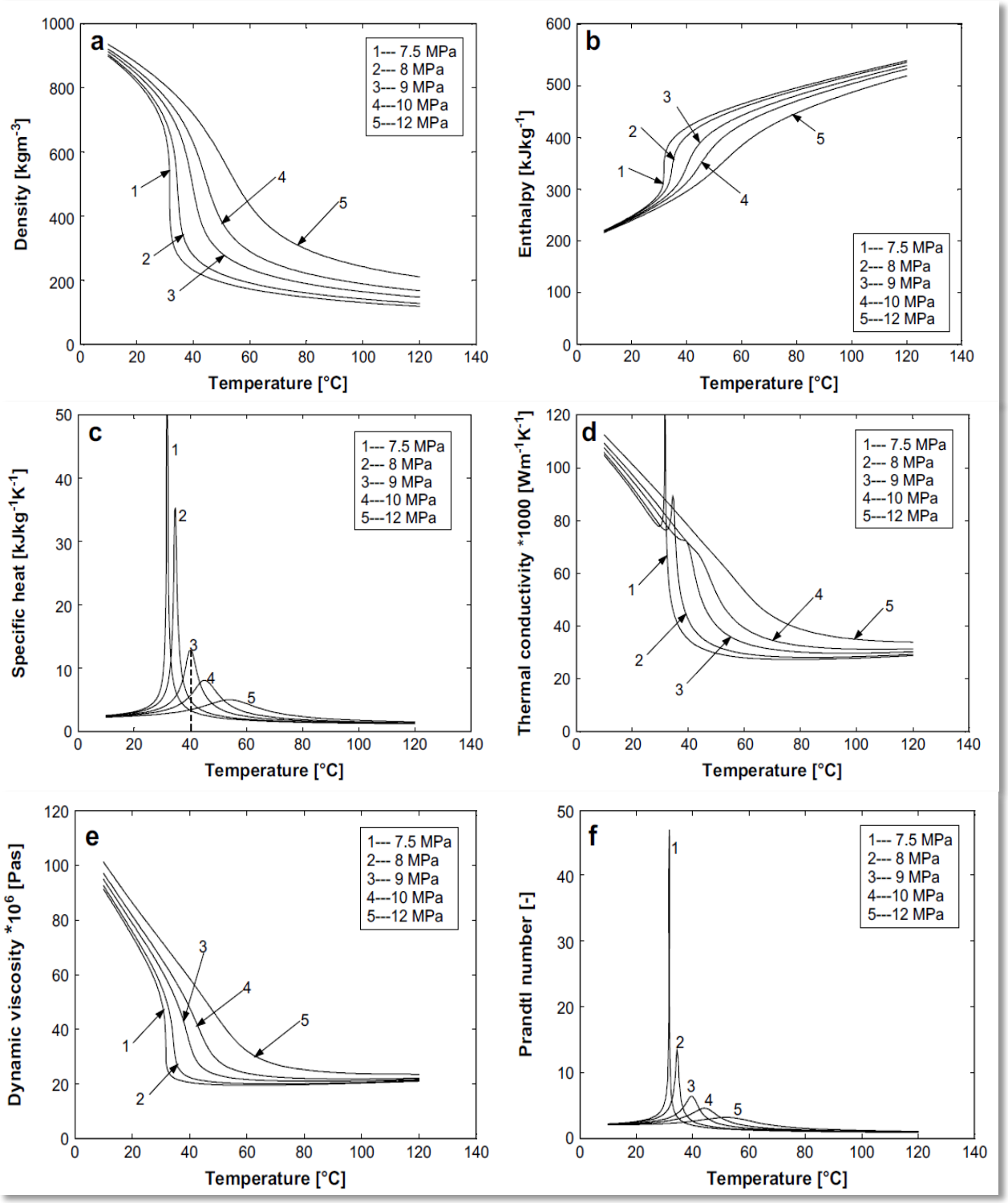

Figure 4 Characteristics versus temperature for supercritical carbon dioxide (REFPROP, 2002). a) Density, b) enthalpy, c) specific heat, d) thermal conductivity, e) dynamic viscosity and f) Prandtl number.

At the pseudocritical temperature the enthalpy has a significant decrease with a decrease in temperature, whereas the density and dynamic viscosity undergo a drastic increase, seen in Figure 4 a, b and e, especially for operating conditions near the critical pressure, (Cheng, et al., 2008). It was also reported that supercritical carbon dioxide expresses liquid-like thermo-physical

properties before the pseudocritical temperature whilst gas-like characteristics were noted after this point, (Aldana, et al., 2002).

The large variations of the physical and transport properties of supercritical carbon dioxide at the pseudocritical temperature during cooling increases the complexity and uncertainty of the heat transfer that takes place in the gas cooler of a trans-critical heat pump cycle. A measure of the heat transfer is given by the Nusselt number (Nu). This number is typically a function of the Reynold's (Re) and Prandtl's (Pr) numbers (that is $Nu = f(Re, Pr)$) when forced convection is present in a turbulent flow. The Reynold's number is affected by the density (ρ) and the viscosity (μ) of a fluid or gas, while the Prandtl's number is a function of the specific heat (c_p), the viscosity (μ) and the thermal conductivity (k), all of which shows large variations at the pseudocritical temperature. Adding to the complexity of the heat transfer is the oil contamination that may be present in the gas cooler. The effects of oil contamination on the heat transfer together with the large variations of the supercritical carbon dioxide's properties makes it difficult to predict the heat transfer. For this reason, an experimental approach is typically done by researchers in an attempt to understand the heat transfer for the cooling of supercritical carbon dioxide and the effects that oil contamination has on it.

2.3 Published test data concerning the cooling of supercritical carbon dioxide with oil entrainment

In this section, studies are examined where experiments were performed on the cooling of supercritical carbon dioxide with the focus directed at the effects of oil contamination on the convection heat transfer coefficients. The outcome for these experiments were to determine heat transfer coefficients (and pressure drops for limited cases) by using test segments that represents the conditions inside the gas cooler of a trans-critical heat pump cycle. The early studies on the heat transfer characteristics of supercritical fluids were performed by Petukhov (1970), Hall (1971), Polyakov (1991), Duffey and Pioro (2004) and Pioro et al. (2005). In these studies, carbon dioxide to water configurations were used to improve the understanding of supercritical heat transfer and pressure drops.

Studies concerning the cooling of supercritical carbon dioxide in micro- and macro tubes have only been conducted in recent years. For this purpose, a micro-tube refers to a pipe diameter equal or less than 3 mm and a macro-tube refers to a diameter above that, (Cheng & Mewes, 2006). The first studies performed on supercritical carbon dioxide only focussed on heating in macro-tubes. The studies performed on the heating of supercritical carbon dioxide far outweighs the studies on the cooling heat transfer, (Cheng & Mewes, 2006).

Eleven different published studies on the cooling of supercritical carbon dioxide were investigated by Cheng et al. (2008). Only four of the 11 studies focused on the cooling heat transfer of supercritical carbon dioxide with oil contamination. The studies including the effects of oil entrainment can be divided into macro-tubes (Mori, et al., 2003; Dang, et al., 2007) and micro-tubes (Dang, et al., 2007; Yun, et al., 2007; Kuang, et al., 2003). The studies neglecting the effects of oil can also be divided in two sections: macro-tubes (Son & Park, 2006; Dang & Hihara, 2004; Yoon, et al., 2003) and micro-tubes (Dang & Hihara, 2004; Liao & Zhao, 2002; Huai & Koyama, 2007; Pettersen, et al., 2000; Kuang, et al., 2004).

Another study was performed on the cooling of oil-contaminated supercritical carbon dioxide by Zhao et al. (2011). In this study, it was noted that the convection coefficients were related to the viscosity and density ratios of the oil to the carbon dioxide. A summary of the published data is reported in Table 3. In all of these tests, oil had a very adverse effect on the convection coefficients: especially near the pseudocritical temperature.

Table 3 Summary of the studies done on the cooling heat transfer of supercritical carbon dioxide with oil entrainment, (Cheng, et al., 2008) and (Zhao, et al., 2011).

Study	**Tube diameter D [mm]**	**Inlet temperature T [^{o}C]**	**Inlet pressure p [MPa]**	**Mass Flux G [kg/m^{2}s]**	**Heat flux q [kW/m^2]**	**Oil concentration ω (wt. %)**
Kuang et al. (2003)	0.79	30-50	9	890	Not mentioned	0-5
Mori et al. (2003)	6	20-70	9.5	100-600	Not mentioned	Up to 0.1
Dang et al. (2007)	1,2,4,6	20-70	8-10	200-1200	12-24	0-5 (up to 13% for some cases)
Yun et al. (2007)	1	40-80	8.4-10.4	200-400	20,25	0-4
Zhao et al. (2011)	1.98,4.14	25-100	8-11	400-1200	Not mentioned	0,1,2

Using experimental data, empirical correlations can be developed in an attempt to describe the Nusselt numbers (and consequently the convection heat transfer coefficients) for a certain type of flow. These empirical correlations are typically a function of the Reynolds and Prandtls numbers when forced convection is present within a turbulent flow, (Incropera, et al., 2013).

2.4 Nusselt number correlations for the cooling of oil-free and oil-contaminated supercritical carbon dioxide

A number of researchers have published Nusselt number correlations for the cooling of oil-free supercritical carbon dioxide. These correlations were mainly developed by modifying previously published correlations to fit experimental data and to include the effects of the varying thermo-physical properties on the convection coefficients. In contrast to this, very few Nusselt number correlations for oil-contaminated conditions can be found in literature. For this reason, correlations developed for oil-free conditions are also included within this study.

Nusselt number correlations for oil-free supercritical carbon dioxide in cooling

2.4.1 Study by Yoon *et al.* (2003)

Experimental tests on the cooling of supercritical carbon dioxide to obtain the heat transfer coefficients and pressure drops were conducted by Yoon *et al*. (2003). These tests were conducted using an inner diameter tube of 7.73mm and varying the inlet pressure between 7.5MPa and 8.8MPa. The Reynolds numbers ranged between 60'000 and 170'000 whilst the inlet temperature of the carbon dioxide was adjusted between 50°C and 80°C. The correlations published by Pitla *et al.* (1998), Petrov & Popov (1985), Baskov *et al.* (1977) and Krasnoshchekov *et al*. (1970) were evaluated against the experimental data. A new Nusselt number correlation, taking the variation of the thermo-physical properties into account, was published by Yoon *et al.* (2003). This correlation is based on the Dittus & Boelter (1930) correlation and was claimed to predict the convection coefficients of the experimental data with a 12.7% average deviation. Other conclusions for this study are as follows:

I. The heat transferred is a maximum at the pseudocritical temperature with a sharp decrease as the temperature diverges from the pseudocritical point.
II. The convection coefficients increase for all pressures as the mass flux becomes larger.
III. The maximum convection coefficient over a temperature range decreases as the pressure moves further away from the critical pressure.

2.4.2 Study by Pitla *et al*. (1998) and (2002)

An investigation on the heat transfer correlations for heating and cooling available at the time were conducted by Pitla *et al*. (1998). A comparison between correlations from Baskov *et al.* (1977), Petrov & Popov (1985), Krasnoshchekov *et al.* (1970) and others were done. These studies were concerned with heating applications and were not developed for carbon dioxide as a refrigerant. Pitla *et al.* (1998) concluded that:

I. Turbulence within a flow affects the heat transfer, but the extent of it is unknown.
II. The published correlations before 1998 are not able to predict the convection coefficients accurately.
III. Further experimental data is needed to obtain accurate correlations.
IV. Fluid temperature has a large impact on the heat transfer coefficients.

A few years later Pitla et al. (2002) published a Nusselt number correlation for the cooling of supercritical carbon dioxide. This correlation consists out of a corrected mean Nusselt number calculated using the Gnielinski (1976) correlation evaluated at the wall and bulk conditions. The authors developed this correlation using experimental data where they cooled supercritical carbon dioxide between the ranges of 120°C and 25°C in a 4.72mm inner diameter tube. The pressure range for these experiments were between 8MPa and 12MPa with Reynolds numbers between 95'000 and 415'000. It was stated that the correlation predicted their experimental data within 20% deviation for up to 85% of the data.

2.4.3 Study by Dang & Hihara (2004)

The effects that the variation of inlet pressure, heat flux and mass flux have on the convection heat transfer coefficients of supercritical carbon dioxide cooling were studied by Dang & Hihara (2004). The experiments were conducted using four tubes with diameters varying from 1mm to 6mm. The pressure ranged between 8MPa and 10MPa whilst the Reynolds numbers changed between 4'000 and 80'000. The carbon dioxide's temperatures were between 30°C and 70°C. The correlations published by Yoon *et al*. (2003), Pitla *et al*. (1998), Liao & Zhao (2002), Petrov & Popov (1985) and Gnielinski (1976) were evaluated against this study's experimental data. Dang & Hihara (2004) published a Nusselt number correlation, which takes the variation of the thermo-physical properties into account. This correlation is a modification on the Gnielinski (1976) prediction correlation and predicted the experimental data within a 20% deviation. The conclusions made for this study are:

I. As the mass flux increases, so do the convection coefficients and pressure drop.
II. When the inlet pressure increases, the pressure drop decreases.
III. The property variations in the flow direction determines how the pressure effects the convection coefficients.
IV. The property variations in the radial direction determines how the heat flux and tube diameter effects the coefficients.

2.4.4 Study by Zhao & Jiang (2011)

The study done by Zhao & Jiang (2011) investigated the heat transfer characteristics of supercritical carbon dioxide in cooling. In these experimental tests, the inner diameter of the tube used was 4.01mm whilst the pressure and inlet temperatures ranged between 4.5MPa to 5.5MPa and 80°C to 140°C, respectively. The Reynolds numbers for this study were between 4'000 and 80'000. The correlations published by Pitla et al. (2002), Yoon *et al*. (2003), Gnielinski (1976) and Dang & Hihara (2004) were evaluated against the experimental data. The following conclusions were made by Zhao & Jiang (2011):

I. The heat transfer is a maximum at the pseudocritical temperature.
II. As the mass flux increases, the heat transfer will increase as well.
III. The effects of pressure change on the heat transfer is relatively small when the bulk temperature is smaller than the pseudocritical temperature, but this effect becomes larger when the bulk temperature is higher than the pseudocritical temperature.
IV. Among the tested correlations, the Gnielinski (1976) correlation predicted the heat transfer most accurately with a deviation of under 25%.

A correlation, based on the Gnielinski (1976) correlation, was developed which according to Zhao & Jiang (2011) predicted the experimental data within 15% for 90% of the data.

Nusselt number correlations for oil-contaminated supercritical carbon dioxide in cooling

2.4.5 Study by Zhao *et al.* (2011)

Within this study, an investigation was done on the convection heat transfer coefficients of oil-contaminated supercritical carbon dioxide cooling within horizontal tubes. The tube inner diameters were 1.98mm and 4.14mm, respectively, whilst the inlet pressures ranged between 8MPa and 11MPa. The inlet temperatures were between 100°C and 25°C and the oil concentrations used for this study were between 0% and 2%. The conclusions of the experimental tests are:

I. For oil-free cases, the Nusselt number correlation by Dang and Hihara (2004) most accurately predicted the heat transfer coefficients. The frictional pressure drops were most accurately calculated using the correlation proposed by Petukhov (1970).
II. When oil was introduced within the flow, the heat transfer coefficients decreased for all cases, especially at the pseudocritical temperature.

Zhao et al. (2011) reported that they could not find a correlation in literature that predicts convection coefficients for oil-contaminated supercritical carbon dioxide in cooling. They however,

then compared published correlations for oil-contaminated refrigerants (such as R22 and R134a) in a condensation process to their test data.

According to Zhao et al. (2011), the viscosity of a fluid or gas has a significant effect on the heat transfer and flow. The convection coefficients for the oil-carbon dioxide mixture is directly affected by the viscosity of each substance. It was also reported that the solubility of the carbon dioxide in the lubrication oil is affected by the density ratio between these two substances. This is seen especially when the bulk temperature is higher than the pseudocritical temperature and the supercritical carbon dioxide is in a gas-like state. The solubility of carbon dioxide in the oil has an effect on the heat transfer, i.e. a pure oil layer forming in the inside of a tube at a certain condition will have a different rate of heat transfer as an oil layer with carbon dioxide dissolved within it.

An empirical correlation, containing a viscosity and a density ratio of the oil to the carbon dioxide, was proposed by the authors to describe the effects of oil contamination on the convection heat transfer coefficients. This correlation uses the convection coefficient for oil-free supercritical carbon dioxide calculated from Dang & Hihara (2004) and adjusts it for oil contamination by multiplying it with a formula taking the viscosity and density ratio into account. The correlation is presented by two independent formulas, one before the pseudocritical temperature and one after. It is reported that this correlation was able to predict 90% of the experimental data within 20%.

2.4.6 Study by Jung and Yun (2013)

An investigation into the convection coefficients and transport properties for oil-contaminated supercritical carbon dioxide in cooling was performed in this study. Two correlations were published to predict the coefficients. The first correlation for when no oil layer was present in the flow (used when the oil contamination was low at approximately 1%) and the second correlation for when such a layer was present (used when the oil contamination reached values up to 5%).

These correlations were compared to the findings of Dang et al. (2007, 2008 and 2010). The mean deviation was reported as 13.2% and 33.4% for the correlations published for an oil layer and without such a layer, respectively. It was stated that the maximum value of the convection heat transfer coefficient (found at the pseudocritical temperature) decreased drastically when the oil contamination reached 5%. It was also observed that as the working pressure increased, the convection coefficient decreased.
The correlations published by Jung and Yun (2013) will not be used within this study, because the evaluation of these correlations require impractical input parameters such as the quality of the dissolved carbon dioxide within the oil layer at the inner tube.

2.5 Flow patterns and interaction of oil in supercritical carbon dioxide while cooling

The addition of oil to the flow and its interaction with the supercritical carbon dioxide increases the complexity of the heat transfer process. Different flow patterns and behaviours may be present at different conditions, which will ultimately effect the heat transfer. A number of studies on the effects of oil on the flow have been performed by Dang et al. (2004, 2007, 2008, and 2010). In these studies PAG-type oil (polyalkylene glycol oil), which is a synthetic compressor lubricant, is used. An investigation on the flow visualization and behaviour of oil contamination in supercritical carbon dioxide was done by Dang et al. in 2008 with the main findings discussed in the next section.

2.5.1 Flow pattern observations at different conditions

The variety of flow patterns observed, as illustrated in Figure 5, are:

The different flow patterns observed are:

I. **Mist flow, M:** In this flow pattern small oil particles move with the supercritical carbon dioxide. No oil layer is formed on the inside of the tube wall.
II. **Annular-dispersed flow, AD:** In this case, an oil film occurs at the wall of the tube while small oil particles flows with the supercritical carbon dioxide.
III. **Annular flow, A:** With this type of flow the amount of oil droplets as compared to mist flow and annular-dispersed flow are much less and almost negligible.
IV. **Wavy flow, W:** This is when the oil film does not occur on the entire wall of the tube, but only on the bottom.
V. **Wavy-dispersed flow, WD:** In this case, an oil layer is observed on the bottom of the tube with oil droplets moving with the supercritical carbon dioxide near the layer.

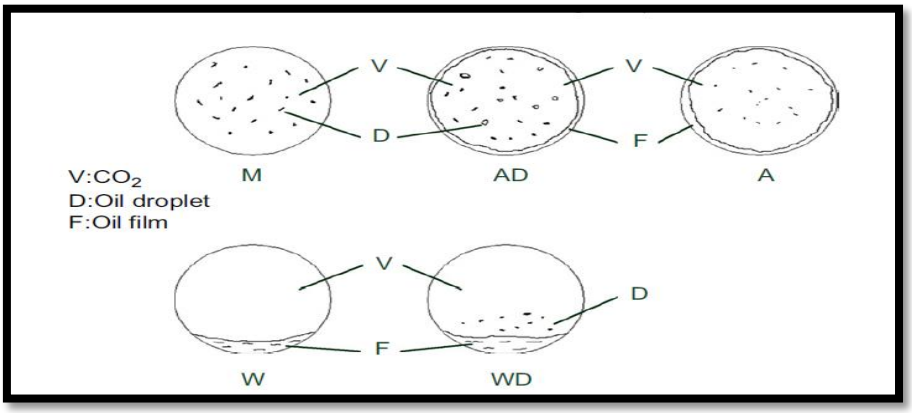

Figure 5 Different flow patterns for oil entrained supercritical carbon dioxide, (Dang, et al., 2008). With: M - mist flow, AD - annular-dispersed flow, A - annular flow, W - wavy flow and WD – wavy-dispersed flow.

The variation of parameters such as pressure, temperature, concentration of oil and tube dimensions results in different flow patterns, (Wang, et al., 2012). Within the study of Dang et al. (2008), a mist type flow was observed when the temperature was 25℃ and the oil contamination was 1%. The oil droplets, with diameters from 50μm to 100μm, flowed with the supercritical carbon dioxide and no oil film was encountered. With the temperature rising, some of the oil particles formed a layer on the inner wall of the tube. As the temperature of the mixture increased further, the oil layer became thicker. The thicker the oil layer became the greater the decrease in the heat transfer coefficients was.

When comparing the flow visualization of a 2mm and 6mm tube it was observed that for the smaller tube the oil layer was thicker with larger oil droplets in the bulk of the carbon dioxide. This caused a larger decrease in the convection coefficients, compared to the 6mm diameter tube, (Dang, et al., 2008).

The findings from the flow patterns of oil-contaminated supercritical carbon dioxide are:

I. From the visual experiments on the 2mm tube, different flow patterns were noted at different temperatures. At lower temperatures, the flow pattern is mist flow. An increase in temperature resulted in an annular-dispersed flow with a further increase leading to annular flow.
II. It was seen that for a 6mm inner diameter tube a wavy flow or wavy-dispersed flow was obtained at a low mass flux (200kg/m^{2}s) whereas an annular-dispersed flow was noted at a higher flux (800kg/m^{2}s).

2.5.2 Main findings with regards to heat transfer performance

The following are the main observations with respects to the convection heat transfer coefficients of oil-contaminated supercritical carbon dioxide, (Dang, et al., 2008):

I. With an increase of oil, the convection coefficients decreased. This reduction was more drastic at the pseudocritical temperature.
II. At low temperatures, the flow pattern was mist flow.
III. At higher temperatures, the oil layer was much thicker which introduced a high thermal resistance and caused a decrease in the convection coefficients.
IV. When the mass flux of the oil and carbon dioxide mixture was low, it is reported that an oil layer formed on the bottom part of the tube. Even with an increase of oil contamination, the convection coefficients do not decrease drastically.
V. At higher mass flux rates, it is seen that the oil film covered the entire inside wall, which resulted in a large decrease in the convection coefficients.

In summery Dang et al. (2008) found the main reason for the decrease of the convection coefficients to be the oil layer forming on the inner wall. The oil droplets did not contribute significantly to the loss of heat transfer.

2.6 Summary

The transport and physical properties of supercritical carbon dioxide changes significantly at the pseudocritical temperature, which increases the complexity of the heat transfer taking place. Oil adds to the complexity as different flow patterns and interactions may exist at different conditions. Limited researchers have published correlations that take the effects of oil into consideration. With oil entrainment, the convection coefficients decrease significantly with the largest reduction at the pseudocritical temperature. In the next chapter, the theory necessary for this study will be discussed.

CHAPTER 3 THEORETICAL BACKGROUND

In Chapter 2, the characteristics of supercritical carbon dioxide in cooling as well as the effects that oil contamination has on the complexity of the heat transfer were described. In this chapter, the relevant theory required to calculate the predicted convection coefficients in this study are reported. This includes the concepts and equations from thermodynamics and heat transfer needed to evaluate a Nusselt number correlation. The theory can then be used to calculate the predicted convection coefficients of different correlations and compare it against published data. This chapter also reports the Nusselt number correlations identified in Chapter 2, which will be used in this study.

The theory discussed in sections 3.1 until 3.5 is based on the work of Incropera et al. (2013), Rousseau (2013), Borgnakke & Sonntag (2014) and Munson et al. (2013).

3.1 Conservation laws

Our understanding of the physical world is largely based on the fundamental definitions and assumptions developed through science. Conservation laws, such as the conservation of mass, momentum and energy, are considered fundamental laws of nature.

An infinitesimal control volume that can be used to derive the conservation equations is seen in Figure 6. This control volume can be used to derive the equations describing the conservation of mass, momentum and energy, (Rousseau, 2013).

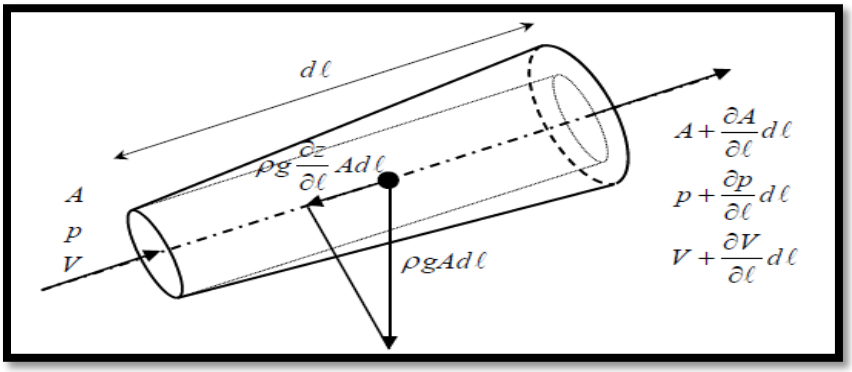

Figure 6 Demonstration of an infinitesimal control volume used for deriving conservation laws, (Rousseau, 2013).

3.1.1 Conservation of mass

The conservation of mass can be applied to a control volume. For such a control volume, the integral form of the conservation of mass is defined as:

$$\frac{\partial}{\partial t}\left(\iiint \rho d\forall\right) + \oiint \rho \bar{V} \cdot \overline{dA} = 0 \tag{1}$$

With $\forall$ [m^3] the volume, V [m/s] the velocity relative to the control volume, ρ [kg/m^3] the density and A [m^2] the cross-sectional free flow area.

Using Figure 6 and equation 1, the conservation of mass equation can be derived to be:

$$\forall \frac{\partial \rho}{\partial t} + \dot{m}_e - \dot{m}_i = 0 \tag{2}$$

With $\dot{m}_e$ [kg/s] and $\dot{m}_i$ [kg/s] referring to the mass flow rates at the outlet and inlet of the control volume. The subscripts 'i' and 'e' will from here on refer to the inlet and outlet conditions of a control volume. For steady-state flow ($\forall \frac{\partial \rho}{\partial t} = 0$), we have:

$$\dot{m}_e - \dot{m}_i = 0 \tag{3}$$

So that:

$$\dot{m}_i = \dot{m}_e = \dot{m} \tag{4}$$

3.1.2 Conservation of momentum

The integral form of the linear momentum conservation equation is given as:

$$\oiint \tau \overline{dA} + \iiint \bar{B} \rho d\forall = \frac{\partial}{\partial t}\left(\iiint \bar{V} \rho d\forall\right) + \oiint \bar{V}\left(\rho \bar{V} \cdot \overline{dA}\right) \tag{5}$$

With $\bar{B}$ [N/m^3] the body forces acting on the control surface and τ [N/m^2] the shearing stress.

For incompressible flow, the following equation is derived:

$$\rho L \frac{\partial V}{\partial t} + (p_{0e} - p_{0i}) + \rho g (z_e - z_i) + \Delta p_{0L} = 0 \tag{6}$$

With L [m] the length of the control volume, p_0 [Pa] the total pressure, Δp_{0L} [Pa] the total pressure drop and z [m] the elevation. The subscript '0' will from here on refer to the total/stagnation properties. For steady state ($\rho L \frac{\partial V}{\partial t} = 0$) incompressible flow, we have:

$$(p_{0e} - p_{0i}) + \rho g(z_e - z_i) + \Delta p_{0L} = 0 \tag{7}$$

For compressible flow, the conservation of momentum becomes:

$$\rho L \frac{\partial V}{\partial t} + \frac{p}{p_0}(p_{0e} - p_{0i}) + \frac{1}{2}\rho V^2 \frac{1}{T_0}(T_{0e} - T_{0i}) + \rho g(z_e - z_i) + \Delta p_{0L} = 0 \tag{8}$$

With T_0 [K] the total temperature and p [Pa] the static pressure. For steady-state compressible flow, we have:

$$\frac{p}{p_0}(p_{0e} - p_{0i}) + \frac{1}{2}\rho V^2 \frac{1}{T_0}(T_{0e} - T_{0i}) + \rho g(z_e - z_i) + \Delta p_{0L} = 0 \tag{9}$$

For steady-state conditions, with no elevation changes ($z_e - z_i = 0$) or pressure drops ($\Delta p_{0L} = 0$) equations 6 and 8 become:

$$p_{0e} = p_{0i} = p_0 \tag{10}$$

3.1.3 Conservation of energy

The integral form of the conservation of energy as applied to a control volume is given as:

$$\dot{Q} + \dot{W} = \frac{\partial}{\partial t}\left(\iiint \left(u + \frac{1}{2}V^2 + gz\right)\rho \, d\forall\right) + \oiint (h + \frac{1}{2}V^2 + gz)\, \rho \bar{V} \cdot \overline{dA} \tag{11}$$

With $\dot{Q}$ [W] the rate of heat transfer into the control volume, $\dot{W}$ [W] the work done on the control volume, u [J/kg] the internal energy and h [J/kg] the static enthalpy. The conservation of energy simplifies to:

$$\dot{Q} + \dot{W} = \cancel{\forall} \frac{\partial}{\partial t}(\rho h_0 - p) + \dot{m}_e h_{0e} - \dot{m}_i h_{0i} + \dot{m}_e g z_e + \dot{m}_i g z_i \tag{12}$$

With h_0 [J/kg] the total enthalpy. For a steady-state flow ($\cancel{\forall}\frac{\partial}{\partial t}(\rho h_0 - p) = 0$) without elevation changes ($z_e - z_i = 0$) or work done on the control volume ($\dot{W} = 0$), we have:

$$\dot{Q} = \dot{m}_e h_{0e} - \dot{m}_i h_{0i} \tag{13}$$

In the following sections, the required theory for the evaluation of Nusselt number correlations is reported.

3.2 Mass flow rates

The generic form for the mass flow rate equation is defined by, (Munson, et al., 2013):

$$\dot{m} = \rho V A_{ff} \tag{14}$$

Where A_{ff} [m^2] is the free flow area perpendicular to the flow. The mass flow rate can also be written as:

$$\dot{m} = GA_{ff} \tag{15}$$

Where G [kg/m^{2}s] is the mass flux.

The perpendicular cross-sectional flow area for a circular tube can be defined as:

$$A_{ff} = \pi r^2 \tag{16}$$

Where r [m] refers to the inner radius of the tube.

3.3 Heat transfer

The heat flux, $\dot{Q}_{flux}$ [W/m^2], can be defined as, (Incropera, et al., 2013):

$$\dot{Q}_{flux} = \frac{\dot{Q}}{A_{heat\ transfer}} \tag{17}$$

Where $A_{heat\ transfer}$ [m^2] is the area perpendicular to the heat transfer direction. For a fluid flowing in a circular tube exchanging heat through the tube wall, the heat transfer area at the inner wall is defined as:

$$A_{heat\ transfer} = A_{wall} = 2\pi rL \tag{18}$$

Where L [m] is the length of the tube.

3.4 Wall and film temperatures

3.4.1 Wall temperature

For a fluid flowing in a circular tube, the wall temperature can be determined using, (Incropera, et al., 2013):

$$\dot{Q} = \frac{\Delta T}{R_{tot}} \tag{19}$$

With ΔT [K or °C] the temperature difference of the fluid at the tube wall and the bulk and where R_{tot} [K/W] is the total thermal resistance between these two points. This equation can also be written as:

$$T_w = \dot{Q}R_{tot} + T_b \tag{20}$$

Where T_b [K] and T_w [K] refers to the bulk and wall temperature, respectively. From here on the subscripts 'b' and 'w' will refer to properties as calculated at the bulk or wall temperature. The total thermal resistance between the bulk of the fluid and the tube wall can defined by:

$$R_{tot} = R_{convection} + R_{fouling} \tag{21}$$

Where $R_{convection}$ is the thermal resistance due to convection and $R_{fouling}$ is the resistance if fouling is present. The resistance due to convection can be defined as, (Incropera, et al., 2013):

$$R_{convection} = \frac{1}{\eta_o h_c A_{wall}} \tag{22}$$

With η_o [-] the overall surface efficiency ($\eta_o = 1$ for a surface without fins such as flow in a circular tube) and h_c [W/m^2-K] the convection heat transfer coefficient. If fouling is present, the thermal resistance it introduces can be defined by:

$$R_{fouling} = \frac{R_{foul}}{\eta_o A_{wall}} \tag{23}$$

Where R_{foul} [m^{2}K/W] is the fouling factor.

3.4.2 Film temperature

The film temperature can be calculated using the following equation:

$$T_f = \frac{T_b + T_w}{2} \tag{24}$$

For the remainder of this study the subscript 'f' will imply a thermodynamic property calculated at the film temperature.

3.5 Non-dimensional parameters

In this section, the relevant non-dimensional parameters for this study are discussed. This is based on the work of Incropera et al. (2013), Rousseau (2013) and Munson et al. (2013). This includes the Nusselt number, the Reynolds number and the Prandtl number.

3.5.1 Nusselt number

The Nusselt number gives a representation of the non-dimensional temperature gradient at the surface. This value gives an indication of the heat being transferred for a certain flow arrangement. The Nusselt number can be described by:

$$Nu = \frac{h_c L_{ch}}{k} \tag{25}$$

With Nu [-] being the Nusselt number, L_{ch} [m] the characteristic length and k [W/m-K] the thermal conductivity of the fluid. For flow within a pipe or duct, the Nusselt number can be written as:

$$Nu = \frac{h_c D_H}{k} \tag{26}$$

With D_H [m] the hydraulic diameter defined by:

$$D_H = \frac{4A_{ff}}{P_w} \tag{27}$$

Where P_w [m] is the wetted perimeter.

3.5.2 Prandtl number

The Prandtl number gives an indication of the ability of a fluid to transport momentum through the velocity boundary layer versus the fluid's ability to transport energy through the thermal boundary layer. The Prandtl number is defined by:

$$Pr = \frac{\nu}{\alpha} = \frac{c_p \mu}{k} \tag{28}$$

Where c_p [J/kg-K] is the specific heat at a constant pressure process and μ [Ns/m^2] is the dynamic viscosity. The momentum diffusivity is defined by $\nu = \frac{\mu}{\rho}$ [m^2/s] and the thermal diffusivity by $\alpha = \frac{k}{\rho c_p}$ [m^2/s].

3.5.3 Reynolds number

The ratio between the inertial and viscous forces found in the velocity boundary layer is defined by the Reynolds number:

$$Re = \frac{\rho V L_{ch}}{\mu} \tag{29}$$

For pipe or duct flow, the Reynolds number can be evaluated as:

$$Re = \frac{G D_H}{\mu} = \left| \frac{\dot{m} D_H}{\mu A_{ff}} \right| \tag{30}$$

Nusselt number correlations are usually a function of the Reynolds and Prandtl numbers when forced convection in a turbulent flow is present.

3.6 Nusselt number correlations

The Nusselt number correlations used in this study are reported within this section. The following correlations are for general flow conditions.

3.6.1 Dittus & Boelter (1930)

The Dittus & Boelter (1930) correlation is accurate for a wide variety of flow conditions and fluids. It can be described by:

$$Nu_{D\&B} = 0.023 Re_b^{0.8} \mathrm{Pr_b^n} \tag{31}$$

With n defined by:

$$n = \begin{cases} 0.4 \;\; when \;\; \dfrac{T_w}{T_b} > 1 \\ 0.3 \;\; when \;\; \dfrac{T_w}{T_b} < 1 \end{cases}$$

It should be noted, $n = 0.3$ for a fluid in cooling.

3.6.2 Gnielinski (1976)

The Nusselt number correlation defined by Gnielinski (1976):

$$Nu_G = \frac{\frac{f_{fil}}{8}(Re_b - 1000)Pr_b}{1.07 + 12.7\sqrt{\frac{f_{fil}}{8}}\left(Pr_b^{\frac{2}{3}} - 1\right)} \tag{32}$$

A modified Nusselt number correlation, with a greater accuracy, defined by Gnielinski (1976):

$$Nu_{G,M} = \frac{f_{fil}}{8}(Re_b - 1000)Pr_b \left[1.07 + 12.7\sqrt{\frac{f_{fil}}{8}}\left(Pr_b^{\frac{2}{3}} - 1\right)\right]^{-1} \left[1 + \left(\frac{D_H}{L}\right)^{\frac{2}{3}}\right] \tag{33}$$

With f_{fil} [-] the Filonenko friction factor defined as:

$$f_{fil} = (1.82 log Re_b - 1.64)^{-2} \tag{34}$$

The following correlations are developed for the cooling of oil-free supercritical carbon dioxide.

3.6.3 Yoon *et al.* (2003)

Based on the Dittus & Boelter (1930) correlation and accounting for the density variation between the pseudocritical (defined in Section 2.2) and bulk temperature, Yoon *et al*. (2003) proposed a correlation defined by:

$$Nu_Y = 0.013 Re_b Pr_b^{-0.05} \left(\frac{\rho_{pc}}{\rho_b}\right)^{1.6} \quad if \quad \frac{T_b}{T_{pc}} \leq 1 \tag{35}$$

And:

$$Nu_Y = 0.14 Re_b^{0.69} Pr_b^{0.66} \quad if \quad \frac{T_b}{T_{pc}} > 1 \tag{36}$$

Where T_{pc} [K] is the pseudocritical temperature and ρ_{pc} [kg/m^3] refers to the density as evaluated at the pseudocritical temperature. For the remainder of this study the subscript 'pc' will imply a thermodynamic property calculated at the pseudocritical temperature.

3.6.4 Pitla *et al.* (2002)

The correlation by Pitla *et al.* (2002) uses the mean of Gnielinski (1976) calculated at the wall and bulk temperature, together with a correction factor. The correlation can be defined by:

$$Nu_P = \left(\frac{Nu_{G,w} + Nu_{G,b}}{2}\right) \frac{k_w}{k_b} \tag{37}$$

This correlation accounts for the variation in thermo-physical properties between the bulk and wall temperature to deliver more accurate results than Gnielinski (1976).

3.6.5 Dang & Hihara (2004)

Dang & Hihara (2004) published a Nusselt number correlation, which takes the variation of thermo-physical properties at the bulk, film and wall temperature into account. The correlation is described by:

$$Nu_{D\&H} = \frac{(f_{fil,f}/8)(Re_b - 1000) Pr_{D\&H}}{1.07 + 12.7\sqrt{f_{fil,f}/8}\left(Pr_{D\&H}^{2/3} - 1\right)} \tag{38}$$

Where $f_{fil,f}$ [-] refers to the Filonenko friction factor calculated using a Reynolds number with properties evaluated at the film temperature:

$$f_{fil,f} = \left(1.82 log Re_f - 1.64\right)^{-2} \tag{39}$$

The Prandtl number, $\mathrm{Pr}_{D\&H}$ [-], is defined by:

$$Pr_{D\&H} = \begin{cases} \frac{c_{p_b}\mu_b}{k_b} \; when \; c_{p_b} \geq \overline{c_p} \\ \frac{\overline{c_p}\mu_b}{k_b} \; when \; c_{p_b} < \overline{c_p} \;\; and \;\; \frac{\mu_b}{k_b} \geq \frac{\mu_f}{k_f} \\ \frac{\overline{c_p}\mu_f}{k_f} \; when \; c_{p_b} < \overline{c_p} \;\; and \;\; \frac{\mu_b}{k_b} < \frac{\mu_f}{k_f} \end{cases} \quad (40)$$

The integrated specific heat, $\overline{c_p}$ [J/kg-K], calculated in the radial direction is defined by:

$$\overline{c_p} = \frac{h_b - h_w}{T_b - T_w} \quad (41)$$

When the convection coefficient is evaluated, the thermal conductivity is calculated at the film temperature instead of at the bulk temperature so that:

$$Nu_{D\&H} = \frac{h_{c,D\&H} D_H}{k_f} \quad (42)$$

3.6.6 Zhao & Jiang (2011)

Using the modified Gnielinski (1976) correlation as a basis, Zhao & Jiang (2011) developed the following prediction correlation:

$$Nu_{Z\&J} = \frac{f_{fil}}{8}(Re_b - 1000)Pr_b \left[1.07 + 12.7\sqrt{\frac{f_{fil}}{8}}\left(Pr_b^{\frac{2}{3}} - 1\right)\right]^{-1} \left[1 + \left(\frac{D_H}{L}\right)^{\frac{2}{3}}\right] C_{vp} \quad (43)$$

Where the property variation coefficient, C_{vp} [-], is defined by:

$$C_{vp} = \begin{cases} 0.93\left(\frac{Pr_w}{Pr_b}\right)^{-0.11}\left(\frac{\overline{c_{p_t}}}{c_{p_b}}\right)^{0.96}\left(\frac{\rho_w}{\rho_b}\right)^{1.06} & when \;\; \frac{T_b}{T_{pc}} \leq 1 \\ 1.07\left(\frac{T_w}{T_b}\right)^{-0.45}\left(\frac{\overline{c_{p_t}}}{c_{p_b}}\right)^{0.61}\left(\frac{\rho_w}{\rho_b}\right)^{-0.18} & when \;\; \frac{T_b}{T_{pc}} > 1 \end{cases} \quad (44)$$

The mean specific heat value over the test section, $\overline{c_{p_t}}$ [J/kg-K], is defined by:

$$\overline{c_{p_t}} = \frac{h_i - h_e}{T_i - T_e} \quad (45)$$

This correlation takes the variation between the thermo-physical properties at the wall and bulk temperatures into account. It also takes into account the variation between the specific heat value and the mean specific heat value.

The next section reports Nusselt number correlations for oil-contaminated refrigerants in a condensation process.

3.6.7 Oil-contaminated refrigerants in a condensation process

A correlation developed for oil-contaminated refrigerants in a condensation process is defined by, (Tincky, et al., 1985):

$$\frac{h_{c,oil-refrigerant}}{h_{c,refrigerant}} = e^{a\omega} \tag{46}$$

Where $h_{c,oil-refrigerant}$ [W/m^2-K], is the convection coefficient predicted for oil-contaminated refrigerants, $h_{c,refrigerant}$ [W/m^2-K] is the convection coefficient predicted for oil-free refrigerants and ω [-] is the oil concentration in the flow. This correlation adjusts a convection coefficient predicted for oil-free conditions, $h_{c,refrigerant}$, by using Euler's number $(e \approx 2.71828)$. The constant, a, is reported as -5.0 by Tricky et al. (1985) when using R12 and 300 SUS naphthenic base oil. Schlager et al. (1990) used a value of -3.2 for R22 with 150/300 SUS oil and Bassi and Bansal (2003) suggested a value of -2.2 for R134a with polyol ester oil.

The next section reports a Nusselt number correlation for oil-contaminated supercritical carbon dioxide in cooling.

3.6.8 Zhao *et al.* (2011)

The correlation by Zhao *et al*. (2011) was developed specifically for oil-contaminated supercritical carbon dioxide in cooling. It uses the convection coefficient calculated from the correlation by Dang & Hihara (2004), $h_{c,D\&H}$, and adjusts it with an oil compensation term containing a coefficient, a density ratio and a viscosity ratio. This correlation can be defined by:

$$h_{c,Z} = h_{c,D\&H}\left(1.186\left(\frac{\rho_{oil}}{\rho_{CO_2}}\right)^{-0.236}\left(\frac{\omega\mu_{oil}}{\mu_{CO_2}}\right)^{-0.114}\right) \quad if \quad \frac{T_b}{T_{pc}} \leq 1 \tag{47}$$

And:

$$h_{c,Z} = h_{c,D\&H}\left(0.764\left(\frac{\rho_{oil}}{\rho_{CO_2}}\right)^{0.53}\left(\frac{\omega\mu_{oil}}{\mu_{CO_2}}\right)^{-0.227}\right) \quad if \quad \frac{T_b}{T_{pc}} > 1 \tag{48}$$

The subscripts 'oil' and 'CO_2' refers to the properties of either the oil or carbon dioxide as evaluated at the bulk temperature. The density of the oil can be calculated with the following equation, (Conde, 1996):

$$\rho_{oil} = \rho_{oil,ref} - 0.6\,(T - T_{ref}) \tag{49}$$

With $\rho_{oil,ref}$ [kg/m^3] the density at a reference temperature, T_{ref} [K]. The oil concentration, ω [-], in the carbon dioxide can be defined with the following equation:

$$\omega = \frac{\dot{m}_{oil}}{\dot{m}_{oil}+\dot{m}_{CO2}} \tag{50}$$

3.7 Statistical concepts

The statistical concepts used in this study are:

- Mean/average
- Relative error
- Average absolute error
- Sum of absolute errors

These statistical concepts are used to evaluate the predicted convection coefficients in this study. The concepts in this section are based on the work of Fang et al. (2013):

3.7.1 Mean

The mean or average, $\bar{x}$, is the sum of numerical values in a sample divided by the number of values within that sample, n:

$$\bar{x} = \frac{1}{n}\sum_{i=1}^{n} x_i \tag{51}$$

Where x_i refers to the $i'th$ numerical value of the sample.

3.7.2 Relative error

The relative error gives a measure of the over or under prediction of a value. The relative error is defined by:

$$E = \frac{x_{i,pred}-x_{i,real}}{x_{i,real}} \tag{52}$$

Where the subscripts $real$ and $pred$ refers to the $i'th$ real and predicted values, respectfully.

3.7.3 Average absolute error

The average absolute error gives a measure of the prediction accuracy. This is defined by:

$$|\bar{E}| = \frac{1}{n}\sum_{i=1}^{n}\left|\frac{x_{i,pred}-x_{i,real}}{x_{i,real}}\right| \tag{53}$$

Where n refers to the number of data points.

3.7.4 Sum of absolute errors

The sum of the absolute relative errors is defined by:

$$\sum|E| = \sum_{i=1}^{n} \left| \frac{x_{i,pred} - x_{i,real}}{x_{i,real}} \right| \quad (54)$$

3.8 Summary

In this section, the necessary theory to calculate the predicted convection coefficients in this study was reported. This included the fundamental principles and formulas needed to evaluate a Nusselt number correlation. The Nusselt number correlations used within this study were then reported. Finally, the statistical concepts to evaluate the predicted convection coefficients were discussed. In the next chapter, a performance consistency evaluation of the correlation published for oil-contaminated supercritical carbon dioxide in cooling will be reported.

CHAPTER 4 CORRELATION EVALUATION

In Chapter 3, the theoretical background needed for this study was described in detail. In this chapter, the correlations published to predict the convection coefficients of oil-contaminated supercritical carbon dioxide during cooling are evaluated on data from literature. However, only one correlation, by Zhao et al. (2011) (Section 3.6.8), was found in literature specifically developed for this type of flow. This correlation will be tested against published data and the performance consistency will be evaluated. The following section reports the published data used for this chapter.

4.1 Experimentally based data obtained from literature

The data for oil-contaminated supercritical carbon dioxide during cooling used in this chapter are published by Dang et al. (2007). In this study, PAG-type (PAG100) oil was used. The test section was a 0.5m long horizontal counter flow tube-in-tube heat exchanger with the carbon dioxide flowing inside the inner tube and water flowing in the annulus. The inner pipe was made out of smooth copper, which has a high thermal conductivity and allows heat to transfer effectively. The outer tube was made out of acrylic with a 25 mm thick polystyrene insulation covering it to minimize heat transfer to the environment.

In Figure 7 (a-f), the experimentally calculated convection coefficients ($h_{c,exp}$) as a function of temperature for the test data are shown for different oil concentrations. The test data include the measured inlet (T_i) and outlet bulk temperatures (T_e) of the carbon dioxide, as well as the experimentally calculated convection coefficients from the measured test parameters. The inner diameter of the inner tube ($d_{in} = d$), the inlet pressure of the carbon dioxide ($p_i = P$), the mass flux of the carbon dioxide (G) and the desired heat flux between the carbon dioxide and the water ($\dot{Q}_{flux} = q_w$) are also given.

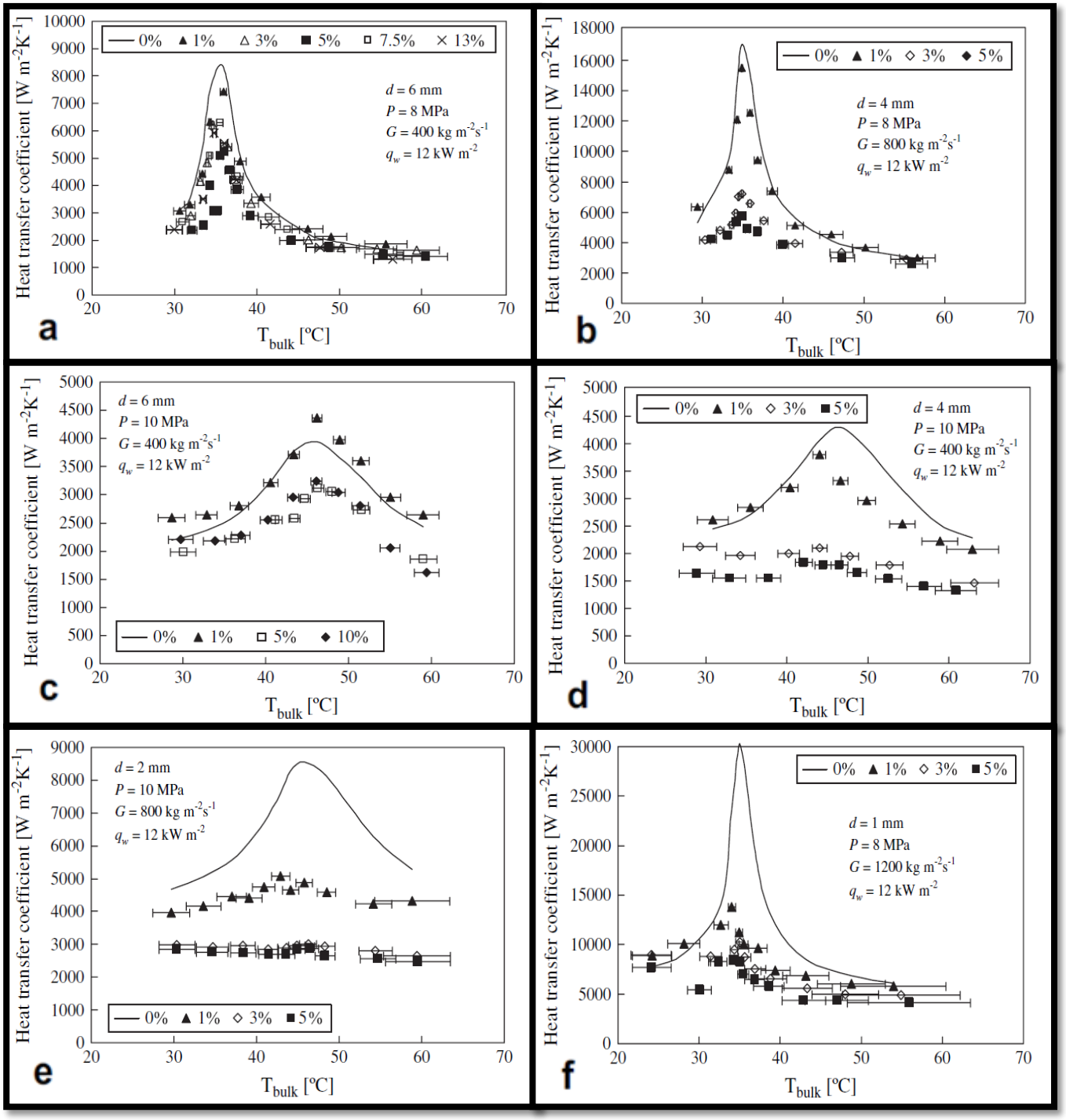

Figure 7 Published data for oil-contaminated supercritical carbon dioxide in cooling, (Dang, et al., 2007)

In Figure 7 (a-f), 189 individual test results are given. As reported by Dang et al. (2007), unlike conventional bar-error representations, each experimental test is represented by a horizontal error bar. Where the right hand side of the horizontal error bar indicates the inlet temperature of the carbon dioxide at the gas cooler and where the left hand side refers to the outlet temperature. The curve is an analytically representation when Dang & Hihara (2004)'s correlation is implemented for oil-free conditions. Refer to Appendix A for more details. It can be seen in Figure 7 that the addition of oil into the carbon dioxide has a negative effect on the

convection. Appendix B contains another data set by Zhao et al. (2011) that will be used as a second set in this study.

The data of Dang et al. (2007) can now be used for the evaluation of Zhao et al. (2011)'s correlation. The following section discusses the method to compute the predicted convection coefficients.

4.2 Method to calculate predicted convection coefficients

To calculate the predicted convection coefficients of a correlation for an experimental data set, certain assumptions are made which simplify the calculations.

4.2.1 Assumptions

The assumptions for the calculations are:

I. Steady-state flow conditions are present.
II. The effects of pressure drops are assumed negligible. This is because the pressure drop over the test sections are relatively small compared to the operating pressure ($p_0 \gg \Delta p_{0L}$).
III. No elevation changes are present for the gas cooler ($z_e - z_i = 0$).
IV. The total pressure can be assumed to represent the static pressure ($p_0 \approx p$), as the difference between these values at the high pressures used within this study is negligible.
V. The total enthalpy can also be assumed to represent the static enthalpy ($h_0 \approx h$) as the dynamic pressure has a negligible effect on the total enthalpy at these conditions.

Based on these assumptions, the method of calculating the predicted convection coefficients can now be discussed. This is reported in the next section.

4.2.2 Method of Calculations

The calculation method discussed in this section, is to compute the predicted/theoretical convection coefficients on the carbon dioxide side of the gas cooler using the measured parameters of an experimental data set. The method of calculation is described by the following:

I. Use the measured values from an experimental test as the input parameters. Inputs include the small tube's inner diameter ($d_{in} = d$), the inlet pressure ($p_i = P$), mass flux (G) and the inlet (T_i) and outlet bulk temperatures (T_e).
II. The mass flow rate of the carbon dioxide can be determined using equation 15 with the free flow area (A_{ff}) calculated by equation 16.

III. The enthalpy (h) at the inlet and outlet can be determined as a function of the pressure and temperature at these points. Now that the mass flow rate and enthalpy at the inlet and outlet are known, the heat transfer rate ($\dot{Q}$) can then be calculated from the conservation of energy (equation 13). The heat flux ($\dot{Q}_{flux}$) can then be calculated from equation 17 with the heat transfer area ($A_{heat\ transfer}$) from equation 18.

IV. Using the heat transfer rate and the average between the inlet and the outlet temperatures as the bulk temperature (T_b), the wall temperature (T_w) can be calculated with equation 20 by incorporating equations 21 to 23. *Note: to evaluate* equation *22 the predicted/theoretical convection coefficient is needed. This however is the objective of these calculations. This can be solved simultaneously within the software package used. In addition, the fouling factor for equation 23 can be obtained from the software package.*

V. With the wall temperature known, the film temperature can be calculated with equation 24. *When thermodynamic properties at the wall or film are needed. These properties can be evaluated by using the temperature at either the wall or the film together with the pressure. This also holds true for properties that needs to be evaluated at the pseudocritical temperature (see Section 2.2).*

VI. From here on the Prandtl and Reynolds numbers can be calculated using equation 28 and equation 30. The hydraulic diameter needed for the Reynolds number can be obtained with equation 27, which reduces to the diameter for a circular tube.

VII. The Prandtl and Reynolds numbers together with certain properties at the wall, film and pseudocritical temperatures are now known. From this, a Nusselt number can be calculated from an empirical correlation.

VIII. With the Nusselt number known, the theoretical/predicted convection coefficient can be calculated with equation 25.

The correlation of Zhao et al. (2011) requires the evaluation of the oil's density and viscosity. The following section discusses the property evaluation of the oils used within this study.

4.2.3 Oil properties

The method of obtaining the density and viscosity of the oils used within this study are presented in this section. *Note: the oil used for the experimental tests of Dang et al. (2007) is PAG100 oil (polyalkylene glycol oil or PAG-oil) while Zhao et al. (2011) used POE solest-68 oil (polyol ester oil or POE-oil).*

(a) Density

The densities of the oils used within this study, i.e. PAG100 and POE solest-68, are calculated using equation 49. Note from equation 49 that a reference temperature and density are required. For PAG100, the density at a reference temperature of 15℃ is 996kg/m^3, (Schmierstoffe, 2009). For POE solest-68 the density at a reference temperature of 15℃ is 957kg/m^3, (CPI Engineering Services, 2009).

(b) Dynamic viscosity

To determine the viscosity of the oils, viscosity graphs are used. The viscosity as a function of temperature for PAG-oil (PAG100) and POE-oil (solest-68) can be seen in Appendix C. A polynomial regression, based on the least squares method, can be obtained for both oils:

$$\mu_{PAG100} = a_{PAG} + b_{PAG}T + c_{PAG}T^2 + d_{PAG}T^3 + e_{PAG}T^4 \tag{55}$$

$$\mu_{POE_{solest68}} = a_{POE} + b_{POE}T + c_{POE}T^2 + d_{POE}T^3 + e_{POE}T^4 \tag{56}$$

Where T [℃] is the temperature of the oil and the regressed coefficients are reported in Table 4:

Table 4 Coefficients for viscosity correlations of PAG100 and POE solest-68 oil

Oil	$a\left[\frac{Ns}{m^2}\right]$	$b\left[\frac{Ns}{m^2℃}\right]$	$c\left[\frac{Ns}{m^2℃^2}\right]$	$d\left[\frac{Ns}{m^2℃^3}\right]$	$e\left[\frac{Ns}{m^2℃^4}\right]$
$PAG100$	$3.17\text{x}10^{-1}$	$-8.48\text{x}10^{-3}$	$1.01\text{x}10^{-4}$	$-6.22\text{x}10^{-7}$	$1.59\text{x}10^{-9}$
$POE\ solest\ 68$	0.41	-0.01	$1.98\text{x}10^{-4}$	$-1.17\text{x}10^{-6}$	$2.37\text{x}10^{-9}$

In the next section, a comparison between the results of Zhao et al. (2011)'s correlation on their own and on Dang et al. (2007)'s data is reported. The performance consistency between the two separate data sets will then be evaluated.

4.3 Evaluation of Zhao et al. (2011)'s correlation

In this section, the accuracy and performance consistency of the correlation published by Zhao et al. (2011) are evaluated on published data. As previously stated, this correlation is the only one found in literature specifically developed for the cooling of oil-contaminated supercritical carbon dioxide.

As reported by Zhao et al. (2011), this correlation predicted 90% of the convection coefficients of their own data with an absolute error below 20%. The percentage of convection coefficients predicted with an absolute error below 20% will be used as a benchmark throughout this study to compare various correlations. The predicted ($h_{c,Z}$) versus experimentally calculated ($h_{c,exp}$) convection coefficients are shown in Figure 8:

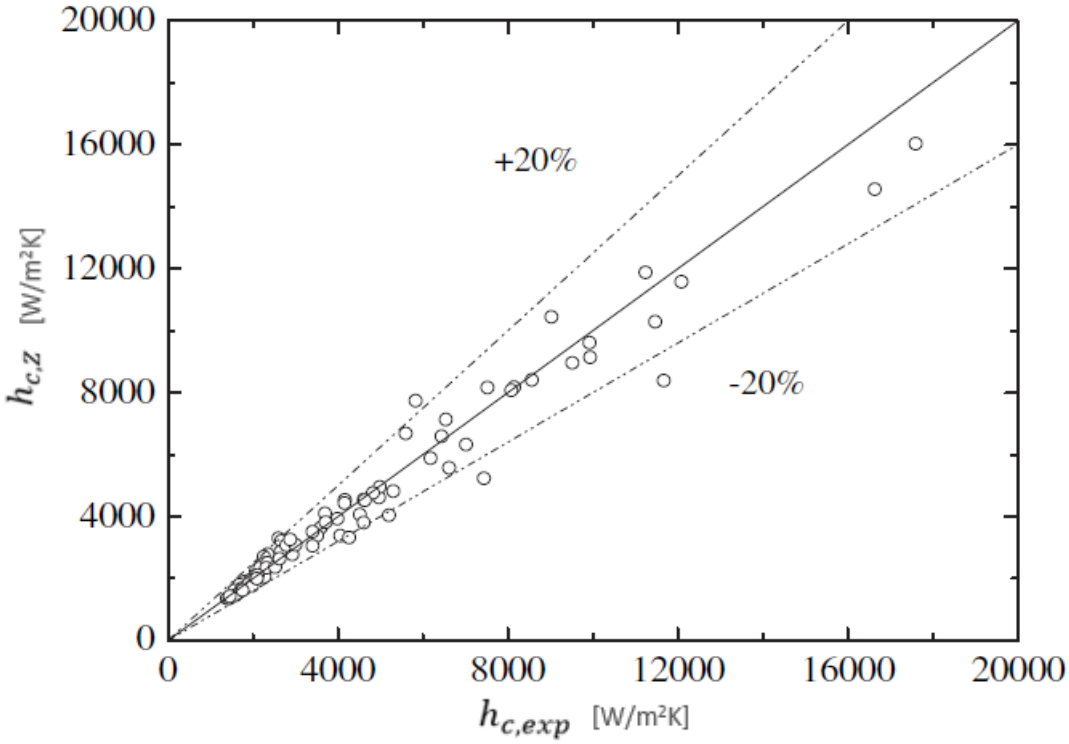

Figure 8 Predicted versus experimentally calculated convection coefficients of Zhao et al. (2011)'s correlation on their own data, Zhao et al. (2011).

When this correlation is evaluated against the data of Dang et al. (2007), it is reported that 39.7% of the predicted coefficients have an absolute error less than 20%. The predicted versus experimentally calculated convection coefficients on Dang et al. (2007)'s data is shown in Figure 9. It can be seen that more convection coefficients are outside of the ±20% deviation region, compared to Figure 8. Refer to Appendix D for detailed calculations and results.

The correlation of Zhao et al. (2011) predicts 90% of their own data with an absolute error of less than 20%. However, when applied to Dang et al. (2007)'s data it only predicts 39.7% within this range. This correlation's accuracy is not consistent between the data sets used. It should be noted however, that lower oil concentrations are used for Zhao et al. (2011)'s data (1% and 2% oil), whereas much higher oil concentrations (typically 1%, 3% and 5% oil and for single cases 7,5%, 10% and 13% oil) are used within the data of Dang et al. (2007). This may be the reason that less

accurate results are obtained on Dang et al. (2007)'s data, because the data used to develop the correlation are for small percentages oil. In addition, this correlation is more complex than most correlations from literature reported in Section 3.6. This is mainly because Zhao et al. (2011) uses the convection coefficient of Dang & Hihara (2004) in their correlation. Typically, a more complex correlation is not always applicable over a wide range of applications outside the parameters used to develop it.

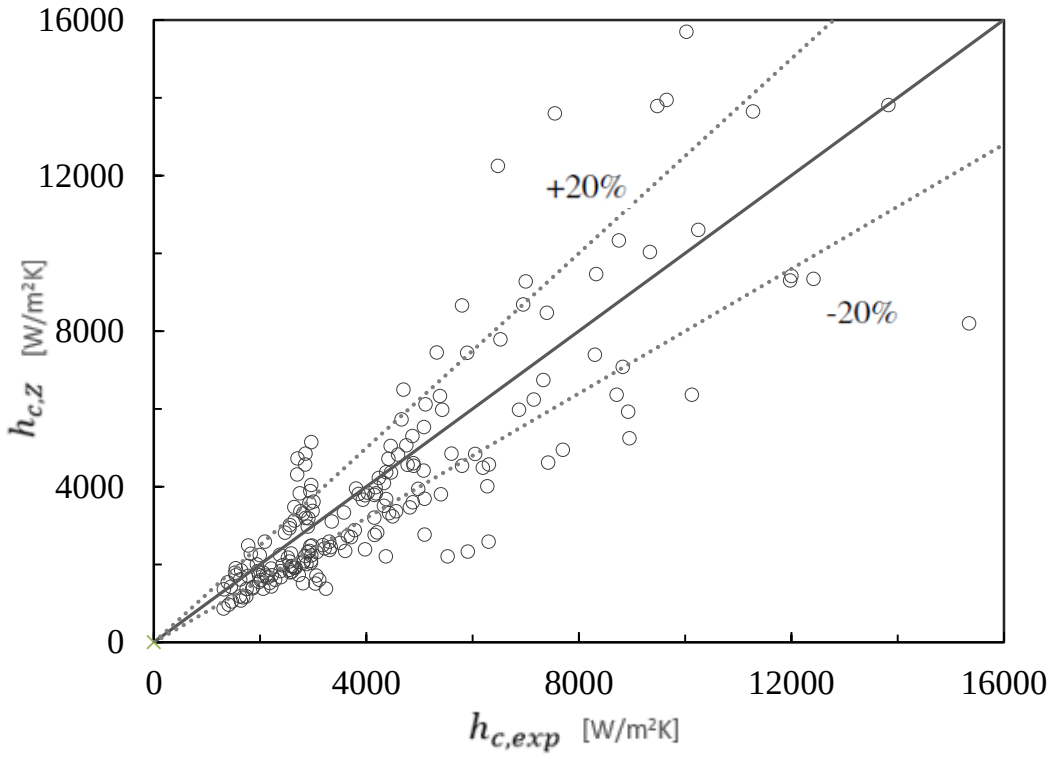

Figure 9 Predicted versus experimentally calculated convection coefficients of Zhao et al. (2011)'s correlation on Dang et al. (2007)'s data.

4.4 Conclusion

In this chapter, the performance consistency of the correlation by Zhao et al. (2011) was evaluated. It was reported that it predicted 90% of the convection coefficients of Zhao et al. (2011)'s data with an absolute error less than 20%, whilst 39.7% of the coefficients were predicted for Dang et al. (2007) within this range. The accuracy of this correlation is not consistent between the two data sets. Based on the results, a new correlation to improve on the performance consistency of Zhao et al. (2011)'s correlation must be investigated. Furthermore, it will be investigated whether the new correlation can deliver results that are more consistent but also have a simpler form than Zhao et al. (2011)'s correlation. However, because of the limited number of correlations found developed specifically for the cooling of oil-contaminated supercritical carbon dioxide, different correlations published for similar flow conditions will firstly be

investigated. This will give an indication of the accuracy and consistency of these correlations, which may form a basis for the development of a new correlation.

CHAPTER 5 INVESTIGATION OF ALTERNATIVE CORRELATIONS

In Chapter 4, the published data sets used for this study was discussed and an evaluation of Zhao et al. (2011)'s correlation was done. It was reported that this correlation is not consistent between the data sets and that a more consistent correlation should be investigated. However, due to the limited number of correlations published for oil-contaminated supercritical carbon dioxide in cooling, alternative correlations developed for similar flow conditions will firstly be evaluated. The results can then be compared to Zhao et al. (2011)'s correlation and may form a basis for the development of a new correlation.

5.1 Evaluation of alternative correlations for similar flow conditions

In this section, the alternative correlations are evaluated to predict the experimentally calculated convection coefficients of Dang et al. (2007)'s and Zhao et al. (2011)'s data. These alternative correlations, discussed in more detail in the literature survey, include those developed for both general flow conditions and for oil-free supercritical carbon dioxide in cooling. The general flow correlations to be evaluated are Dittus & Boelter-1930 ($D\&B$), Gnielinski-1976 (G) and modified Gnielinski-1976 (G,M) as reported in Sections 3.6.1 and 3.6.2. The oil-free supercritical carbon dioxide cooling correlations include Yoon et al.-2003 (Y), Pitla et al.-2002 (P), Dang & Hihara-2004 ($D\&H$) and Zhao & Jiang-2011 ($Z\&J$), presented in Sections 3.6.3 to 3.6.6. The detailed calculations and results for these correlations are provided in Appendix E, with the following table showing the percentage convection coefficients predicted with an error less than 20%.

Table 5 Percentage convection coefficients predicted with absolute error less than 20% for alternative correlations.

	$D\&B$	G	G,M	Y	P	$D\&H$	$Z\&J$
On Dang et al. (2007)'s data	44.4	47.6	46	4.8	39.2	29.6	39.2
On Zhao et al. (2011)'s data	59.5	39.2	38	0	25.3	20.3	30.4
On both data sets	**48.9**	**45.2**	**43.7**	**3.4**	**35.1**	**26.9**	**36.6**

From the results in Table 5, the most accurate correlation on Dang et al. (2007)'s data is Gnielinski (1976) with 47.6% of the coefficients predicted under an absolute error of 20%. This correlation is followed closely by the modified Gnielinski (1976) and Dittus & Boelter (1930) with 46% and 44.4%, respectively. On Zhao et al. (2011)'s data the most accurate correlation is Dittus & Boelter

(1930) with 59.5%. This is followed by 39.2% for Gnielinski (1976) and 38% for the modified Gnielinski (1976).

The best (most consistent) performing correlation on both sets is Dittus & Boelter (1930) with 48.9% of the coefficients predicted with an absolute error less than 20%. When compared to the results of Zhao et al. (2011)'s correlation (Section 4.3), Dittus & Boelter (1930) reports a much more consistent performance between the two data sets, whilst still being comparably accurate. As stated, it predicts 44.4% of Dang et al. (2007)'s data with an absolute error of less than 20% and 59.5% on Zhao et al. (2011)'s data (15.1% difference between sets). This is in contrast with the results of Zhao et al. (2011)'s correlation: 39.7% on Dang et al. (2007)'s data and 90% on Zhao et al. (2011)'s data (50.3% difference). Dittus & Boelter (1930) reports an increase in accuracy on Dang et al. (2007)'s data, whilst a slight decrease is noted on Zhao et al. (2011)'s data. However, this correlation's performance is much more consistent over the data sets compared to Zhao et al. (2011)'s correlation. It can then be expected that Dittus & Boelter (1930) will have a more consistent performance on a wider range of test conditions than Zhao et al. (2011)'s correlation, which may be more data specific. In addition, Dittus & Boelter (1930) is a much simpler correlation than Zhao et al. (2011), which makes it easier to apply and which may be more applicable to a wider range of data. From the results, Dittus & Boelter (1930) is an improvement on Zhao et al. (2011)'s correlation. This correlation is the best alternative for Zhao et al. (2011)'s correlation in this section.

Further remarks on results

In general, the alternative correlations' accuracies decreases as the oil concentration increases as seen in Table 6 for ranges between 1% and 5% oil contamination of Dang et al. (2007)'s data. This trend can be expected as the correlations were developed for oil-free conditions.

Table 6 Percentage coefficients predicted with absolute error less than 20% at different oil concentrations on Dang et al. (2007).

ω [%]	$D\&B$	G	G,M	Y	P	$D\&H$	$Z\&J$
1	46.2	63.5	65.4	11.5	48.1	51.9	55.8
3	43.5	32.6	28.3	2.2	28.3	19.6	23.9
5	25	18.6	16.7	2.1	12.5	6.25	14.6

From this table, it is noted that Dittus & Boelter (1930) is more consistent over the different oil concentrations, especially between 1% and 3% oil, compared to the other correlations.

During the evaluation of the alternative correlations, inaccuracies were observed when predicting conditions at the pseudocritical temperature. For some correlations, a curve that has a similar shape than the data curve was predicted; whilst for other correlations this was not seen. This can be seen in Figure 10 within the rectangles.

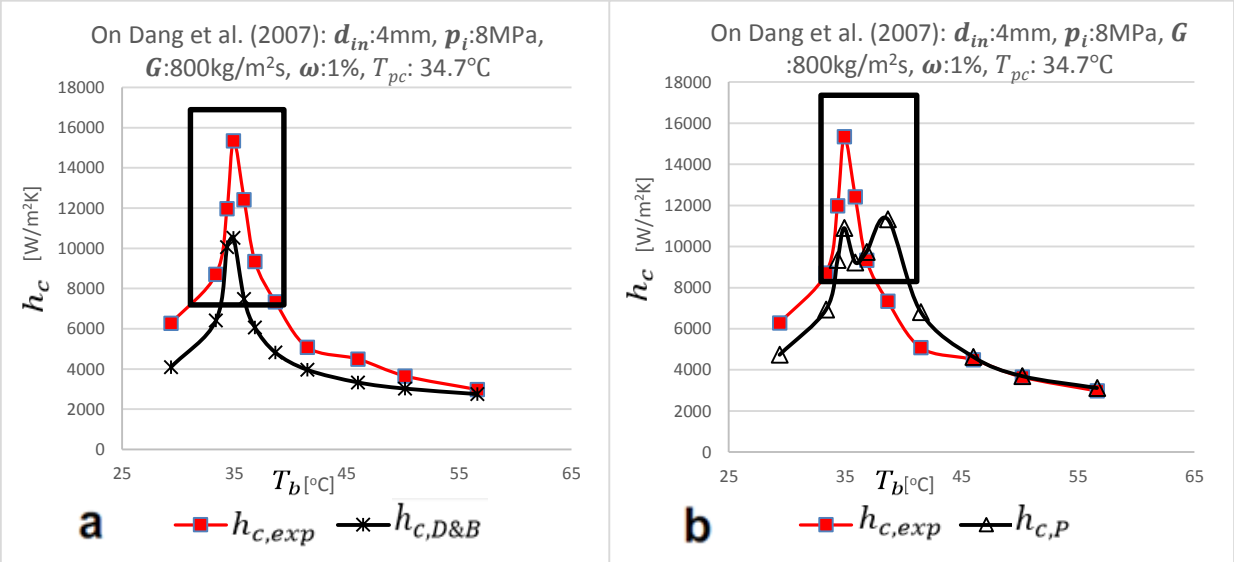

Figure 10 a) Similar shape as data using Dittus & Boelter (1930). b) Dissimilar shape than data using Pitla et al. (2002).

The correlations predicting similar shaped curves than the data curves at the pseudocritical temperature for all cases are: Dittus & Boelter, Gnielinski, modified Gnielinski and Zhao & Jiang.

In this section, it was reported that Dittus & Boelter (1930) showed an improvement on the correlation of Zhao et al. (2011). Dittus & Boelter (1930) reports a more consistent performance and is a much simpler correlation. The correlations in this section were developed for oil-free conditions. In the following section, the focus will be to see if these correlations can be enhanced to take the effect of oil contamination into account.

5.2 Enhancement of alternative correlations to include the effects of oil contamination

In the previous section, alternative correlations developed for similar flow conditions were evaluated to predict the convection coefficients of the data sets. Even though these correlations were developed for oil-free conditions, the correlations such as Dittus & Boelter (1930) showed an improvement on the performance consistency of Zhao et al (2011)'s correlation. Oil contamination reduces the convection coefficients with the largest reduction at the pseudocritical temperature. In this section, it is attempted to enhance the alternative correlations to take the effect of oil contamination to account.

The correlation by Zhao et al. (2011), Section 3.6.8, uses the convection coefficient predicted by Dang & Hihara (2004), $h_{c,D\&H}$, and adjusts it with an oil compensation term to obtain $h_{c,Z}$. For this

section, this same approach will be followed by applying the oil compensation terms of Zhao et al. (2011) to the alternative correlations and evaluating the effects thereof. To enhance the alternative correlations with the oil compensation terms, the following equations are used for this section:

$$h_{c,comp} = h_c \left(1.186 \left(\frac{\rho_{oil}}{\rho_{CO_2}} \right)^{-0.236} \left(\frac{\omega \mu_{oil}}{\mu_{CO_2}} \right)^{-0.114} \right) \; if \; \frac{T_b}{T_{pc}} \leq 1$$

And:

$$h_{c,comp} = h_c \left(0.764 \left(\frac{\rho_{oil}}{\rho_{CO_2}} \right)^{0.53} \left(\frac{\omega \mu_{oil}}{\mu_{CO_2}} \right)^{-0.227} \right) \; if \; \frac{T_b}{T_{pc}} > 1$$

Where h_c is the convection coefficient determined from one of the alternative correlations in the previous section and $h_{c,comp}$ is the convection coefficient adjusted to compensate for the effect of oil. The detailed calculations and results for each of the enhanced correlations are reported in Appendix F, with a summary given in Table 7. *Note: 'compensated' or 'comp' refers to a correlation enhanced by the oil compensation terms of Zhao et al. (2011).*

Table 7 Percentage convection coefficients predicted with absolute error less than 20% for enhanced alternative correlations.

	$D\&B, comp$	$G, comp$	$G, M, comp$	$Y, comp$	$P, comp$	$Z\&J, comp$
On Dang et al. (2007)'s data	17.5	28	29.6	43.4	37.6	36.5
On Zhao et al. (2011)'s data	53.2	53.2	51.9	11.4	65.8	45.6
On both data sets	**28**	**35.4**	**36.2**	**34**	**45.9**	**39.2**

When the oil compensation terms of Zhao et al. (2011) is used with the alternative correlations the accuracy of Dittus & Boelter (1930), Gnielinski and modified Gnielinski (1976) decreased, whilst the rest increased. Pitla et al. (2002) now reports the highest accuracy on both data sets with 45.9% of the coefficients predicted with an absolute error of less than 20%. This is less accurate than Dittus & Boelter (1930) without the oil compensation terms in the previous section. It should be remembered that the oil compensation terms of Zhao et al. (2011) were not developed to be used with the alternative correlations in this chapter. This may be the reason that some correlations' accuracy increases, whilst other do not. This may also be the reason that a higher accuracy on both data sets is not reported compared to the previous section.

5.3 Conclusion

In this chapter, alternative correlations developed for oil-free conditions were used to calculate the convection coefficients of Dang et al. (2007)'s and Zhao et al. (2011)'s data. Dittus & Boelter (1930) reported the highest accuracy among the alternative correlations. It also showed an improvement on Zhao et al. (2011)'s correlation as its performance is more consistent and is a much simpler correlation, while still being comparably accurate. The alternative correlations were then enhanced by the oil compensation terms published by Zhao et al. (2011) in an attempt to account for the effects of oil contamination. This however, did not improve on the accuracy on both data sets.

From this chapter, Dittus & Boelter (1930) is an improvement on Zhao et al. (2011)'s correlation even though it does not account for the effect of oil contamination. In the following chapter, it will be attempted to enhance Dittus & Boelter (1930) to take the effect of oil into account by developing new oil compensation terms specifically to be used with this correlation. It will also be attempted to improve on the performance consistency of Dittus & Boelter (1930).

CHAPTER 6 CORRELATION DEVELOPMENT

In the previous chapter, it was reported that Dittus & Boelter (1930) is an improvement on Zhao et al. (2011)'s correlation. It shows an improvement on the performance consistency and simplicity, whilst still being comparably accurate. This correlation however, does not account for the effect of oil contamination. In this chapter, a new correlation will be developed for the cooling of oil-contaminated supercritical carbon dioxide. This correlation will use Dittus & Boelter (1930) as a basis together with newly developed oil compensation terms to account for oil. This new correlation should improve on the performance consistency of Dittus & Boelter, whilst still being comparably accurate.

6.1 Approach of new correlations

In this section, the approach taken to develop the new correlation is discussed in detail. From the data of Dang et al. (2007) and Zhao et al. (2011) it was noted that the addition of oil to the flow of supercritical carbon dioxide resulted in a reduction of the convection coefficients with the largest decrease at the pseudocritical temperature (T_{pc} – Section 2.2). A requirement for the new correlation developed within this chapter is to take the effect of oil into account. The basis of the correlation will be a convection coefficient for oil-free conditions predicted by Dittus & Boelter (1930) and then enhanced for the effects of oil by using an oil compensation term. In other words, the new correlation in this section will have the following form:

$$h_{c,CO_2oil} = h_{c,CO_2} \times (oil\ compensation\ term) \tag{57}$$

Where h_{c,CO_2oil} [W/m^2-K], is the convection coefficient predicted for oil-contaminated supercritical carbon dioxide in cooling and h_{c,CO_2} [W/m^2-K] the convection coefficient predicted for oil-free conditions using Dittus & Boelter (1930). The ratio $h_{c,CO_2oil}/h_{c,CO_2}$ represents the effects of oil contamination. In the next section, the oil compensation terms will be developed.

6.2 Oil compensation terms

As previously stated, the oil compensation term is equal to $h_{c,CO_2oil}/h_{c,CO_2}$. In other words, the oil compensation terms should predict the convection ratio of the oil-contaminated to oil-free conditions. To develop the compensation terms, it is necessary to understand the thermodynamic

property ratios that significantly influence the convection heat transfer ratio. This is discussed in the following sections.

6.2.1 Thermodynamic property ratios

The following thermodynamic property ratios show a relationship with the convection ratio ($h_{c,CO_2oil}/h_{c,CO_2}$).

a) Viscosity and density ratios

As stated in Section 2.4.5, Zhao et al. (2011) reported that the convection coefficients of oil-contaminated carbon dioxide are affected by the viscosity of both the carbon dioxide and the oil. It was also reported that the solubility of the carbon dioxide in the oil affects the convection coefficients of the flow. According to these researchers, the solubility of the carbon dioxide in the oil is affected by the density ratio between these two fluids. Zhao et al. (2011) then presented two ratios, which showed a relationship with the convection ratio namely a density ratio (ρ_{oil}/ρ_{CO_2}) and an effective viscosity ratio ($\omega\mu_{oil}/\mu_{CO_2}$).

In Figure 11a, the effective viscosity ratio and convection ratio as a function of temperature are shown, while in Figure 11b the density ratio is shown. The results shown are for a test condition: d_{in}:2mm, p_i:10MPa, G:800kg/m^{2}s, ω:3% and T_{pc}: 45℃ of Dang et al. (2007). To calculate the convection ratio ($h_{c,CO_2oil}/h_{c,CO_2}$), the convection coefficient of Dittus & Boelter 1930 ($h_{c,D\&B}$) was used to obtain h_{c,CO_2}, while the experimental convection coefficient ($h_{c,exp}$) was used for h_{c,CO_2oil}.

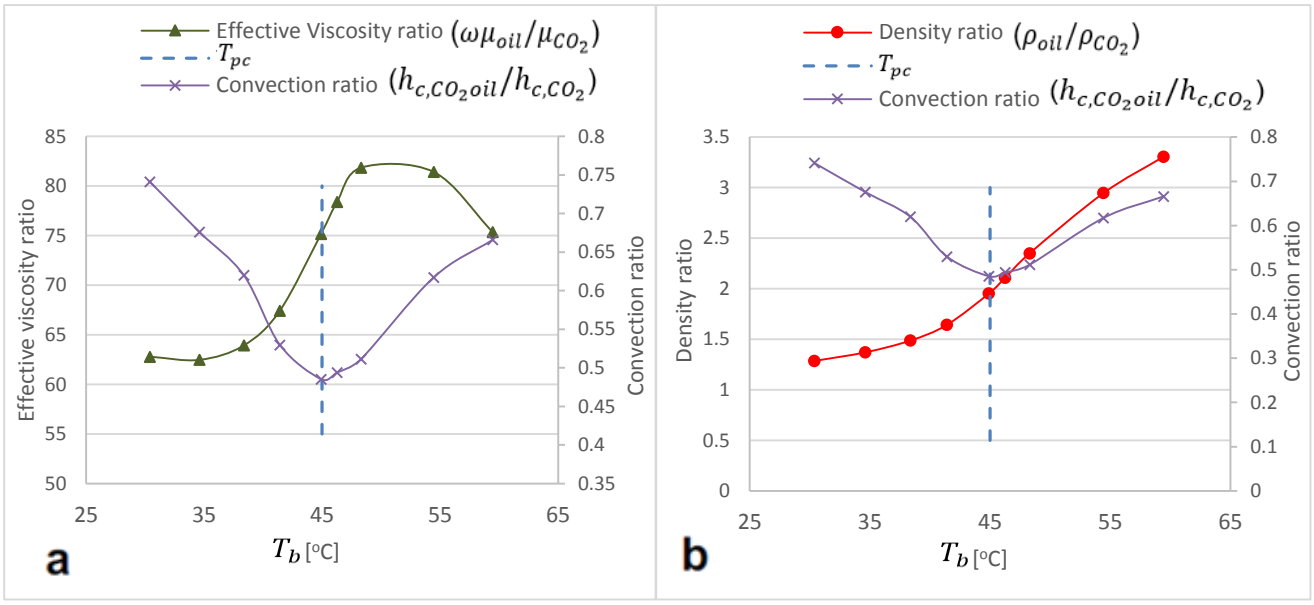

Figure 11 a) Effective viscosity ratio and convection ratio over bulk temperature. b) Density ratio and convection ratio over bulk temperature.

From Figure 11a, it can be seen that when the convection ratio ($h_{c,CO_2oil}/h_{c,CO_2}$) decreases, an increase is seen in the effective viscosity ratio ($\omega\mu_{oil}/\mu_{CO_2}$) and vice versa. In Figure 11b, it is noted that for bulk temperatures (T_b) smaller than the pseudocritical temperature (T_{pc}) a decrease of $h_{c,CO_2oil}/h_{c,CO_2}$ is accompanied by an increase of ρ_{oil}/ρ_{CO_2}. However, for temperatures larger than T_{pc} an increase of $h_{c,CO_2oil}/h_{c,CO_2}$ is accompanied by an increase of ρ_{oil}/ρ_{CO_2}. This is the same trend as reported by Zhao et al. (2011).

b) Euler's number

As stated in Section 2.4.5, Zhao et al. (2011) tested correlations developed for oil-contaminated refrigerants in a condensation process against their data of oil contaminated supercritical carbon dioxide in cooling. These correlations are published by Tricky et al. (1985), Schlager et al. (1990) and Bassi and Bansal (2003) who reported a relationship between Euler's number (in the form of $e^{a\omega}$, where $e \approx 2.71828$) and the convection ratio (see equation 46).

In Figure 12, the correlations of Tricky et al. (1985), Schlager et al. (1990) and Bassi and Bansal (2003) are plotted for different oil concentrations. Also plotted on this figure is the average convection ratio ($h_{c,CO_2oil}/h_{c,CO_2}$) for the data of Dang et al. (2007) at different oil concentrations.

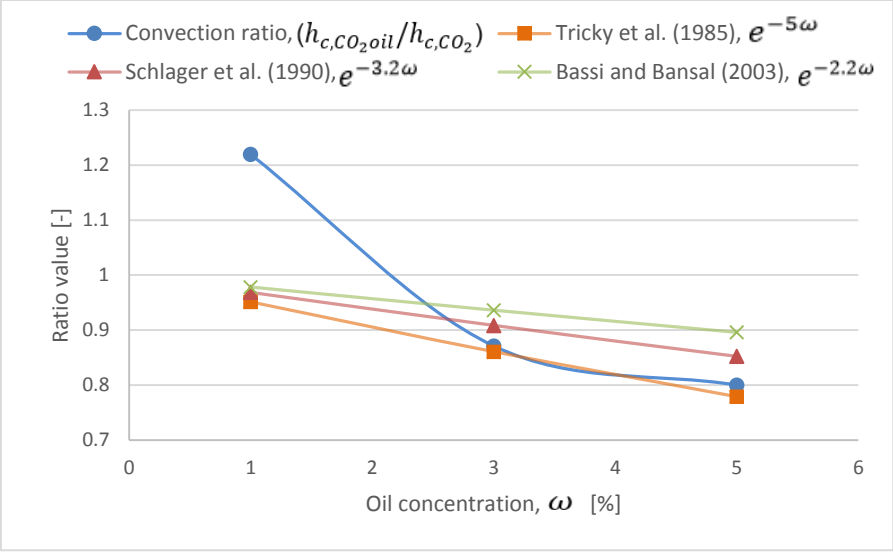

Figure 12 Convection ratio and correlations of Tricky et al. (1985), Schlager et al. (1990) and Bassi and Bansal (2003) for different oil concentrations.

From Figure 12, it seems that ($h_{c,CO_2oil}/h_{c,CO_2}$) resembles an exponentially decreasing function over the oil concentration. The correlations of Tricky et al. (1985), Schlager et al. (1990) and Bassi and Bansal (2003) also show solutions that are exponentially decreasing over the oil concentration. These solutions may appear to be linearly decreasing lines, but this is due to the

values used in the exponents. For example: if the constant, a, is adjusted to a value of -75 an exponentially decreasing solution is clearly seen. This is presented in Figure 13.

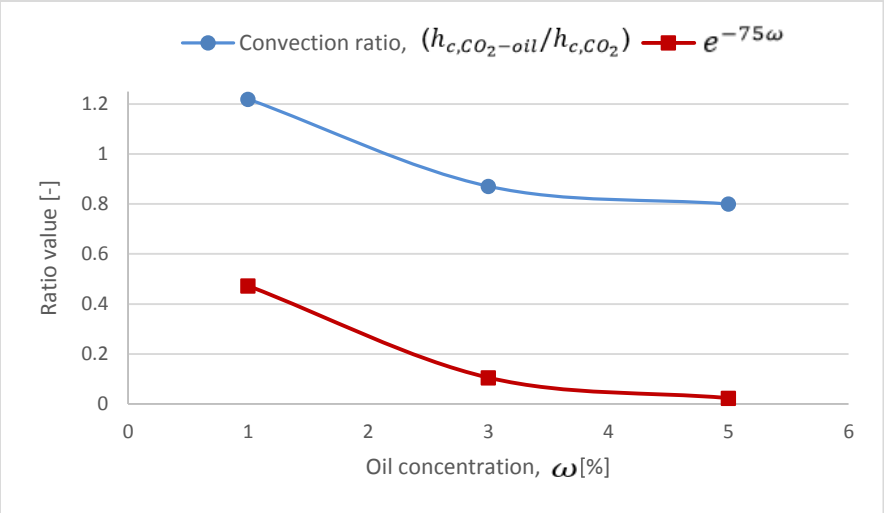

Figure 13 Convection ratio and modified Euler's number correlation at different oil concentrations.

From Figure 13, it can be noted that $(h_{c,CO_2oil}/h_{c,CO_2})$ resembles the shape of $e^{-75\omega}$. As stated previously, Zhao et al. (2011) tested correlations in the form of $e^{a\omega}$ (from Tricky et al. (1985), Schlager et al. (1990) and Bassi and Bansal (2003)) against their data and therefore it is proposed that $e^{a\omega}$ can be used to describe $(h_{c,CO_2oil}/h_{c,CO_2})$.

c) Correction ratio

As stated in Section 2.2, the large variations of the physical and transport properties of supercritical carbon dioxide at the pseudocritical temperature (T_{pc}) increase the complexity of predicting the heat transfer taking place at this point.

For example: when Dittus & Boelter (1930) is used to predict the convection coefficients of the data sets in this study, it is noted that for most cases a larger absolute error is reported at T_{pc}, compared to points away from this temperature. The absolute error represents either an under or over prediction of the convection coefficients. In Figure 14, the absolute errors of Dittus & Boelter (1930) for test condition: d_{in}:4mm, p_i:8MPa, G:800kg/m^{2}s, ω:3% and T_{pc}:34.7℃ of Dang et al. (2007)'s data are shown.

From Figure 14 it is noted that the absolute error it much larger at T_{pc} than at temperatures away from this point. To reduce the absolute error at T_{pc} the convection coefficients at this point must either be increased or decreased, depending on the specific situation. A correction ratio is now defined to reduce the error at T_{pc}.

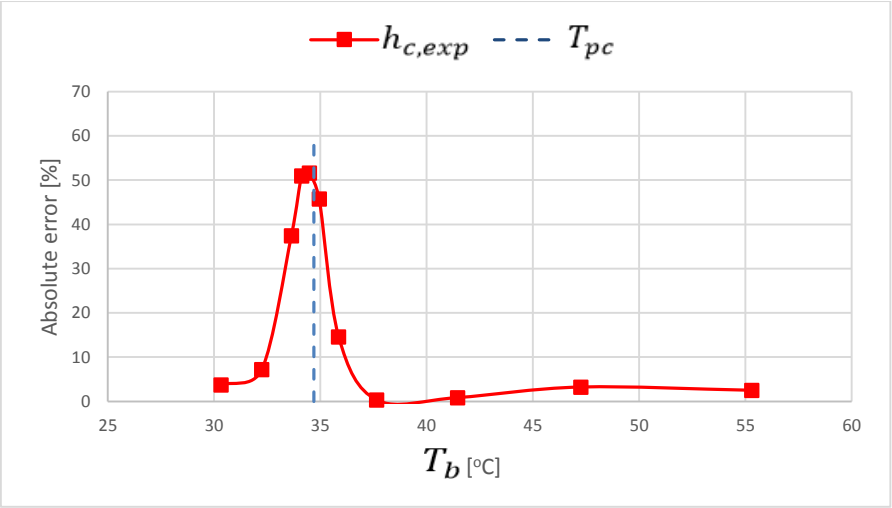

Figure 14 Absolute error versus bulk temperature for Dittus & Boelter (1930).

A ratio, $c_{p_{b,CO_2}}/c_{p_{pc,CO_2}}$, is introduced. Where $c_{p_{b,CO_2}}$ [J/kgK] and $c_{p_{pc,CO_2}}$ [J/kgK] are the carbon dioxide's specific heats at the bulk and pseudocritical temperature (T_{pc}), respectively. In Figure 15, $\left(c_{p_{b,CO_2}}/c_{p_{pc,CO_2}}\right)^{1}$ and $\left(c_{p_{b,CO_2}}/c_{p_{pc,CO_2}}\right)^{-1}$ are plotted for test condition: d_{in}:4mm, p_i:8MPa, G:800kg/m^{2}s, ω:3% and T_{pc}:34.7℃ of Dang et al. (2007)'s data. From this figure it can be seen that $\left(c_{p_{b,CO_2}}/c_{p_{pc,CO_2}}\right)^{1}$ reaches a maximum at T_{pc}, while $\left(c_{p_{b,CO_2}}/c_{p_{pc,CO_2}}\right)^{-1}$ shows a minimum at this point. The ratio $\left(c_{p_{b,CO_2}}/c_{p_{pc,CO_2}}\right)^{a}$ can now be used as a scaling factor in the oil compensation terms to either increase or decrease the convection coefficients at T_{pc} (depending on the value used for a).

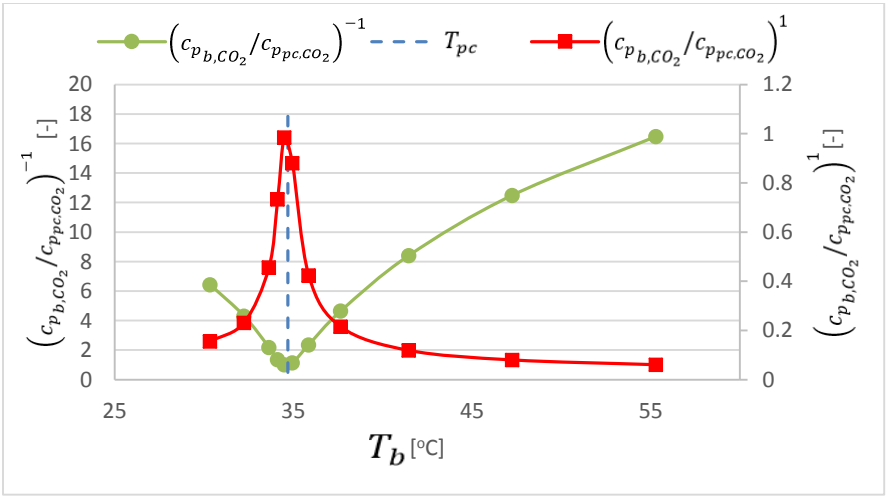

Figure 15 Specific heat ratios versus bulk temperature.

In the next section, different cases for the oil compensation term in equation 57 are developed.

6.2.2 Oil compensation terms cases

The following section reports the cases for the oil compensation term in equation 57 used in this study.

Case I

For the first case, the focus is to predict $h_{c,CO_2oil}/h_{c,CO_2}$ using Euler's number. This will allow the convection ratio to change exponentially over the oil concentration. This is the simplest form for the oil compensation term and can be defined as:

$$\frac{h_{c,CO_2oil}}{h_{c,CO_2}} = oil\ compensation\ term = e^{a_I\omega}$$

Where a_I is a constant.

Case II

For case II, the density and effective viscosity ratios presented by Zhao et al. (2011) are used to predict $h_{c,CO_2oil}/h_{c,CO_2}$. This allows the convection ratio to change with the density and effective viscosity ratio. The oil compensation term for case II is then defined as:

$$\frac{h_{c,CO_2oil}}{h_{c,CO_2}} = oil\ compensation\ term = a_{II}\left(\frac{\rho_{oil}}{\rho_{CO_2}}\right)^{b_{II}}\left(\frac{\omega\mu_{oil}}{\mu_{CO_2}}\right)^{c_{II}}$$

Where a_{II} is a scaling constant and b_{II} and c_{II} are constants used to adjust the effects of the density and effective viscosity ratios on $h_{c,CO_2-oil}/h_{c,CO_2}$.

Case III

For case III, the scaling constant, a_{II}, of Case II is replaced by a scaling factor that changes exponentially with the oil concentration. For this case a_{II} of Case II is replaced by $e^{a_I\omega}$ of Case I. This allows the convection ratio to change with the density and effective viscosity ratio, whilst also decreasing exponentially over the oil concentration. The oil compensation term for case III is defined as:

$$\frac{h_{c,CO_2oil}}{h_{c,CO_2}} = oil\ compensation\ term = e^{a_{III}\omega}\left(\frac{\rho_{oil}}{\rho_{CO_2}}\right)^{b_{III}}\left(\frac{\omega\mu_{oil}}{\mu_{CO_2}}\right)^{c_{III}}$$

Where a_{III}, b_{III} and c_{III} are constants.

Case IV

For the final case, the correction ratio is added to Case III to reduce the absolute error at T_{pc}. This will be used to either increase or decrease the values at the pseudocritical temperature. The oil compensation term for case IV is then defined as:

$$\frac{h_{c,CO_2oil}}{h_{c,CO_2}} = oil\ compensation\ term = e^{a_{IV}\omega}\left(\frac{\rho_{oil}}{\rho_{CO_2}}\right)^{b_{IV}}\left(\frac{\omega\mu_{oil}}{\mu_{CO_2}}\right)^{c_{IV}}\left(\frac{c_{p_{b,CO_2}}}{c_{p_{pc,CO_2}}}\right)^{d_{IV}}$$

Where a_{IV}, b_{IV}, c_{IV} and d_{IV} are constants.

In the next section, the constants present in the oil compensation term cases are determined.

6.3 Constants

For equation 57, h_{c,CO_2} is predicted using the convection coefficient of Dittus & Boelter (1930), $h_{c,D\&B}$, whilst the oil compensation term can be one of the cases presented in Section 6.2.2 above. This then leads to four combinations for equation 57 to be evaluated. For each of the combinations the constants in the oil compensation term need to be determined, that results in the smallest percentage error. The values of the constants are calculated by minimizing the sum of the absolute errors (equation 54) between the predicted and published convection coefficients. The constants are calculated using Dang et al. (2007)'s data, whilst the data of Zhao et al. (2011) are kept as an independent data set for the verification of the combinations in the next section. The calculated constants are presented in Table 8.

Table 8 Constants for different combinations using Dang et al. (2007)'s data.

Case	Correlation	Constants	
		$T_b \leq T_{pc}$	$T_b > T_{pc}$
I	$\frac{h_{c,CO_2oil}}{h_{c,D\&B}} = e^{a_I\omega}$	$a_I = -6.089$	$a_I = -1.614$
II	$\frac{h_{c,CO_2oil}}{h_{c,D\&B}} = a_{II}\left(\frac{\rho_{oil}}{\rho_{CO_2}}\right)^{b_{II}}\left(\frac{\omega\mu_{oil}}{\mu_{CO_2}}\right)^{c_{II}}$	$a_{II} = 3.008,$ $b_{II} = -1.019,$ $c_{II} = -0.193$	$a_{II} = 0.767,$ $b_{II} = 0.739,$ $c_{II} = -0.179$
III	$\frac{h_{c,CO_2oil}}{h_{c,D\&B}} = e^{a_{III}\omega}\left(\frac{\rho_{oil}}{\rho_{CO_2}}\right)^{b_{III}}\left(\frac{\omega\mu_{oil}}{\mu_{CO_2}}\right)^{c_{III}}$	$a_{III} = 1.662,$ $b_{III} = -0.542,$ $c_{III} = 0.006$	$a_{III} = 5.266,$ $b_{III} = 0.733,$ $c_{III} = -0.277$
IV	$\frac{h_{c,CO_2oil}}{h_{c,D\&B}} = e^{a_{IV}\omega}\left(\frac{\rho_{oil}}{\rho_{CO_2}}\right)^{b_{IV}}\left(\frac{\omega\mu_{oil}}{\mu_{CO_2}}\right)^{c_{IV}}\left(\frac{c_{p_{b,CO_2}}}{c_{p_{pc,CO_2}}}\right)^{d_{IV}}$	$a_{IV} = -0.183,$ $b_{IV} = 0.552,$ $c_{IV} = -0.173,$ $d_{IV} = -0.368$	$a_{IV} = 0.029,$ $b_{IV} = 0.365,$ $c_{IV} = -0.168,$ $d_{IV} = -0.099$

The constants for each combination are calculated separately for temperatures smaller and larger than the pseudocritical temperature (T_{pc}), due to liquid-like thermo-physical properties before T_{pc} and gas-like characteristics after this point, (Aldana, et al., 2002).

The four combinations reported in Table 8 can now be tested against the data sets.

6.4 Evaluation of combinations against data sets

The four combinations in the previous section is now tested against the data set used to develop them, Dang et al. (2007), and verified against the independent data set, Zhao et al. (2011), to evaluate the consistency of their performance. For this section, the average absolute error ($|\bar{E}|$) of each combination against the data sets is reported and based on the results one of the combinations will be chosen. The results are reported in Table 9.

Table 9 Combinations tested against data sets.

Case	Correlation	On Dang et al. (2007)'s data	On Zhao et al. (2011)'s data
		$\lvert\bar{E}\rvert$ [%]	$\lvert\bar{E}\rvert$ [%]
I	$\frac{h_{c,CO_2oil}}{h_{c,D\&B}} = e^{a_I\omega}$	28.76	16.65
II	$\frac{h_{c,CO_2oil}}{h_{c,D\&B}} = a_{II}\left(\frac{\rho_{oil}}{\rho_{CO_2}}\right)^{b_{II}}\left(\frac{\omega\mu_{oil}}{\mu_{CO_2}}\right)^{c_{II}}$	23.71	33.82
III	$\frac{h_{c,CO_2oil}}{h_{c,D\&B}} = e^{a_{III}\omega}\left(\frac{\rho_{oil}}{\rho_{CO_2}}\right)^{b_{III}}\left(\frac{\omega\mu_{oil}}{\mu_{CO_2}}\right)^{c_{III}}$	24.38	25.62
IV	$\frac{h_{c,CO_2oil}}{h_{c,D\&B}} = e^{a_{IV}\omega}\left(\frac{\rho_{oil}}{\rho_{CO_2}}\right)^{b_{IV}}\left(\frac{\omega\mu_{oil}}{\mu_{CO_2}}\right)^{c_{IV}}\left(\frac{c_{p_{b,CO_2}}}{c_{p_{pc,CO_2}}}\right)^{d_{IV}}$	22.23	28.05

The best performing combination on Dang et al. (2007)'s data is case IV with an error of 22.23%, closely followed by cases II and III with 23.71% and 24.38% respectively. On the independent data set, the best performing combination is case I with 16.65%, followed with 25.62% by case III.

The most consistent combination however, is case III with only a 1.24% difference between the errors calculated on the data sets. An error of 24.38% was calculated on Dang et al. (2007)'s data, whilst 25.62% was obtained on the independent data. For this reason, this correlation is chosen among the combinations, because a consistent correlation is required for this study.

In the next section, the chosen correlation will be evaluated and compared to Dittus & Boelter (1930).

6.5 Proposed correlation for oil-contaminated supercritical carbon dioxide in cooling

In this section, the proposed correlation for oil contaminated supercritical carbon dioxide in cooling from the previous section is evaluated and compared to Dittus & Boelter (1930). The correlation chosen is defined by:

$$\frac{h_{c,CO_2oil,new}}{h_{c,D\&B}} = e^{1.662\omega}\left(\frac{\rho_{oil}}{\rho_{CO_2}}\right)^{-0.542}\left(\frac{\omega\mu_{oil}}{\mu_{CO_2}}\right)^{0.006} \quad if \quad \frac{T_b}{T_{pc}} \leq 1 \tag{58}$$

$$\frac{h_{c,CO_2oil,new}}{h_{c,D\&B}} = e^{5.266\omega}\left(\frac{\rho_{oil}}{\rho_{CO_2}}\right)^{0.733}\left(\frac{\omega\mu_{oil}}{\mu_{CO_2}}\right)^{-0.277} \quad if \quad \frac{T_b}{T_{pc}} > 1 \tag{59}$$

Where $h_{c,D\&B}$ is the convection coefficient predicted by Dittus & Boelter (1930) and $h_{c,CO_2oil,new}$ is the convection coefficient enhanced to take the effect of oil contamination into account. This correlation allows the convection ratio, $\frac{h_{c,CO_2oil,new}}{h_{c,D\&B}}$, to change with the density and viscosity ratio, whilst also allowing it to change exponentially over the oil concentration.

When the new correlation is used to predict the data of Dang et al. (2007), 47.1% of the results have an absolute error less than 20%. On the independent data set of Zhao et al. (2011), it predicts 49.4% of the data within this range. This is a 2.3% difference between the results on the data sets. When Dittus & Boelter (1930) is used on Dang et al. (2007), 44.4% of the coefficients are predicted with an absolute error less than 20%, while on Zhao et al. (2011)'s data 59.5% are predicted in this range. This shows a much larger difference between the results (15.1%) compared to the new correlation. It must be remembered that lower oil concentrations are used for Zhao et al. (2011)'s data (1% and 2% oil), whereas much higher oil concentrations (typically 1%, 3% and 5% oil and for single cases 7,5%, 10% and 13% oil) are used for the data of Dang et al. (2007). This may be the reason why Dittus & Boelter (1930) is slightly more accurate on the data of Zhao et al. (2011). Dittus & Boelter (1930), developed for oil-free conditions, seems to predict the convection coefficients at the low oil concentrations of Zhao et al. (2011)'s data slightly more accurate than the new correlation. However, when the oil increases the new correlation shows a more consistent accuracy, whereas Dittus & Boelter (1930) becomes less accurate. Table 10 reports the average absolute error for these correlations per oil concentration.

Table 10 Average absolute error for different oil concentrations on Dang et al. (2007)'s data.

ω [%]	$Dittus\ \&\ Boelter\ (1930)$	$New\ correlation$
1	22,4	26
3	35,5	19,6
5	42,7	25,3

From this table it can be observed that as the oil increases, the error of Dittus & Boelter (1930) increases. An error of 22.4% is reported for 1% oil and increased to 42.7% for 5% oil. For the new correlation however, an increase of the error is not noted, with 26% error for 1% oil and 25.3% error for 5%. From these results, it can be concluded that the enhanced new correlation that takes the effect of oil into account predicts the convection coefficients more accurate as the oil increases, compared to the oil-free correlation by Dittus & Boelter (1930). In addition, it is noted that Dittus & Boelter (1930) can be used to predict the convection coefficients for low oil concentrations of up to 2%. However, as the oil increases this correlation becomes inaccurate and it is then advised to rather use the new correlation for all oil concentrations even though it is slightly less accurate at low oil concentrations. The new correlation's performance is much more consistent over the data sets used and it can then be expected to have a more consistent accuracy over a wider range of conditions compared to Dittus & Boelter (1930). The detailed results for when the new correlation is tested on the data sets are reported in Appendix G.

In addition, a higher consistency is reported on the average absolute error by the new correlation, compared to Dittus & Boelter (1930). The average absolute error of the new correlation on Dang et al. (2007) is 24.38% and 25.62% on Zhao et al. (2011) (1.24% difference). When Dittus & Boelter (1930) is tested against the data sets, an error of 30.42% is obtained on Dang et al. (2007) and 21.48% on Zhao et al. (2011) (8.94% difference).

From the results in this section, the new correlation is an improvement on Dittus & Boelter (1930). It takes the effect of oil into account and consequently reports a more consistent performance over the data sets and oil concentrations. The predicted versus experimentally calculated convection coefficients on the data of Dang et al. (2007) and Zhao et al. (2011) are shown in Figure 16 and Figure 17, respectively.

From Figure 16, it can be seen that the new correlation under predicts more convection coefficients than over predicts. In Figure 17, over prediction is seen for lower values of the convection coefficients, while under prediction is observed for higher values.

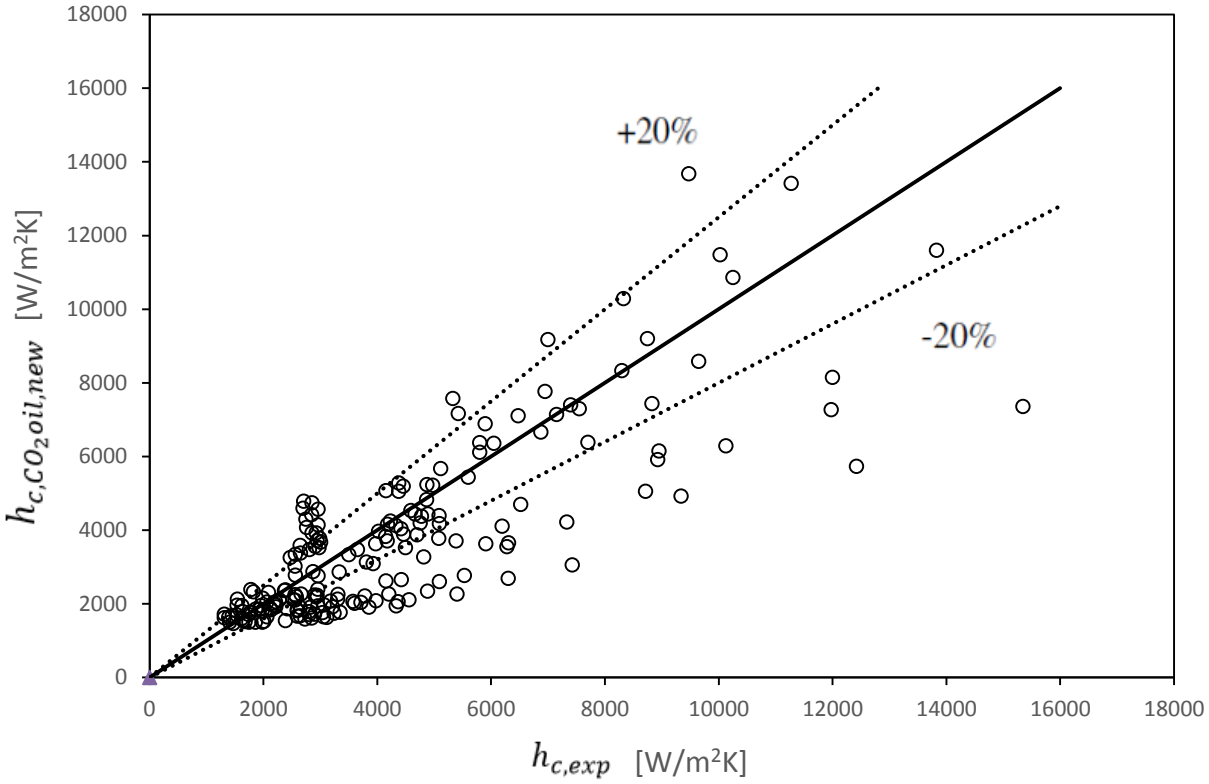

Figure 16 Predicted versus experimentally calculated convection coefficients of new correlation on Dang et al. (2007)'s data.

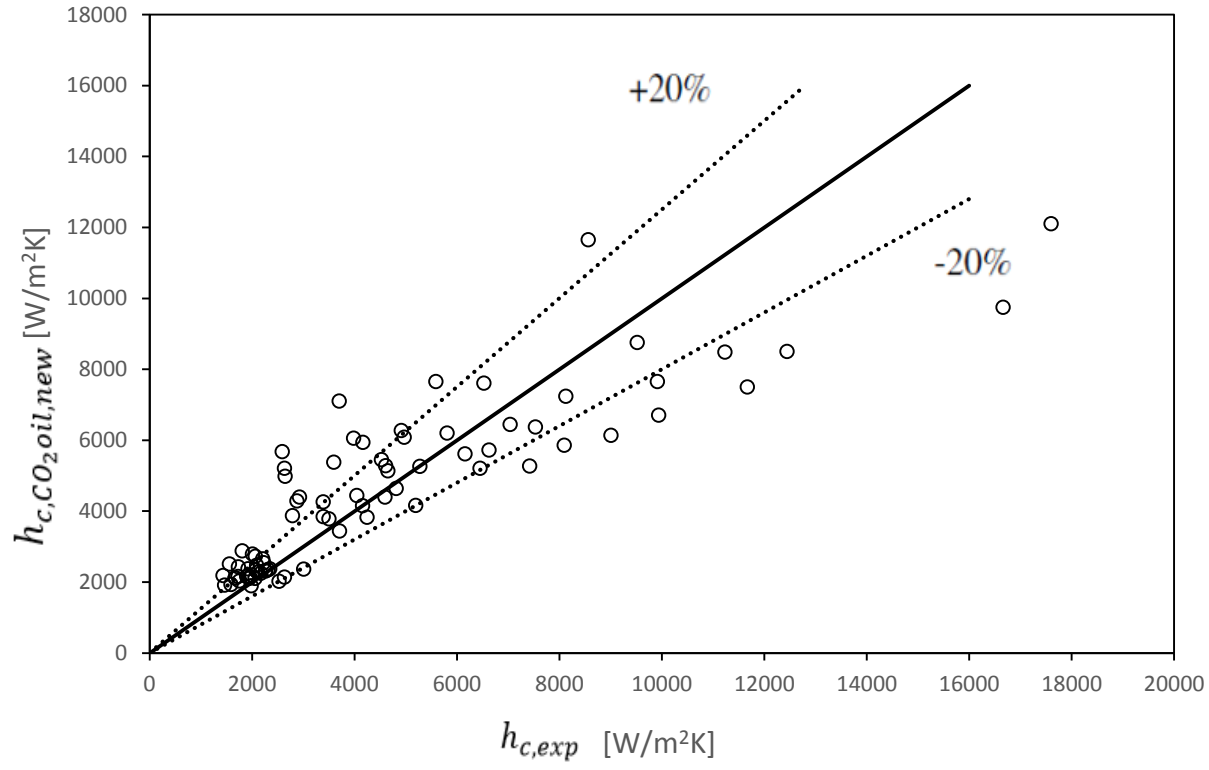

Figure 17 Predicted versus experimentally calculated convection coefficients of new correlation on Zhao et al. (2011)'s data.

Finally, the new correlation developed in this chapter is less complex than Zhao et al. (2011)'s correlation for oil contaminated supercritical carbon dioxide in cooling (Section 4.3), which reported non consistent accuracies over the data sets. Both correlations are given below to show the less complex form of the newly proposed correlation:

Zhao et al. (2011)'s correlation:

$For\ \frac{T_b}{T_{pc}} \leq 1$:

$$h_{c,Z} = \frac{\left(\frac{((1.82logRe_f - 1.64)^{-2}/8)(Re_b - 1000)Pr_{D\&H}}{1.07 + 12.7\sqrt{\frac{(1.82logRe_f - 1.64)^{-2}}{8}}\left(Pr_{D\&H}^{\frac{2}{3}} - 1\right)} \right) k_f}{D_H} \left(1.186 \left(\frac{\rho_{oil}}{\rho_{CO_2}} \right)^{-0.236} \left(\frac{\omega \mu_{oil}}{\mu_{CO_2}} \right)^{-0.114} \right)$$

$For\ \frac{T_b}{T_{pc}} > 1$:

$$h_{c,Z} = \frac{\left(\frac{((1.82logRe_f - 1.64)^{-2}/8)(Re_b - 1000)Pr_{D\&H}}{1.07 + 12.7\sqrt{\frac{(1.82logRe_f - 1.64)^{-2}}{8}}\left(Pr_{D\&H}^{\frac{2}{3}} - 1\right)} \right) k_f}{D_H} \left(0.764 \left(\frac{\rho_{oil}}{\rho_{CO_2}} \right)^{0.53} \left(\frac{\omega \mu_{oil}}{\mu_{CO_2}} \right)^{-0.227} \right)$$

$With$:

$$Pr_{D\&H} = \begin{cases} \frac{c_{p_b}\mu_b}{k_b}\ when\ c_{p_b} \geq \frac{h_b - h_w}{T_b - T_w} \\ \frac{\left(\frac{h_b - h_w}{T_b - T_w}\right)\mu_b}{k_b}\ when\ c_{p_b} < \frac{h_b - h_w}{T_b - T_w}\ \ and\ \frac{\mu_b}{k_b} \geq \frac{\mu_f}{k_f} \\ \frac{\left(\frac{h_b - h_w}{T_b - T_w}\right)\mu_f}{k_f}\ when\ c_{p_b} < \frac{h_b - h_w}{T_b - T_w}\ \ and\ \frac{\mu_b}{k_b} < \frac{\mu_f}{k_f} \end{cases}$$

New correlation:

$For\ \frac{T_b}{T_{pc}} \leq 1$:

$$h_{c,CO_2oil,new} = \frac{(0.023Re_b^{0.8}\mathrm{Pr_b^{0.3}})k}{D_H} \left(e^{1.662\omega} \left(\frac{\rho_{oil}}{\rho_{CO_2}} \right)^{-0.542} \left(\frac{\omega \mu_{oil}}{\mu_{CO_2}} \right)^{0.006} \right)$$

$For\ \frac{T_b}{T_{pc}} > 1$:

$$h_{c,CO_2oil,new} = \frac{(0.023Re_b^{0.8}\mathrm{Pr_b^{0.3}})k}{D_H}\left(e^{5.266\omega}\left(\frac{\rho_{oil}}{\rho_{CO_2}}\right)^{0.733}\left(\frac{\omega\mu_{oil}}{\mu_{CO_2}}\right)^{-0.277}\right)$$

A more simplified correlation eases the calculation process and typically reduces the calculation times of large simulations. A less complex correlation is often also more applicable to a wider range of applications.

6.6 Summary

In this chapter, Dittus & Boelter (1930) was enhanced to take the effect of oil contamination into account. The newly proposed correlation allowed the convection ratio to change with the density and viscosity ratio, whilst also allowing it to change exponentially over the oil concentration. It was reported that the new correlation's accuracy is much more consistent over the data sets compared to Dittus & Boelter (1930). In addition, the error was more consistent as the oil increased; whereas Dittus & Boelter (1930) became less accurate. Lastly, it was reported that the new correlation is much less complex than the correlation of Zhao et al. (2011).

CHAPTER 7 CONCLUSION AND RECOMMENDATIONS

This study includes a literature survey (Chapter 2), a theoretical background study (Chapter 3), an evaluation of Zhao et al. (2011)'s correlation (Chapter 4), an investigation of alternative correlations (Chapter 5) and a correlation development (Chapter 6). The focus of this study was to investigate the performance consistency of currently published correlations for the cooling of oil-contaminated supercritical carbon dioxide. In addition, develop an improved Nusselt number correlation, if possible, whilst having a simpler form.

7.1 Chapter 2

In this chapter, the current literature on the cooling of supercritical carbon dioxide especially with oil contamination was discussed. It was reported that the properties of supercritical carbon dioxide changes significantly at the pseudocritical temperature, which in addition to oil contamination, increases the complexity of predicting the heat transfer. A number of Nusselt number correlations for the cooling of supercritical carbon dioxide, found in literature, were discussed. It was reported however, that very few correlations are published which takes the adverse effects of oil contamination into account. The study of Zhao et al. (2011) was the only study that published a correlation for the cooling of oil-contaminated supercritical carbon dioxide

7.2 Chapter 3

In this chapter, the theory necessary for this study was reported. This included the concepts and equations from thermodynamics and heat transfer needed to evaluate a Nusselt number correlation at the carbon dioxide side of a tube-in-tube gas cooler using the measured parameters of published data. The relevant Nusselt number correlations and statistical concepts were also presented in this chapter.

7.3 Chapter 4

In Chapter 4, the data sets used for this study was reported. The method of calculating the theoretical/predicted convection coefficients of an experimental test was then discussed. Finally, the correlation for oil-contaminated supercritical carbon dioxide in cooling, published by Zhao et al. (2011), was then used to predict the convection coefficients of Dang et al. (2007)'s data. This was compared to the results of Zhao et al. (2011)'s correlation on their own data. It was reported that this correlation's accuracy is not consistent between the data sets used. It predicts 90% of

Zhao et al. (2011)'s data with an absolute error less than 20%, whilst only 39.7% are within this range for Dang et al. (2007)'s data. Based on the results, it was decided to investigate a new correlation to improve on the performance consistency and to reduce on the complexity of the correlation.

7.4 Chapter 5

In this chapter, alternative correlations developed for similar flows were used to predict the convection coefficients of the data sets. Dittus & Boelter (1930) reported the highest accuracy among the alternative correlations. It also showed an improvement on Zhao et al. (2011)'s correlation as its performance is more consistent and is a much simpler correlation, while still being comparably accurate. Dittus & Boelter (1930) predicted 44.4% and 59.5% of Dang et al. (2007)'s and Zhao et al. (2011)'s data within 20%. The alternative correlations were then enhanced by the oil compensation terms published by Zhao et al. (2011) in an attempt to account for the effects of oil contamination. This however, did not improve on the accuracy on both data sets. It was then decided to investigate the enhancement of Dittus & Boelter (1930) to take the effect of oil into account by developing new oil compensation terms specifically to be used with this correlation. It should also be attempted to improve on the performance consistency of Dittus & Boelter (1930).

7.5 Chapter 6

In this chapter, Dittus & Boelter (1930) was enhanced to take the effect of oil contamination into account. The newly proposed correlation allowed the convection ratio to change with the density and viscosity ratio, whilst also allowing it to change exponentially over the oil concentration. It was reported that the new correlation's accuracy is much more consistent over the data sets compared to Dittus & Boelter (1930). The new correlation predicted 47.1% of Dang et al. (2007)'s data within 20% and 49.4% for the data of Zhao et al. (2011). In addition, the error was more consistent as the oil increased; whereas Dittus & Boelter (1930) became less accurate. Lastly, it was reported that the new correlation is much less complex than the correlation of Zhao et al. (2011).

7.6 Recommendations for future studies

Even though the test data used on this study covers a large variety of test conditions, it might be useful to obtain test conditions out of this range (especially for diameters larger than 6mm) so that further verification of the new correlation can be done. The ideal would be to construct a test bench facility for this purpose. This facility can also then be used to vary one parameter (such as pressure, mass flux etc.) while keeping the other conditions constant and noting the effect on the

convection coefficients. However, such facilities have proven to be expensive and complex, as reported by (Kalinger, 2005).

BIBLIOGRAPHY

Aldana, J., Georgiadis, J. & Jacobi, A., 2002. Critical Heat Flux of CO2 in a Microchannel at Elevated Subcritical Pressures. In: *Air-conditioning and Refrigeration Center, CRC TR-195.* s.l.:The University of Illinois, Urbana-Champaign, p. 90.

Arora, R., 2010. *Refrigeration and Air Conditioning.* New Delhi: PHI Learning Private Limited.

Atlanta, G., 2004. *The Systems and Equipment volume of ASHRAE Handboek.* s.l.:ASHRAE, Inc.

Austin, B. & Sumathy, K., 2011. Transcritical carbon dioxide heat pump systems: A review. *Renewable and Sustainable Energy Reviews,* Issue 15, pp. 4013-4028.

Baskov, V., Kuraeva, I. & Protopopov, V., 1977. Heat transfer with the turbulent flow of a liquid at supercritical pressure in tubes under cooling conditions. *Teplofizika Vysokikh Temperatur,* 15(1), pp. 96-102.

Bassi, R. & Bansal, P., 2003. In tube condensation of mixture of R134a and ester oil: empirical correlations. *International Journal of Refrigeration,* Issue 26, pp. 402-409.

Borgnakke, C. & Sonntag, R., 2014. *Fundamentals of Thermodynamics.* Eighth edition ed. s.l.:Wiley & Sons.

Borgnakke, C. & Sonntag, R., 2014. *Fundamentals of thermodynamics eigth edition.* Michigan: Wiley.

Budisa, N. & Schulze-Makuch, D., 2014. Supercritical Carbon Dioxide and Its Potential as a Life-Sustaining Solvent in a Planetary Environment.. *Life,* Issue 4, pp. 331-340.

Calm, J., 2008. The next generation of refrigerants - Historical review, considerations, and outlook. *International Journal of Refrigeration,* 31(7), pp. 1123-1133.

Cavallini, A., 2004. *Properties of CO2 as a refrigerant,* Universita Degli Studi Di Milano Centro Di Ricerca Per L'Ambiente E L'Impresa: Centro Studi Galileo Industria & Formazone.

Cheng, L. & Mewes, D., 2006. Review of two-phase flow and flow boiling of mixtures in small and mini channels. *International Journal of Multiphase Flow,* Volume 32, pp. 183-207.

Cheng, L., Ribatski, G. & Thome, J., 2008. Analysis of supercritical CO2 cooling in macro- and micro-channels. *International Journal of Refrigeration,* Volume 31, pp. 1301-1316.

Conde, M., 1996. Estimation of thermophysical properties of lubricating oils and their solutions with refrigerants: an appraisal of existing methods. *Appl. Therm. Eng.,* 16(1), pp. 51-61.

CPI Engineering Services, I., 2009. *Solest polyol ester lubricants,* U.S.A: s.n.

Dang, C. & Hihara, E., 2004. In-tube cooling heat transfer of supercritical carbon dioxide - part 1: experimental measurement. *International Journal of Refrigeration,* Volume 27, pp. 736- 747.

Dang, C. & Hihara, E., 2004. In-tube cooling heat transfer of supercritical carbon dioxide - part 2: comparison of numerical calculation with different turbulance models. *International Journal of Refrigeration,* Volume 27, pp. 748-760.

Dang, C., Lino, K., Fukuoka, K. & Hihara, E., 2007. Effect of lubricating oil on cooling heat transfer of supercritical carbon dioxide. *International Journal of Refrigeration,* Volume 30, pp. 724-731.

Dang, C., Lino, K. & Hihara, E., 2008. Study on two-phase flow pattern of supercritical carbon dioxide with entrained PAG type lubricating oil in a gas cooler. *International Journal of Refrigeration,* 31(72), p. 1265.

Dang, C., Lino, K. & Hihara, K., 2010. Effect of PAG-type lubricating oil on heat transfer characteristics of supercritical carbon dioxide cooled inside a small internally grooved tube. *International Journal of Refrigeration,* 33(558), p. 65.

Dittus, F. & Boelter, L., 1930. Heat transfer in automobile radiators of the tubular type. *International Communications in Heat and Mass Transfer,* 12(1), pp. 3-22.

Duffey, R. & Pioro, I., 2004. Heat transfer to supercritical fluids flowing in channels - empirical correlations (survey). *Nuclear Engineering,* Volume 230, pp. 69-91.

Fang, X., Zhou, Z. & Li, D., 2013. Review of correlations of flow boiling heat transfer coefficients for carbon dioxide.. *International Journal of Refrigeration,* Issue 36, pp. 2017-2039.

Filho, E., Cheng, L. & Thome, J., n.d. Flow boiling characteristics and flow pattern visualization of refrigerant/lubricant oil mixtures.

Frank, P. & Incropera, D., 2013. *Principles of Heat and Mass Transfer.* Seventh Edition ed. s.l.:John Wiley & Sons.

Gao, L. & Honda, T., 2002. Experiments on heat transfer characteristics of heat exchanger for CO2 heat pump system, in: Proceedings of the Asian Conference on Refrigeration and Air Conditioning 2002. *Japan Society of Refrigeration and Air Conditioning Engineers,* pp. A2-A4.

Gao, L. & Honda, T., 2006. *Flow and heat transfer characteristics of refrigerant and PAG oil in the evaporator of a CO2 heat pump system.* Trondheim, Normway, 7th IIR-Gustav Lorentzen Conference.

Gnielinski, V., 1976. New equations for heat and mass transfer in the turbulent flow in pipes and channels. *Internation Chemical Engineering,* 16(2), pp. 359-368.

Hall, W., 1971. Heat transfer near the critical point. *Adv. Heat Transfer,* Volume 7, pp. 359-368.

Harris, P., 2014. *Theoretical and experimental analysis of supercritical carbon dioxide cooling,* Potchefstroom: North-West University.

Huai, X. & Koyama, S., 2007. Heat transfer characteristics of supercritical CO2 flow in small-channeled structures. *Exp. Heat Transf.,* Volume 20, pp. 19-33.

Huai, X., Koyama, S. & Zhao, T., 2005. An experimental study of flow and heat transfer of supercritical carbon dioxide in multiport mini channels under cooling conditions. *Chem. Eng. Sci.,* Volume 60, pp. 3337-3345.

Incropera, F., Dewit, D., Bergman, T. & Lavine, A., 2013. *Principles of heat and mass transfer.* Seventh ed. s.l.:Wiley & Sons.

Jung, J. & Yun, R., 2013. Prediction of gas cooling heat transfer coefficients for CO2-oil mixtures. *International Journal of Refrigeration,* Volume 36, pp. 129-135.

Kalinger, J., 2005. *Heat Transfer Coefficient and Pressure Drop Measurements for CO2/Oil Mixture in a Micro Channel Tube,* Maryland: University of Maryland, Center for Environmental Energy Engineering (CEEE).

Krasnoshchekov, E. K. I. P. V., 1970. Local heat transfer of carbon dioxide at supercritical pressure under cooling conditions. *Teplofizika Vysokikh Temperatur,* 7(5), pp. 922-930.

Kuang, G., Ohadi, M. & Zhao, Y., 2003. *Experimental study of miscible and immiscible oil effects on heat transfer coefficients and pressure drop in microchannel gas cooling of supercritical CO2.* Las Vegas, Navada, USA, HT ASME Summer Heat Transfer Conference.

Kuang, G., Ohadi, M. & Zhao, Y., 2004. *Experimental study on gas cooling heat transfer for supercritical CO2 in microchannels.* Rochester, New York, USA, The Second International Conference on Microchannels and Minichannels.

Liao, S. & Zhao, C., 2002. Measurements of heat transfer coefficients from supercritical carbon dioxide flowing in horizontal mini/micro channels. *Journal of Heat Transfer,* pp. 124,413.

Liao, S. & Zhao, T., 2002. Measurement of heat transfer coefficient from supercritical carbon dioxide flowing in horizontal mini/micro channels. *J. Heat Transf.,* Volume 124, pp. 413-430.

Lorentzen, G., 1994. Revival of Carbon Dioxide as a Refrigerant. *International Journal of Refrigeration,* 17(5), pp. 292-301.

Mori, K. et al., 2003. Cooling heat transfer characteristics of CO2 and CO2-oil mixture at supercritical pressure conditions. *Trans. Jpn. Soc. Refrig. Air Cond. Eng.,* 20(3), pp. 121-126.

Munson, B., Okiishi, T., Huebsch, W. & Rothmayer, A., 2013. *Fluid Mechanics.* Seventh Edition ed. s.l.:Wiley & Sons.

Nations, U., 1997. *Kyoto Protocol to the United Nations Framework Convention on Climate Change,* Kyoto: s.n.

Nation, U., 1987. *Montreal Protocol on Subtances that Deplete the Ozone Layer,* s.l.: s.n.

Nekså, P., 2002. CO2 heat pump systems.. *Internation Journal of Refrigeration,* 161(8), p. 12.

Nekså, P. et al., 1999. Development of semi-hermetic CO2-compressors. *20th International Congress of Refrigeration IIR/IIF. Sydney. Australia.*

Nekså, P., Rekstad, H. & Reza Zakeri, G. A. S. P., 1998. CO2 - heatpump water heater: characteristics, system design and experimental results. *International Journal of Refrigeration,* 21(3), pp. 172-179.

Padrela, L. et al., 2009. Formation of indomethacin-saccharin cocrystals using supercritical fluid technology. *European Journal of Pharmaceutical Sciences,* Volume 38, pp. 9-17.

Pearson, A., 2005. Carbon dioxide - new uses for an old refrigerant. *International Journal of Refrigeration 28,* pp. 1140-1148.

Petrov, N. & Popov, V., 1985. Heat transfer and resistance of carbon dioxide being cooled in the supercritical region. *Thermal Engineering,* 32(3), pp. 131-134.

Pettersen, J., Rieberer, R. & Munkejord, S., 2000. *Heat Transfer and Pressure Drop for flow of Supercritical and Subcritical CO2 in Microchannel Tubes. Final Technical Report for United States Army,* London, England: European Research Office of The U.S. Army.

Petukhov, B., 1970. Heat transfer and friction in turbulent pipe flow with variable physical properties. *Adv. Heat Transfer.,* Volume 6, pp. 503-564.

Pioro, I., Khartail, H. & Duffey, R., 2005. Experimental heat transfer of supercritical carbon dioxide flowing inside channels (survey). *Nuclear Engineering,* Volume 235, pp. 913-924.

Pitla, S., Groll, E. & Ramadhyani, S., 2002. New correlation to predict the heat transfer coefficient during in-tube cooling of turbulent supercritical CO2. *International Journal of Refrigeration 11,* 25(7), pp. 887-895.

Pitla, S., Robinson, D., Groll, E. & Ramadhyani, S., 1998. Heat transfer from supercritical carbon dioxide in tube flow: a critical review. *Hvac&R Research,* 4(3), pp. 281-301.

Polyakov, A., 1991. Heat transfer under supercritical pressures. *Adv. Heat Transfer,* Volume 21, pp. 1-53.

REFPROP, 2002. *NIST Refrigerant Properties Database 23,* Gaithersburg: MD Version 7.0.

Rousseau, P., 2013. *Thermal-Fluid systems modelling 1.* Potchefstroom: North-West University.

Schlager, L., Pate, M. & Bergles, A., 1990. Performance predictions of refrigerant-oil mixtures in smooth and internally finned tubes. *ASHRAE Trans,* Issue 96, pp. 170-182.

Schmierstoffe, F., 2009. *RENISO PAG 46 and RENISO PAG 100 Fully synthetic refrigeration oils based on special polyglycols (PAG) for R134a A/C systems,* Germany: Fuchs.

Son, C. & Park, S., 2006. An experimental study on heat transfer and pressure drop characteristics of carbon dioxide during gas cooling process in a horizontal tube. *International Journal of Refrigeration,* Volume 29, pp. 539-546.

Tincky, J., Macken, N. & W.M.B., 1985. An experimental investigation of heat transfer in forced convection condensation of oil-refrigerant mixtures. *ASHRAE Trans. 91,* pp. 297-309.

Wang, C., Hafner, A., Kuo, C. & Hsieh, W., 2012. An overview of the effect of lubricant on the heat transfer performance on conventional refrigerant and natural refrigerant R-744. *Renewable and Sustainable Energy Reviews,* Volume 16, pp. 2071-5086.

Wang, C., Hafner, A., Kuo, C. & Hsieh, W., 2012. An overview of the effect of lubricant on the heat transfer performance on conventional refrigerant and natural refrigerant R-744. *Renewable and Sustainable Energy Reviews,* Volume 16, pp. pp 2071-5086.

White, S., Yarall, M., Cleland, D. & Hedley, R., 2002. Modelling the performance of a transcritical CO2 heat pump for high temperature heating. *International Journal of Refrigeration,* 24(5), pp. 479-486.

Wolfram, S., 2002. A New Kind of Science. In: s.l.:Wolfram Media, p. 1019.

Yoon, S. et al., 2003. Heat transfer and pressure drop characteristics during the in-tube cooling process of carbon dioxide in the supercritical region. *International Journal of Refrigeration,* Volume 26, pp. 857-864.

Yun, R., Hwang, Y. & Radermacher, R., 2007. Convective gas cooling heat transfer and pressure drop characteristics of supercritical CO2/oil mixture in a mini-channel tube. *International Journalof Heat and Mass Transfer,* Volume 50, p. 804.

Zhao, C. & Jiang, P., 2011. Experimental study of in-tube cooling heat transfer and pressure drop characteristics of R134a at supercritical pressures. *Experimental Thermal and Fluid Science 10,* 35(7), pp. 1293-1303.

Zhao, C. & Jiang, P., 2014. Predictions of in-tube cooling pressure drops for CO2 mixed with lubricating oil at supercritical pressures. *Applied Thermal Engineering,* Volume 73, pp. 529-538.

Zhao, C., Jiang, P. & Zhang, Y., 2011. Flow and convection heat transfer characteristics of CO2 mixed with lubricating oil at super-critical pressures in small tube during cooling. *International Journal of Refrigeration,* Volume 34, pp. 29-39.

Zhao, X. & Bansal, P., 2009. Critical review of flow boiling heat transfer of CO2-lubricant mixtures. *International Journal of Heat and Mass Transfer ,* Volume 52, pp. 870-879.

Zingerli, A. & Groll, E., 2000. *Influence of refrigeration oil on the heat transfer and pressure drop of supercritical CO2 during in-tube cooling.* Purdue, IN, 4th IIR-Gustave Lorentzen Conference.

APPENDIX A: TEST DATA OF DANG ET AL. (2007)

The graphically read data from Dang et al. (2007) is reported in this appendix. Where 'd_{in}', 'p_i', 'G' and 'ω' refers to the inner diameter [mm] of the inner tube, the inlet pressure of the carbon dioxide [MPa], the mass flux [kg/m^{2}s] of the carbon dioxide and the oil concentration [%] respectively.

Test condition 1		
d_{in}:1, p_i:8, G:1200, ω:1		
T_i	T_e	$h_{c,exp}$
26,57	21,75	8925
30,06	26,1	10125
33,58	31,81	12000
34,5	33,58	13825
35,35	34,5	11275
36,02	34,94	10025
38,4	36,1	9650
41,23	37,6	7400
46	40,29	6875
52,98	44,56	6050
60,44	47,44	5800

Test condition 2		
d_{in}:1, p_i:8, G:1200, ω:3		
T_i	T_e	$h_{c,exp}$
26,57	21,61	8950
32,78	30,06	8825
34,8	33,83	9475
35,47	34,5	10250
36,35	34,77	8750
38,21	35,6	7550
46,41	40,23	5600
52,12	43,89	4975
62,18	47,66	4875

Test condition 3		
d_{in}:1, p_i:8, G:1200, ω:5		
T_i	T_e	$h_{c,exp}$
26,54	21,77	7700
31,47	28,54	5425
33,41	31,14	8300
35,49	34,61	8325
36,1	34,77	7000
38,04	35,6	6475
40,45	36,69	5800
45,58	40,23	4375
50,88	43,06	4375
63,49	48,27	4150

Test condition 4		
d_{in}:2, p_i:10, G:800, ω:1		
T_i	T_e	$h_{c,exp}$
31,92	27,43	3972
35,72	31,53	4175
38,81	35,21	4460
40,69	37,54	4415
42,26	39,51	4753
44,09	41,84	5084
45,15	43,16	4662
46,81	44,82	4888
49,62	47,4	4594
56,39	52,04	4232
63,44	54,34	4329

Test condition 5		
d_{in}:2, p_i:10, G:800, ω:3		
T_i	T_e	$h_{c,exp}$
32,57	28,21	2986
36,64	32,57	2925
39,87	36,86	2962
42,62	40,21	2849
45,91	43,91	2961
47,28	45,23	3006
49,53	47,06	2946
56,47	52,42	2810
63,49	55,4	2651

Test condition 6		
d_{in}:2, p_i:10, G:800, ω:5		
T_i	T_e	$h_{c,exp}$
32,62	28,21	2851
36,53	32,73	2760
39,92	36,89	2744
42,62	40,26	2698
44,64	42,65	2706
45,85	43,94	2856
47,03	45,91	2908
49,5	47,14	2645
56,89	52,56	2561
63,49	55,63	2470

Test condition 7		
d_{in}:4, p_i:8, G:800, ω:1		
T_i	T_e	$h_{c,exp}$
30,09	28,64	6278
33,64	33,08	8712
34,47	34,22	11975
35	34,84	15345
36,17	35,56	12419
37,26	36,4	9339
39,3	38,01	7332
42,5	40,5	5079
47,44	44,54	4495
51,79	48,61	3652
58,82	54,44	2975

Test condition 8		
d_{in}:4, p_i:8, G:800, ω:3		
T_i	T_e	$h_{c,exp}$
31,02	29,65	4148
32,72	31,77	4776
33,89	33,39	5112
34,28	33,97	5894
34,56	34,42	6950
35,06	34,84	7149
36,06	35,67	6521
38,1	37,21	5387
42,42	40,5	3930
48,69	45,82	3331
57,28	53,32	2869

Test condition 9		
d_{in}:4, p_i:8, G:800, ω:5		
T_i	T_e	$h_{c,exp}$
31,77	30,62	4179
33,47	32,8	4454
34,36	34,14	5327
35,84	35,34	4867
37,18	36,54	4698
40,66	39,21	3808
48,86	45,91	2963
57,93	53,91	2562

Test condition 10		
d_{in}:4, p_i:10, G:400, ω:1		
T_i	T_e	$h_{c,exp}$
32,81	28,98	2597
37,08	33,95	2823
41,41	39,32	3181
44,83	43,23	3782
47,53	45,72	3308
50,94	48,79	2945
55,82	52,67	2523
61,05	56,63	2211
66,1	59,73	2061

Test condition 11		
d_{in}:4, p_i:10, G:400, ω:3		
T_i	T_e	$h_{c,exp}$
31,38	27,22	2115
36,1	32,44	1953
41,58	38,92	1990
44,98	43,17	2088
48,87	46,71	1939
54,34	51,02	1776
66,1	60,23	1451

Test condition 12		
d_{in}:4, p_i:10, G:400, ω:5		
T_i	T_e	$h_{c,exp}$
31,13	26,71	1624
34,95	30,87	1539
39,25	36,27	1543
43,17	41,07	1824
45,48	43,47	1777
47,55	45,48	1777
49,87	47,47	1640
54,17	50,93	1529
59,06	54,81	1392
63,39	58,33	1315

Test condition 13		
d_{in}:6, p_i:8, G:400, ω:1		
T_i	T_e	$h_{c,exp}$
31,37	29,85	3066
32,42	31,17	3301
33,66	33	4424
34,38	34,05	6309
36,21	35,46	7424
38,64	37,2	4884
41,52	39,28	3576
47,88	44,14	2418
50,75	46,88	2133
58,05	52,94	1864

Test condition 14		
d_{in}:6, p_i:8, G:400, ω:3		
T_i	T_e	$h_{c,exp}$
32,5	31,31	2898
33,41	32,75	4155
34,05	33,72	4817
34,71	34,44	6192
36,87	35,9	5404
40,11	38,34	3350
47,88	44,45	2008
52,27	47,88	1747
56,81	52,27	1679
61,92	56,81	1637

Test condition 15		
d_{in}:6, p_i:8, G:400, ω:5		
T_i	T_e	$h_{c,exp}$
32,69	31,48	2370
33,83	33,25	2554
34,41	34,05	4021
35,79	35,24	5094
37,23	36,04	4557
38,31	36,79	3853
40,02	38,17	2897
45,58	42,65	1982
57,64	52,91	1469
62,92	57,61	1409

Test condition 16		
d_{in}:6, p_i:8, G:400, ω:7.5		
T_i	T_e	$h_{c,exp}$
31,75	30,18	2664
34,41	34,08	5094
35,82	35,1	6301
38,28	36,87	4331
42,59	40,11	2847
45,06	42,07	2385

Test condition 17		
d_{in}:6, p_i:8, G:400, ω:13		
T_i	T_e	$h_{c,exp}$
30,92	29,02	2387
33,74	33,03	3502
34,96	34,57	5907
36,4	35,46	5530
38,11	36,7	4205
42,76	40,35	2595
49,2	45,8	1739
58,63	53,99	1310

Test condition 18		
d_{in}:6, p_i:10, G:400, ω:1		
T_i	T_e	$h_{c,exp}$
30,24	27,03	2593
34,15	31,58	2643
37,94	35,68	2803
41,48	39,75	3215
44,05	42,71	3712
46,79	45,61	4364
49,6	48,18	3977
52,48	50,5	3603
56,3	53,87	2955
60,9	57,03	2643

Test condition 19		
d_{in}:6, p_i:10, G:400, ω:5		
T_i	T_e	$h_{c,exp}$
31,55	28,51	1978
37,55	35,04	2218
41,99	40,31	2555
44,16	42,8	2580
45,39	44,14	2929
47,04	45,64	3114
48,79	47,29	3056
52,59	50,58	2727
60,65	57,42	1856

Test condition 20		
d_{in}:6, p_i:10, G:400, ω:10		
T_i	T_e	$h_{c,exp}$
31,22	28,26	2210
35,21	32,47	2180
38,11	35,88	2281
41,18	39,34	2555
43,97	42,66	2955
46,79	45,45	3241
49,58	48,01	3039
52,39	50,41	2803
56,22	53,79	2058
60,93	57,92	1620

APPENDIX B: TEST DATA OF ZHAO ET AL. (2011)

Where 'd_{in}', 'p_i', 'G' and 'ω' refers to the inner diameter [mm] of the inner tube, the inlet pressure of the carbon dioxide [MPa], the mass flux [kg/m^{2}s] of the carbon dioxide and the oil concentration [%] respectively.

Test condition 1		
d_{in}:1.98, p_i:8, G:800, ω:1		
T_i	T_e	$h_{c,exp}$
26,28	17,29	3501,27
32,31	26,06	5194,66
34,45	31,00	7419,85
35,39	33,91	9519,08
35,84	34,19	12444,02
36,82	35,06	9938,93
38,18	35,50	8091,60
40,15	36,26	6454,20
44,30	37,84	4816,79
51,97	39,98	4592,88
61,23	41,95	4047,07
81,55	58,76	2633,59
93,98	66,81	2591,60

Test condition 2		
d_{in}:1.98, p_i:8, G:800, ω:2		
T_i	T_e	$h_{c,exp}$
26,71	18,33	2787,53
32,36	26,17	3389,31
34,11	30,66	4648,85
35,38	34,12	6524,17
36,25	35,05	5810,43
43,21	36,91	4159,03
52,19	38,93	4243,00
60,46	41,40	3389,31
79,52	54,16	2927,48
98,80	64,13	2647,58

Test condition 3		
d_{in}:1.98, p_i:8, G:1200, ω:1		
T_i	T_e	$h_{c,exp}$
27,05	20,59	5279,11
30,93	27,05	6624,77
34,13	31,67	11670,98
35,18	34,32	17597,04
35,98	35,42	16665,43
38,69	36,10	9911,28
39,92	36,35	8125,69
43,86	38,01	7038,82
50,81	40,10	4968,58
62,76	47,06	4916,82

Test condition 4		
d_{in}:1.98, p_i:8, G:1200, ω:2		
T_i	T_e	$h_{c,exp}$
27,36	20,71	3597,04
31,55	27,54	4166,36
34,38	31,42	5589,65
35,36	34,44	8565,62
37,02	36,10	9005,55
36,10	35,30	11231,05
39,30	36,59	7530,50
43,86	37,89	6158,96
52,78	40,10	4606,28
63,74	46,01	4528,65
77,65	55,37	3985,21
98,83	71,68	3700,55

Test condition 5		
d_{in}:1.98, p_i:11, G:400, ω:1		
T_i	T_e	$h_{c,exp}$
32,01	15,36	1667,85
37,03	19,61	1667,85
41,58	24,09	1944,94
46,18	33,07	1992,90
43,29	28,05	2056,84
48,42	36,26	2168,74
50,96	40,04	2264,65
53,32	42,04	2264,65
57,64	43,93	2227,35
59,88	45,94	2211,37
71,81	51,26	2067,50
84,80	58,64	2008,88
96,14	62,78	1806,39

Test condition 6		
d_{in}:1.98, p_i:11, G:400, ω:2		
T_i	T_e	$h_{c,exp}$
35,44	12,70	1726,47
39,57	19,19	1896,98
41,58	26,63	1955,60
47,83	34,66	2110,12
51,43	38,62	2312,61
53,62	42,34	2344,58
62,13	45,94	2072,82
74,41	51,38	1918,29
85,22	58,59	1731,79
95,02	65,26	1561,28

Test condition 7		
d_{in}:4.14, p_i:11, G:400, ω:2		
T_i	T_e	$h_{c,exp}$
26,67	17,90	1467,11
31,83	23,66	1750,00
34,19	30,07	2092,11
35,06	33,58	2875,00
35,83	34,63	3710,53
38,79	36,16	3006,58
41,37	36,82	2631,58
43,89	37,26	2526,32
51,68	39,67	1980,26
61,83	45,10	1592,11
78,17	56,29	1434,21

APPENDIX C: VISCOSITY GRAPHS

The variation of the viscosity of POE-oil (solest-68), PAG-oil (PAG100) and carbon dioxide can be seen in Figure 18.

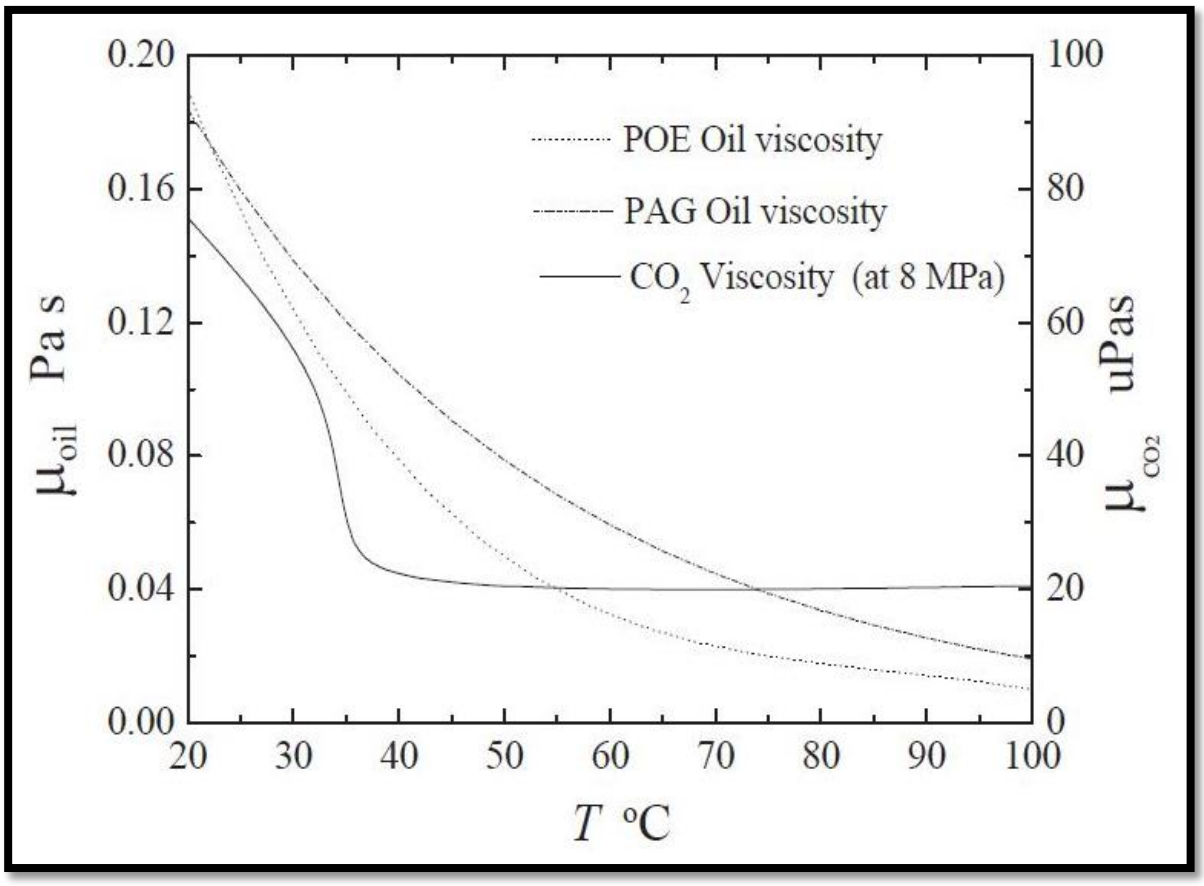

Figure 18 Viscosity versus temperature for POE-oil (solest-68), PAG-oil (PAG100) and carbon dioxide, (Zhao & Jiang, 2014).

APPENDIX D: CORRELATION OF ZHAO ET AL. (2011) TESTED ON DANG ET AL. (2007)'S TEST DATA

I. EES coding

```
"Engineering Equation Solver program"
"Testing of Zhao et al. (2011) on the test data of Dang et al. (2007)"
"Leander Kleyn"
"============================================================"
                          {Functions}
"============================================================"
Function convection(h_c_CO2,rho_oil,rho_b_CO2,omega,mu_oil,mu_b_CO2,T_ave,T_pc)

    If (T_ave<=T_pc) Then
        convection = h_c_CO2*(1.186*((rho_oil/rho_b_CO2)^(-0.236))*(omega*mu_oil/mu_b_CO2)^(-0.114))
    Else
        convection = h_c_CO2*(0.764*((rho_oil/rho_b_CO2)^(0.53))*(omega*mu_oil/mu_b_CO2)^(-0.227))
    Endif

End
"============================================================"
Function prandltnumber_D&H(cp_b_CO2,cp_ave_CO2_D&H,mu_b_CO2,mu_f_CO2_D&H,k_b_CO2,k_f_CO2_D&H,
Ratio_b,Ratio_f)

    If (cp_b_CO2>=cp_ave_CO2_D&H) Then
        prandltnumber_D&H = cp_b_CO2*mu_b_CO2/k_b_CO2
    Else
            If (Ratio_b>=Ratio_f) Then
              prandltnumber_D&H = cp_ave_CO2_D&H*mu_b_CO2/k_b_CO2
            Else
              prandltnumber_D&H = cp_ave_CO2_D&H*mu_f_CO2_D&H/k_f_CO2_D&H
            Endif
    Endif

End
"============================================================"
                          {Main program}
"============================================================"
"-----------------------------------------GENERAL-------------------------------------------------"
"Input parameters"
d_input = 1 [mm]                        "Diameter of inner tube"
P_input = 8 [MPa]                       "Absolute static pressure"
G = 1200 [kg/m^2-s]                     "Mass flux of carbon dioxide"
T_pc = 34.7 [C]                         "Pseudocritical temperature"
omega_input = 5 [%]                     "Oil concentration"
T_i_input = 30.09 [C]                   "Inlet bulk temperature"
T_e_input = 28.644 [C]                  "Outlet bulk temperature"
h_c_exp = 8925 [W/m^2-K]                "Convection heat transfer coefficient from test"
L = 0.5 [m]                             "Length of test section"

"SI Calculations"
d_in = d_input/1000                     "Diameter of inner tube"
P = P_input*10^6                        "Absolute static pressure"
omega = omega_input/100                 "Oil concentration"
T_i = T_i_input+273.15                  "Inlet bulk temperature"
T_e = T_e_input+273.15                  "Outlet bulk temperature"
T_ave = (T_i_input+T_e_input)/2         "Average bulk temperature"
T_ave_Kelvin = T_ave+273.15             "Average bulk temperature"
T_pc_Kelvin = T_pc+273.15


"Area calculations"
A_ff = pi*(d_in/2)^2                    "Free flow area of inner tube"
```

```
A_wall = pi*d_in*L                                  "Inner wall area"

"Mass flow rate calculations"
m_dot_CO2 = G*A_ff                                  "Mass flow rate of CO2"
omega = (m_dot_oil/(m_dot_oil+m_dot_CO2))     "Mass flow rate of oil"

"Heat transfer and real wall temperature"
Q_dot = m_dot_CO2*(h_i-h_e)
Q_dot_flux = Q_dot/A_wall
T_ave_Kelvin-T_wall = Q_dot*(1/(h_c_exp*A_wall) + F/A_wall)

"Fouling factor"
F=foulingfactor('CO2 vapor')


"---------------------------------------FLUID PROPERTIES----------------------------------------"
"Oil properties"
"Polyalkylene glycol: PAG100"

{Density calculation}
A = 0.6
T_ref = 15 [C]                                  "Reference temperature"
rho_oil_ref = 996 [kg/m^3]                      "Reference density"

rho_oil = rho_oil_ref - A*(T_ave - T_ref)          "Oil density"

{Viscosity calculation}
mu_oil = (3.17343e-01) - (8.48149e-03)*T_ave + (1.01243e-04)*T_ave^2 - (6.21890e-07)*T_ave^3 + (1.59488e-
09)*T_ave^4   "Oil viscosity"


"Carbon dioxide properties"

//At bulk temperature
rho_b_CO2 = density(CarbonDioxide,T=T_ave_Kelvin,P=P)            "Density of CO2"
mu_b_CO2 = viscosity(CarbonDioxide,T=T_ave_Kelvin,P=P)           "Viscosity"
k_b_CO2 = conductivity(CarbonDioxide,T=T_ave_Kelvin,P=P)         "Thermal conductivity"
cp_b_CO2 = cp(CarbonDioxide,T=T_ave_Kelvin,P=P)                  "Specific heat"
h_b_CO2 = enthalpy(CarbonDioxide,T=T_ave_Kelvin,P=P)             "Enthalpy at average temperature"
h_i =  enthalpy(CarbonDioxide,T=T_i,P=P)                        "Enthalpy at inlet temperature"
h_e =  enthalpy(CarbonDioxide,T=T_e,P=P)                        "Enthalpy at outlet temperature"

//At pseudo-critical temperature
rho_pc_CO2 = density(CarbonDioxide,T=T_pc_Kelvin,P=P)

{Dimensionless parameters}
//At bulk temperature
Re_b = G*d_in/mu_b_CO2                          "Reynolds number"
Pr_b = cp_b_CO2*mu_b_CO2/k_b_CO2                "Prandtl number"


"----------------------------------------CORRELATIONS-----------------------------------------"
"============================================================="
"============================================================="
{Correlation by Dang & Hihara - 2004}

Nusselt_D&H = (f_fil_G_f_D&H/8)*(Re_b-1000)*Pr_D&H*(1.07+12.7*sqrt(f_fil_G_f_D&H/8)*(Pr_D&H^(2/3)-1))^(-1)

f_fil_G_f_D&H = (1.82*log10(Re_f_D&H)-1.64)^(-2)
T_f_D&H = (T_w_D&H+T_ave_Kelvin)/2
cp_ave_CO2_D&H = (h_b_CO2-h_w_CO2_D&H)/(T_ave_Kelvin-T_w_D&H)

T_ave_Kelvin-T_w_D&H = Q_dot*(1/(h_c_D&H_comp*A_wall)+ F/A_wall)

{Prandtl number}
Ratio_b = mu_b_CO2/k_b_CO2
Ratio_f = mu_f_CO2_D&H/k_f_CO2_D&H
```

```
Pr_D&H =
prandltnumber_D&H(cp_b_CO2,cp_ave_CO2_D&H,mu_b_CO2,mu_f_CO2_D&H,k_b_CO2,k_f_CO2_D&H,Ratio_b,
Ratio_f)

"Dimensionless parameters"
//At film temperature
Re_f_D&H = G*d_in/mu_f_CO2_D&H

"Carbon dioxide properties"
//At film temperature
rho_f_CO2_D&H = density(CarbonDioxide,T=T_f_D&H,P=P)
mu_f_CO2_D&H = viscosity(CarbonDioxide,T=T_f_D&H,P=P)
k_f_CO2_D&H = conductivity(CarbonDioxide,T=T_f_D&H,P=P)
cp_f_CO2_D&H = cp(CarbonDioxide,T=T_f_D&H,P=P)
h_w_CO2_D&H = enthalpy(CarbonDioxide,T=T_w_D&H,P=P)

h_c_D&H = Nusselt_D&H*k_f_CO2_D&H/d_in
Error_D&H = (100*((h_c_D&H-h_c_exp)/h_c_exp))

{Correlation by Zhao et al. - 2011}
//Compensated
h_c_D&H_comp = convection(h_c_D&H,rho_oil,rho_b_CO2,omega,mu_oil,mu_b_CO2,T_ave,T_pc)
Error_D&H_comp = (100*((h_c_D&H_comp-h_c_exp)/h_c_exp))
"============================================================"
"============================================================"
```

II. Numerical results

Test condition 1		
d_{in}:1, p_i:8, G:1200, ω:1		
$h_{c,exp}$	$h_{c,Z}$	$E_{\%}$
8925	5924	-33,62
10125	6361	-37,18
12000	9412	-21,57
13825	13811	-0,1028
11275	13644	21,02
10025	15690	56,5
9650	13940	44,46
7400	8472	14,49
6875	5978	-13,04
6050	4841	-19,98
5800	4535	-21,81

Test condition 2		
d_{in}:1, p_i:8, G:1200, ω:3		
$h_{c,exp}$	$h_{c,Z}$	$E_{\%}$
8950	5241	-41,44
8825	7081	-19,76
9475	13786	45,49
10250	10602	3,439
8750	10326	18,01
7550	13596	80,08
5600	4850	-13,4
4975	3944	-20,72
4875	3596	-26,23

Test condition 3		
d_{in}:1, p_i:8, G:1200, ω:5		
$h_{c,exp}$	$h_{c,Z}$	$E_{\%}$
7700	4949	-35,73
5425	5973	10,1
8300	7389	-10,98
8325	9469	13,74
7000	9273	32,48
6475	12244	89,1
5800	8660	49,3
4375	4373	-0,054
4375	3682	-15,84
4150	3206	-22,76

Test condition 4		
d_{in}:2, p_i:10, G:800, ω:1		
$h_{c,exp}$	$h_{c,Z}$	$E_{\%}$
3972	3777	-4,903
4175	3984	-4,576
4460	4365	-2,121
4415	4716	6,831
4753	5066	6,595
5084	5529	8,753
4662	5732	22,96
4888	4535	-7,214
4594	4821	4,94
4232	4227	-0,1183
4329	4089	-5,561

Test condition 5		
d_{in}:2, p_i:10, G:800, ω:3		
$h_{c,exp}$	$h_{c,Z}$	$E_{\%}$
2986	3376	13,05
2925	3574	22,17
2962	4040	36,39
2849	4568	60,32
2961	5142	73,65
3006	3618	20,36
2946	3890	32,04
2810	3312	17,89
2651	3133	18,18

Test condition 6		
d_{in}:2, p_i:10, G:800, ω:5		
$h_{c,exp}$	$h_{c,Z}$	$E_{\%}$
2851	3196	12,1
2760	3364	21,91
2744	3827	39,45
2698	4317	59,98
2706	4722	74,51
2856	4848	69,74
2908	3185	9,516
2645	3473	31,33
2561	3013	17,64
2470	2817	14,05

Test condition 7		
d_{in}:4, p_i:8, G:800, ω:1		
$h_{c,exp}$	$h_{c,Z}$	$E_{\%}$
6278	4012	-36,09
8712	6366	-26,93
11975	9299	-22,35
15345	8201	-46,55
12419	9339	-24,8
9339	10029	7,382
7332	6740	-8,067
5079	4410	-13,17
4495	3233	-28,08
3652	2734	-25,12
2975	2491	-16,28

Test condition 8		
d_{in}:4, p_i:8, G:800, ω:3		
$h_{c,exp}$	$h_{c,Z}$	$E_{\%}$
4148	3791	-8,614
4776	4564	-4,423
5112	6120	19,71
5894	7444	26,31
6950	8683	24,92
7149	6238	-12,75
6521	7787	19,42
5387	6326	17,43
3930	3660	-6,885
3331	2445	-26,59
2869	2008	-30,01

Test condition 9		
d_{in}:4, p_i:8, G:800, ω:5		
$h_{c,exp}$	$h_{c,Z}$	$E_{\%}$
4179	3831	-8,326
4454	5043	13,23
5327	7452	39,9
4867	5302	8,939
4698	6497	38,29
3808	3953	3,791
2963	2235	-24,57
2562	1797	-29,88

Test condition 10		
d_{in}:4, p_i:10, G:400, ω:1		
$h_{c,exp}$	$h_{c,Z}$	$E_{\%}$
2597	1962	-24,45
2823	2082	-26,24
3181	2494	-21,58
3782	2884	-23,75
3308	2370	-28,35
2945	2474	-16,01
2523	2176	-13,75
2211	1897	-14,17
2061	1791	-13,07

Test condition 11		
d_{in}:4, p_i:10, G:400, ω:3		
$h_{c,exp}$	$h_{c,Z}$	$E_{\%}$
2115	1711	-19,1
1953	1832	-6,183
1990	2237	12,39
2088	2582	23,64
1939	2003	3,339
1776	1964	10,58
1451	1425	-1,777

Test condition 12		
d_{in}:4, p_i:10, G:400, ω:5		
$h_{c,exp}$	$h_{c,Z}$	$E_{\%}$
1624	1619	-0,3532
1539	1726	12,18
1543	1903	23,32
1824	2277	24,84
1777	2485	39,86
1777	1704	-4,081
1640	1844	12,45
1529	1787	16,92
1392	1543	10,87
1315	1358	3,34

Test condition 13		
d_{in}:6, p_i:8, G:400, ω:1		
$h_{c,exp}$	$h_{c,Z}$	$E_{\%}$
3066	2315	-24,49
3301	2584	-21,71
4424	3317	-25,02
6309	4572	-27,54
7424	4621	-37,76
4884	4600	-5,823
3576	3336	-6,711
2418	1977	-18,27
2133	1663	-22,03
1864	1421	-23,76

Test condition 14		
d_{in}:6, p_i:8, G:400, ω:3		
$h_{c,exp}$	$h_{c,Z}$	$E_{\%}$
2898	2318	-20,01
4155	2756	-33,69
4817	3470	-27,97
6192	4484	-27,58
5404	3800	-29,67
3350	3108	-7,212
2008	1602	-20,2
1747	1368	-21,73
1679	1157	-31,09
1637	1071	-34,58

Test condition 15		
d_{in}:6, p_i:8, G:400, ω:5		
$h_{c,exp}$	$h_{c,Z}$	$E_{\%}$
2370	2252	-4,991
2554	2935	14,89
4021	3844	-4,405
5094	2765	-45,72
4557	3371	-26,02
3853	3816	-0,9506
2897	2969	2,494
1982	1726	-12,95
1469	1049	-28,6
1409	966,1	-31,45

Test condition 16		
d_{in}:6, p_i:8, G:400, ω:7.5		
$h_{c,exp}$	$h_{c,Z}$	$E_{\%}$
2664	1920	-27,94
5094	3688	-27,6
6301	2583	-59,01
4331	3505	-19,08
2847	2216	-22,14
2385	1827	-23,41

Test condition 17		
d_{in}:6, p_i:8, G:400, ω:13		
$h_{c,exp}$	$h_{c,Z}$	$E_{\%}$
2387	1673	-29,94
3502	2553	-27,1
5907	2330	-60,56
5530	2205	-60,13
4205	2828	-32,76
2595	1949	-24,89
1739	1181	-32,07
1310	863	-34,14

Test condition 18		
d_{in}:6, p_i:10, G:400, ω:1		
$h_{c,exp}$	$h_{c,Z}$	$E_{\%}$
2593	1810	-30,17
2643	1914	-27,6
2803	2039	-27,25
3215	2411	-25,03
3712	2699	-27,3
4364	2210	-49,36
3977	2386	-40,01
3603	2351	-34,75
2955	2045	-30,77
2643	1930	-26,97

Test condition 19		
d_{in}:6, p_i:10, G:400, ω:5		
$h_{c,exp}$	$h_{c,Z}$	$E_{\%}$
1978	1552	-21,54
2218	1718	-22,55
2555	2075	-18,78
2580	2280	-11,63
2929	2344	-20
3114	1604	-48,51
3056	1712	-43,95
2727	1729	-36,62
1856	1381	-25,6

Test condition 20		
d_{in}:6, p_i:10, G:400, ω:10		
$h_{c,exp}$	$h_{c,Z}$	$E_{\%}$
2210	1432	-35,21
2180	1525	-30,05
2281	1609	-29,45
2555	1859	-27,25
2955	2095	-29,08
3241	1375	-57,56
3039	1505	-50,47
2803	1514	-45,99
2058	1377	-33,1
1620	1181	-27,13

III. Graphical results

Note: The x-axis refers to the bulk temperature, T_b [℃], while the y-axis represents the convection heat transfer coefficients, h_c $\left[\frac{W}{m^2K}\right]$.

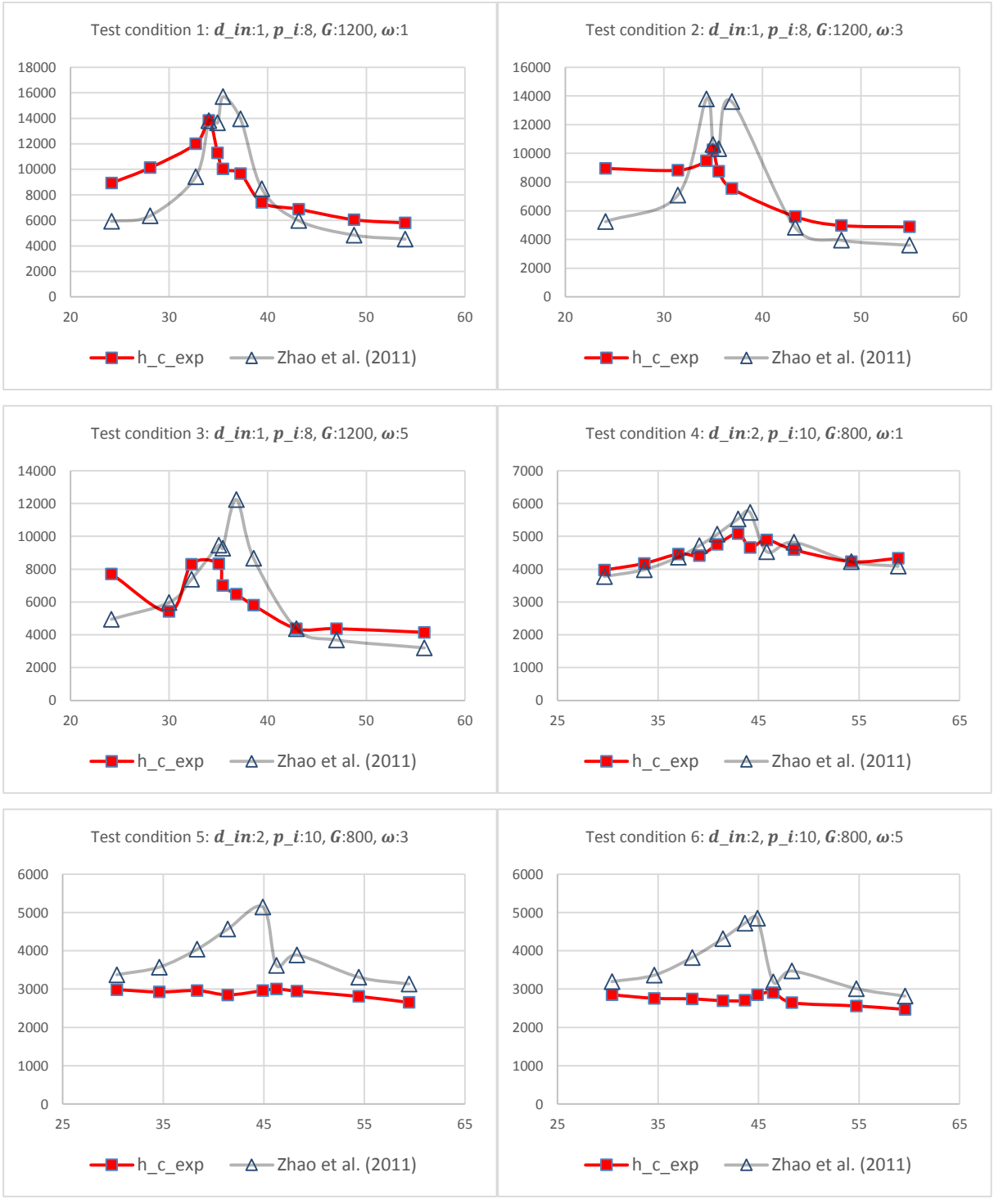

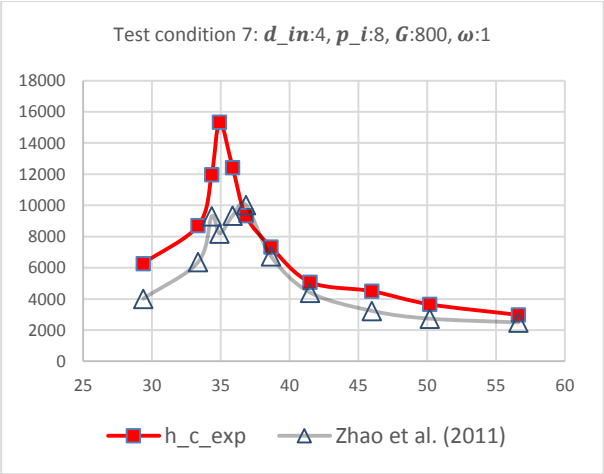
Test condition 7: d_in:4, p_i:8, G:800, ω:1
18000
16000
14000
12000
10000
8000
6000
4000
2000
0
25
30
35
40
45
50
55
60
h_c_exp
Zhao et al. (2011)

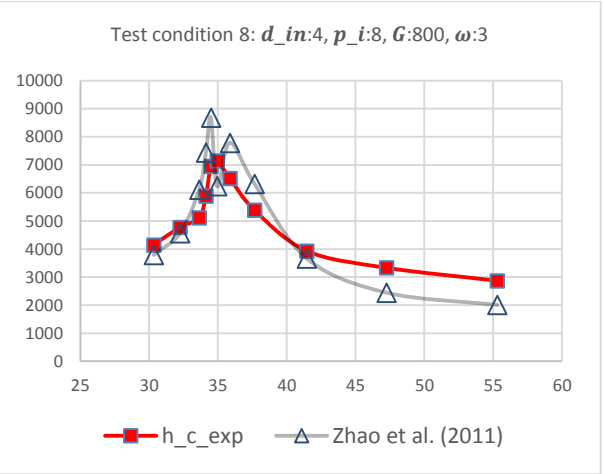
Test condition 8: d_in:4, p_i:8, G:800, ω:3
10000
9000
8000
7000
6000
5000
4000
3000
2000
1000
0
25
30
35
40
45
50
55
60
h_c_exp
Zhao et al. (2011)

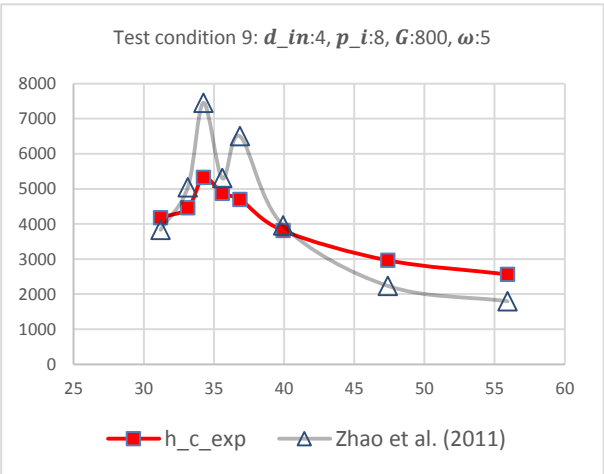
Test condition 9: d_in:4, p_i:8, G:800, ω:5
8000
7000
6000
5000
4000
3000
2000
1000
0
25
30
35
40
45
50
55
60
h_c_exp
Zhao et al. (2011)

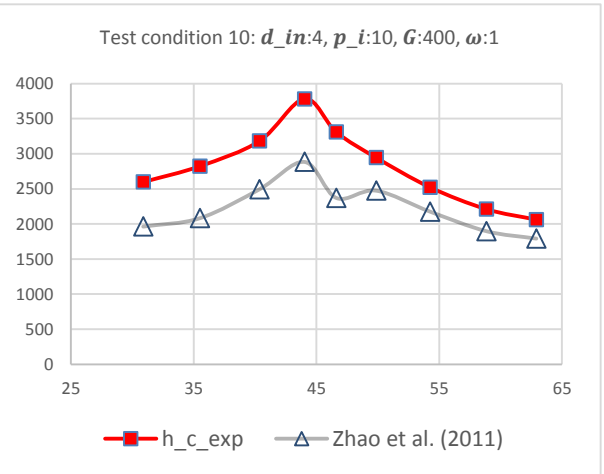
Test condition 10: d_in:4, p_i:10, G:400, ω:1
4000
3500
3000
2500
2000
1500
1000
500
0
25
35
45
55
65
h_c_exp
Zhao et al. (2011)

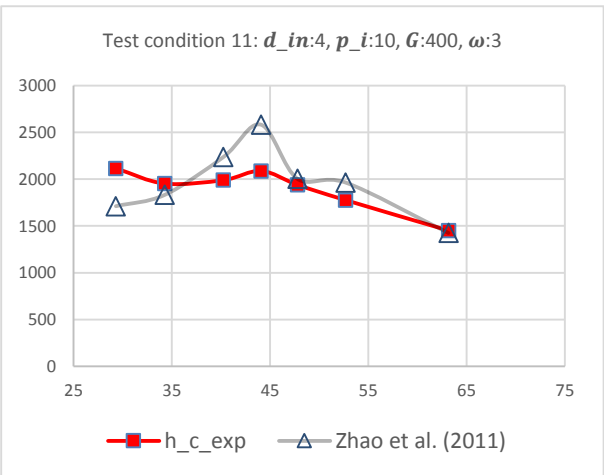
Test condition 11: d_in:4, p_i:10, G:400, ω:3
3000
2500
2000
1500
1000
500
0
25
35
45
55
65
75
h_c_exp
Zhao et al. (2011)

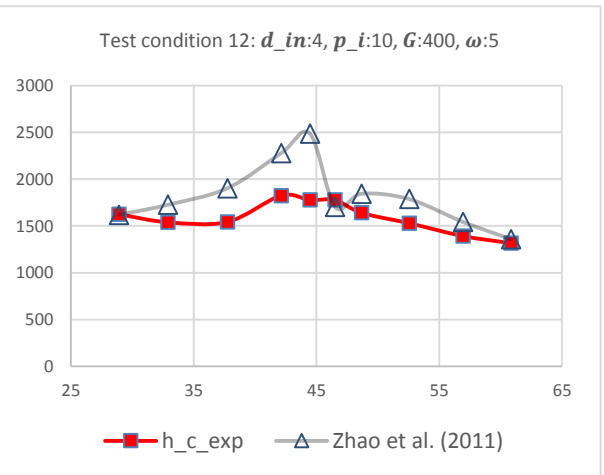
Test condition 12: d_in:4, p_i:10, G:400, ω:5
3000
2500
2000
1500
1000
500
0
25
35
45
55
65
h_c_exp
Zhao et al. (2011)

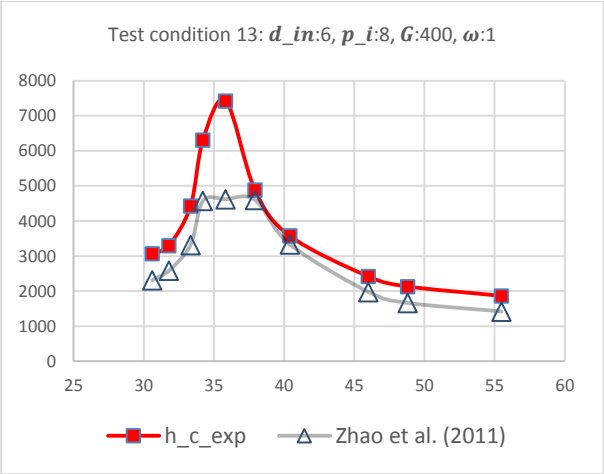
Test condition 13: d_in:6, p_i:8, G:400, ω:1
8000
7000
6000
5000
4000
3000
2000
1000
0
25
30
35
40
45
50
55
60
h_c_exp
Zhao et al. (2011)

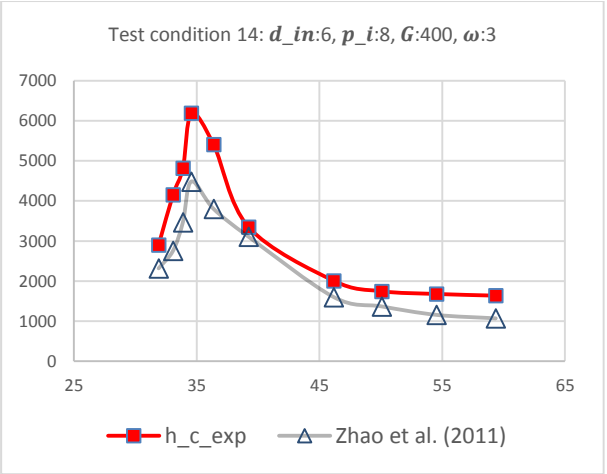
Test condition 14: d_in:6, p_i:8, G:400, ω:3
7000
6000
5000
4000
3000
2000
1000
0
25
35
45
55
65
h_c_exp
Zhao et al. (2011)

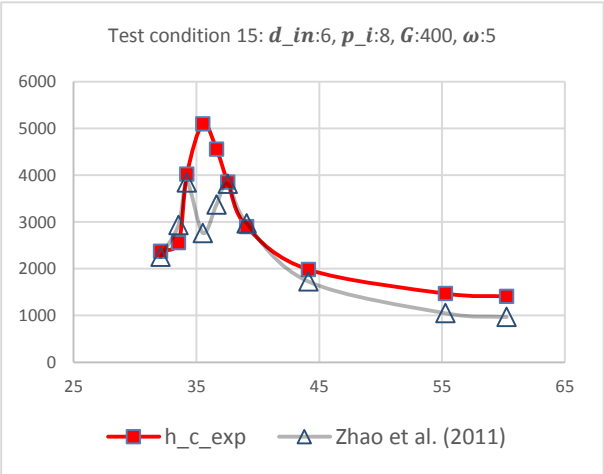
Test condition 15: d_in:6, p_i:8, G:400, ω:5
6000
5000
4000
3000
2000
1000
0
25
35
45
55
65
h_c_exp
Zhao et al. (2011)

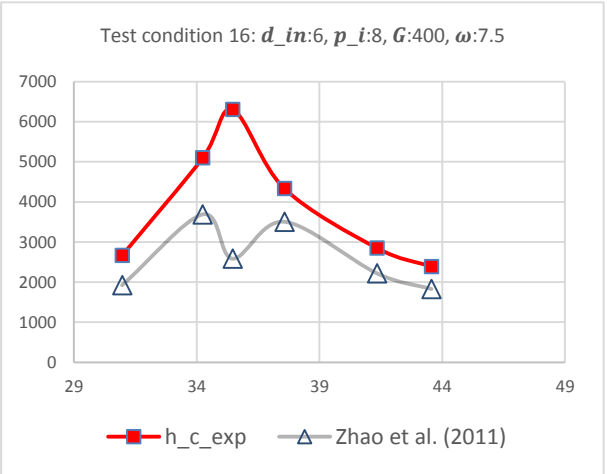
Test condition 16: d_in:6, p_i:8, G:400, ω:7.5
7000
6000
5000
4000
3000
2000
1000
0
29
34
39
44
49
h_c_exp
Zhao et al. (2011)

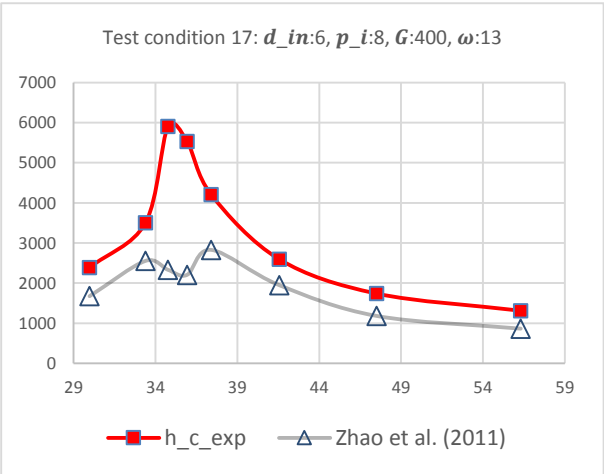
Test condition 17: d_in:6, p_i:8, G:400, ω:13
7000
6000
5000
4000
3000
2000
1000
0
29
34
39
44
49
54
59
h_c_exp
Zhao et al. (2011)

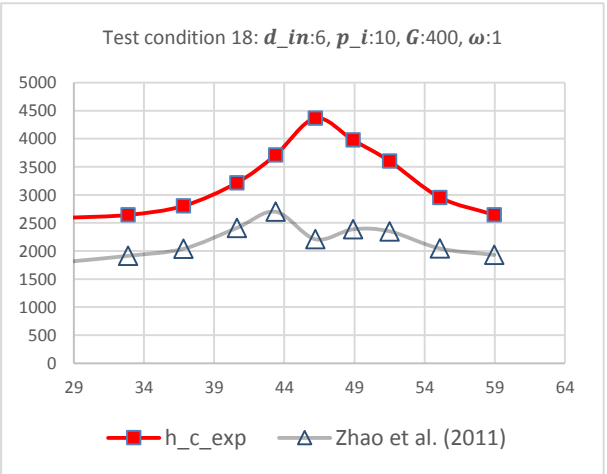
Test condition 18: d_in:6, p_i:10, G:400, ω:1
5000
4500
4000
3500
3000
2500
2000
1500
1000
500
0
29
34
39
44
49
54
59
64
h_c_exp
Zhao et al. (2011)

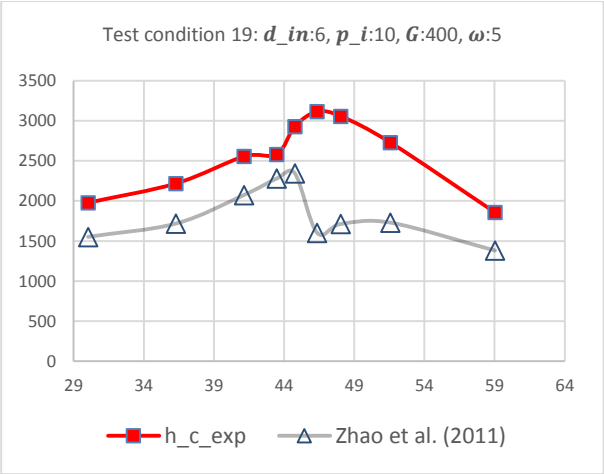
Test condition 19: d_in:6, p_i:10, G:400, ω:5
3500
3000
2500
2000
1500
1000
500
0
29
34
39
44
49
54
59
64
h_c_exp
Zhao et al. (2011)

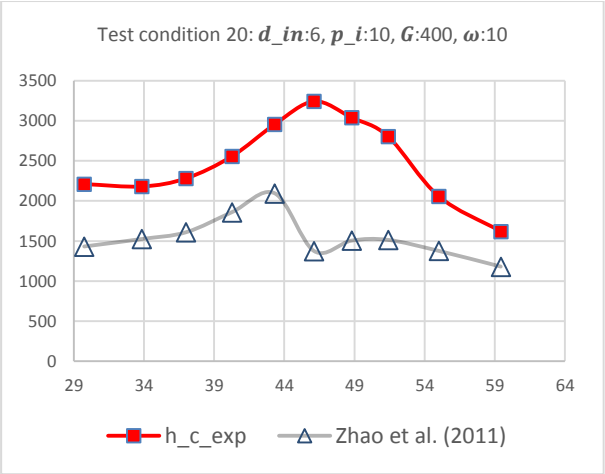
Test condition 20: d_in:6, p_i:10, G:400, ω:10
3500
3000
2500
2000
1500
1000
500
0
29
34
39
44
49
54
59
64
h_c_exp
Zhao et al. (2011)

APPENDIX E: ALTERNATIVE CORRELATIONS TESTED ON THE DATA OF DANG ET AL. (2007) AND ZHAO ET AL. (2011)

I. EES coding

```
"Engineering Equation Solver program"
"Alternative correlations tested on Dang et al. (2007)"
"Leander Kleyn"
"============================================================"
                        {Functions}
"============================================================"
Function nusselt_Y(Re_b,Pr_b,T_ave,T_pc,rho_b_CO2,rho_pc_CO2)

    If (T_ave<=T_pc) Then
        nusselt_Y =  0.013*Re_b*(Pr_b^(-0.05))*(rho_pc_CO2/rho_b_CO2)^1.6
    Else
        nusselt_Y =  0.14*(Re_b^0.69)*(Pr_b^0.66)
    Endif

End
"============================================================"
Function prandltnumber_D&H(cp_b_CO2,cp_ave_CO2_D&H,mu_b_CO2,mu_f_CO2_D&H,k_b_CO2,k_f_CO2_D&H,
Ratio_b,Ratio_f)

    If (cp_b_CO2>=cp_ave_CO2_D&H) Then
        prandltnumber_D&H = cp_b_CO2*mu_b_CO2/k_b_CO2
    Else
            If (Ratio_b>=Ratio_f) Then
              prandltnumber_D&H = cp_ave_CO2_D&H*mu_b_CO2/k_b_CO2
            Else
              prandltnumber_D&H = cp_ave_CO2_D&H*mu_f_CO2_D&H/k_f_CO2_D&H
            Endif
    Endif

End
"============================================================"
Function c_vp_Z&J(T_ave,T_pc,Pr_w_Z&J,Pr_b,cp_ave_Z&J,cp_b_CO2,rho_w_CO2_Z&J,rho_b_CO2,T_w_Z&J,
T_ave_Kelvin)

    If (T_ave<=T_pc) Then
        c_vp_Z&J = 0.93*((Pr_w_Z&J/Pr_b)^(-
0.11))*((cp_ave_Z&J/cp_b_CO2)^(0.96))*(rho_w_CO2_Z&J/rho_b_CO2)^1.06
    Else
        c_vp_Z&J = 1.07*((T_w_Z&J/T_ave_Kelvin)^(-
0.45))*((cp_ave_Z&J/cp_b_CO2)^(0.61))*(rho_w_CO2_Z&J/rho_b_CO2)^(-0.18)
    Endif

End

"============================================================"
                        {Main program}
"============================================================"
"----------------------------------------GENERAL-------------------------------------------------"
"Input parameters"
d_input = 1 [mm]                        "Diameter of inner tube"
P_input = 8 [MPa]                       "Absolute static pressure"
G = 1200 [kg/m^2-s]                     "Mass flux of carbon dioxide"
T_pc = 34.7 [C]                         "Pseudocritical temperature"
omega_input = 5 [%]                     "Oil concentration"
T_i_input = 30.09 [C]                   "Inlet bulk temperature"
T_e_input = 28.644 [C]                  "Outlet bulk temperature"
h_c_exp = 8925 [W/m^2-K]                "Convection heat transfer coefficient from test"
L = 0.5 [m]                             "Length of test section. Note: 1m for Zhao et al. (2011)'s data"
```

```
"SI Calculations"
d_in = d_input/1000                          "Diameter of inner tube"
P = P_input*10^6                             "Absolute static pressure"
omega = omega_input/100                      "Oil concentration"
T_i = T_i_input+273.15                       "Inlet bulk temperature"
T_e = T_e_input+273.15                       "Outlet bulk temperature"
T_ave = (T_i_input+T_e_input)/2              "Average bulk temperature"
T_ave_Kelvin = T_ave+273.15                  "Average bulk temperature"
T_pc_Kelvin = T_pc+273.15


"Area calculations"
A_ff = pi*(d_in/2)^2                         "Free flow area of inner tube"
A_wall = pi*d_in*L                           "Inner wall area"

"Mass flow rate calculations"
m_dot_CO2 = G*A_ff                           "Mass flow rate of CO2"
omega = (m_dot_oil/(m_dot_oil+m_dot_CO2))    "Mass flow rate of oil"

"Heat transfer and real wall temperature"
Q_dot = m_dot_CO2*(h_i-h_e)
Q_dot_flux = Q_dot/A_wall
T_ave_Kelvin-T_wall = Q_dot*(1/(h_c_exp*A_wall) + F/A_wall)

"Fouling factor"
F=foulingfactor('CO2 vapor')


"---------------------------------------FLUID PROPERTIES----------------------------------------"
"Oil properties"
"Polyalkylene glycol: PAG100"

{Density calculation}
A = 0.6
T_ref = 15 [C]                               "Reference temperature"
rho_oil_ref = 996 [kg/m^3]                   "Reference density. Use 957kg/m^3 for POE solest-68"

rho_oil = rho_oil_ref - A*(T_ave - T_ref)    "Oil density"

{Viscosity calculation}
mu_oil = (3.17343e-01) - (8.48149e-03)*T_ave + (1.01243e-04)*T_ave^2 - (6.21890e-07)*T_ave^3 + (1.59488e-
09)*T_ave^4                                  "Oil viscosity. Use equation 56 for POE solest-68"


"Carbon dioxide properties"

//At bulk temperature
rho_b_CO2 = density(CarbonDioxide,T=T_ave_Kelvin,P=P)        "Density of CO2"
mu_b_CO2 = viscosity(CarbonDioxide,T=T_ave_Kelvin,P=P)       "Viscosity"
k_b_CO2 = conductivity(CarbonDioxide,T=T_ave_Kelvin,P=P)     "Thermal conductivity"
cp_b_CO2 = cp(CarbonDioxide,T=T_ave_Kelvin,P=P)              "Specific heat"
h_b_CO2 = enthalpy(CarbonDioxide,T=T_ave_Kelvin,P=P)         "Enthalpy at average temperature"
h_i =  enthalpy(CarbonDioxide,T=T_i,P=P)                     "Enthalpy at inlet temperature"
h_e =  enthalpy(CarbonDioxide,T=T_e,P=P)                     "Enthalpy at outlet temperature"

//At pseudo-critical temperature
rho_pc_CO2 = density(CarbonDioxide,T=T_pc_Kelvin,P=P)

{Dimensionless parameters}
//At bulk temperature
Re_b = G*d_in/mu_b_CO2                       "Reynolds number"
Pr_b = cp_b_CO2*mu_b_CO2/k_b_CO2             "Prandtl number"


"---------------------------------------CORRELATIONS--------------------------------------------"
```

```
"============================================================"
{Correlation by Dittus & Boelter - 1985}

Nusselt_D&B = 0.023*(Re_b^0.8)*(Pr_b^n_D&B)
n_D&B = 0.3


h_c_D&B = Nusselt_D&B*k_b_CO2/d_in
Error_D&B = (100*((h_c_D&B-h_c_exp)/h_c_exp))

"============================================================"
"============================================================"
{Correlation 1 by Gnielinksi - 1975}

Nusselt_G = (f_fil_G/8)*(Re_b-1000)*Pr_b*(1.07+12.7*sqrt(f_fil_G/8)*(Pr_b^(2/3)-1))^(-1)
f_fil_G = (1.82*log10(Re_b)-1.64)^(-2)


h_c_G = Nusselt_G*k_b_CO2/d_in
Error_G = (100*((h_c_G-h_c_exp)/h_c_exp))

"============================================================"
"============================================================"
{Modified correlation by Gnielinksi - 1975}

Nusselt_G_M = ((f_fil_G/8)*(Re_b-1000)*Pr_b*(1.07+12.7*sqrt(f_fil_G/8)*(Pr_b^(2/3)-1))^(-1))*(1+(d_in/L)^(2/3))

h_c_G_M = Nusselt_G_M*k_b_CO2/d_in
Error_G_M = (100*((h_c_G_M-h_c_exp)/h_c_exp))

"============================================================"
"============================================================"
{Correlation by Yoon et al. - 2003}

Nusselt_Y = nusselt_Y(Re_b,Pr_b,T_ave,T_pc,rho_b_CO2,rho_pc_CO2)

h_c_Y = Nusselt_Y*k_b_CO2/d_in
Error_Y = (100*((h_c_Y-h_c_exp)/h_c_exp))

"============================================================"
"============================================================"
{Correlation by Pitla et al. - 2002}

Nusselt_P = ((Nusselt_P_w+Nusselt_P_b)/2)*(k_w_CO2_P/k_b_CO2)
Nusselt_P_b = (f_fil_G/8)*(Re_b-1000)*Pr_b*(1.07+12.7*sqrt(f_fil_G/8)*(Pr_b^(2/3)-1))^(-1)
Nusselt_P_w = (f_fil_G_w_P/8)*(Re_w_P-1000)*Pr_w_P*(1.07+12.7*sqrt(f_fil_G_w_P/8)*(Pr_w_P^(2/3)-1))^(-1)
f_fil_G_w_P = (1.82*log10(Re_w_P)-1.64)^(-2)

"Dimensionless parameters"
//At wall temperature
Re_w_P = G*d_in/mu_w_CO2_P
Pr_w_P = cp_w_CO2_P*mu_w_CO2_P/k_w_CO2_P

"Carbon dioxide properties"
//At wall temperature
rho_w_CO2_P = density(CarbonDioxide,T=T_w_P,P=P)          "Density of CO2"
mu_w_CO2_P = viscosity(CarbonDioxide,T=T_w_P,P=P)         "Viscosity"
k_w_CO2_P = conductivity(CarbonDioxide,T=T_w_P,P=P)       "Thermal conductivity"
cp_w_CO2_P = cp(CarbonDioxide,T=T_w_P,P=P)                "Specific heat"

T_ave_Kelvin-T_w_P = Q_dot*(1/(h_c_P*A_wall) + F/A_wall)

h_c_P = Nusselt_P*k_b_CO2/d_in
Error_P = (100*((h_c_P-h_c_exp)/h_c_exp))

"============================================================"
"============================================================"
```

{Correlation by Dang & Hihara - 2004}

Nusselt_D&H = (f_fil_G_f_D&H/8)*(Re_b-1000)*Pr_D&H*(1.07+12.7*sqrt(f_fil_G_f_D&H/8)*(Pr_D&H^(2/3)-1))^(-1)

f_fil_G_f_D&H = (1.82*log10(Re_f_D&H)-1.64)^(-2)
T_f_D&H = (T_w_D&H+T_ave_Kelvin)/2
cp_ave_CO2_D&H = (h_b_CO2-h_w_CO2_D&H)/(T_ave_Kelvin-T_w_D&H)

T_ave_Kelvin-T_w_D&H = Q_dot*(1/(h_c_D&H*A_wall)+ F/A_wall)

{Prandtl number}
Ratio_b = mu_b_CO2/k_b_CO2
Ratio_f = mu_f_CO2_D&H/k_f_CO2_D&H
Pr_D&H =
prandltnumber_D&H(cp_b_CO2,cp_ave_CO2_D&H,mu_b_CO2,mu_f_CO2_D&H,k_b_CO2,k_f_CO2_D&H,Ratio_b,
Ratio_f)

"Dimensionless parameters"
//At film temperature
Re_f_D&H = G*d_in/mu_f_CO2_D&H

"Carbon dioxide properties"
//At film temperature
rho_f_CO2_D&H = density(CarbonDioxide,T=T_f_D&H,P=P)
mu_f_CO2_D&H = viscosity(CarbonDioxide,T=T_f_D&H,P=P)
k_f_CO2_D&H = conductivity(CarbonDioxide,T=T_f_D&H,P=P)
cp_f_CO2_D&H = cp(CarbonDioxide,T=T_f_D&H,P=P)
h_w_CO2_D&H = enthalpy(CarbonDioxide,T=T_w_D&H,P=P)

h_c_D&H = Nusselt_D&H*k_f_CO2_D&H/d_in
Error_D&H = (100*((h_c_D&H-h_c_exp)/h_c_exp))

"=="
"=="
{Correlation by Zhao & Jiang - 2011}

Nusselt_Z&J = ((f_fil_G/8)*(Re_b-1000)*Pr_b*(1.07+12.7*sqrt(f_fil_G/8)*(Pr_b^(2/3)-1))^(-
1))*(1+(d_in/L)^(2/3))*C_vp_Z&J

C_vp_Z&J =
c_vp_Z&J(T_ave,T_pc,Pr_w_Z&J,Pr_b,cp_ave_Z&J,cp_b_CO2,rho_w_CO2_Z&J,rho_b_CO2,T_w_Z&J,T_ave_Kelvi
n)

cp_ave_Z&J = (h_i-h_e)/(T_i-T_e)

T_ave_Kelvin-T_w_Z&J = Q_dot*(1/(h_c_Z&J*A_wall) + F/A_wall)

"Dimensionless parameters"
//At wall temperature
Pr_w_Z&J = cp_w_CO2_Z&J*mu_w_CO2_Z&J/k_w_CO2_Z&J

"Carbon dioxide properties"
//At wall temperature
rho_w_CO2_Z&J = density(CarbonDioxide,T=T_w_Z&J,P=P)
mu_w_CO2_Z&J = viscosity(CarbonDioxide,T=T_w_Z&J,P=P)
k_w_CO2_Z&J = conductivity(CarbonDioxide,T=T_w_Z&J,P=P)
cp_w_CO2_Z&J = cp(CarbonDioxide,T=T_w_Z&J,P=P)

h_c_Z&J = Nusselt_Z&J*k_b_CO2/d_in
Error_Z&J = (100*((h_c_Z&J-h_c_exp)/h_c_exp))

"=="
"=="

II. Graphical results on Dang et al. (2007)'s data

Note: The x-axis refers to the bulk temperature, T_b [°C], while the y-axis represents the convection heat transfer coefficients, h_c $\left[\frac{W}{m^2K}\right]$. Also, the results for Yoon et al. (2003) are not included in these graphs, because this correlation shows large errors relative to the other correlations used and then makes it difficult to observe the other correlations' results.

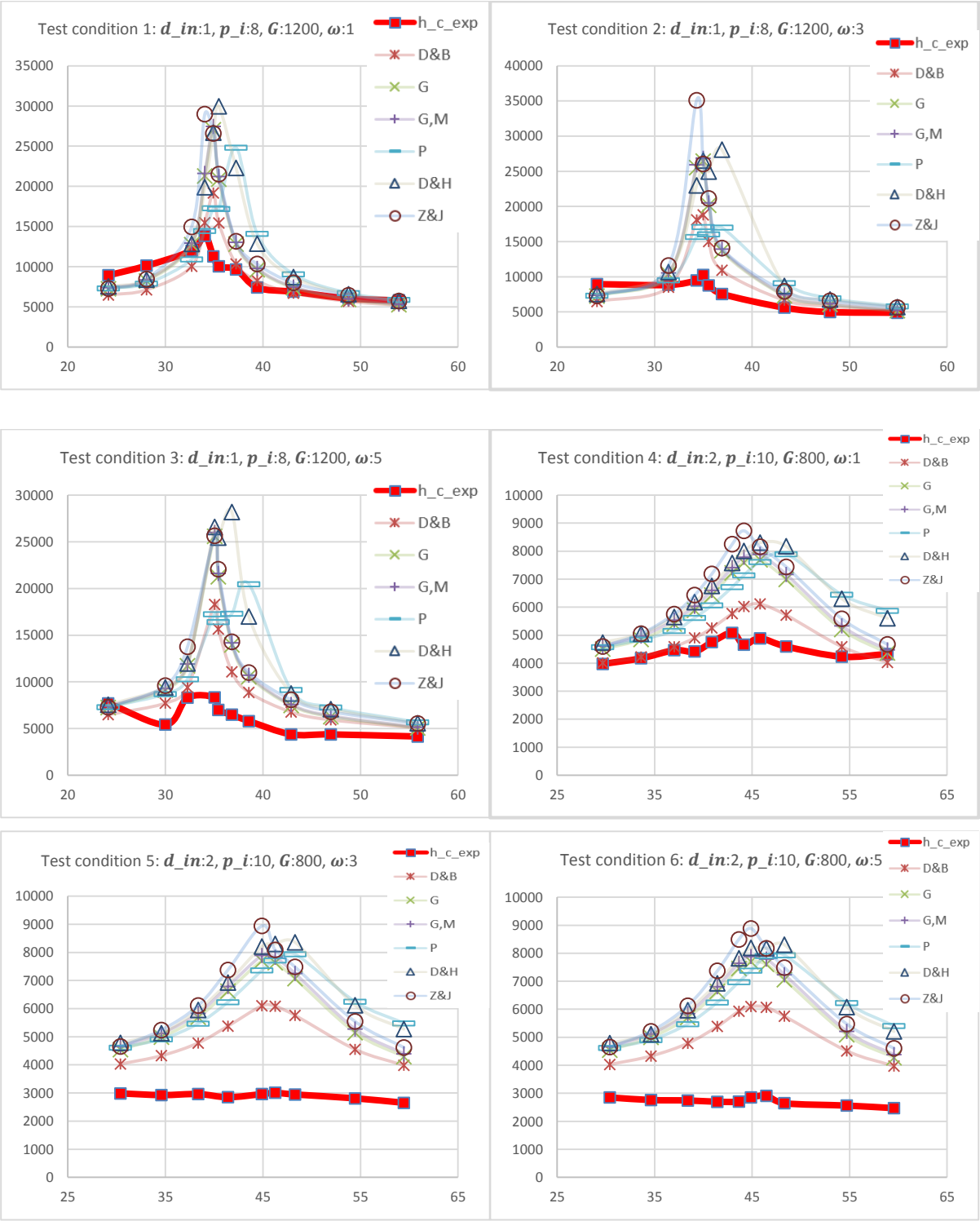

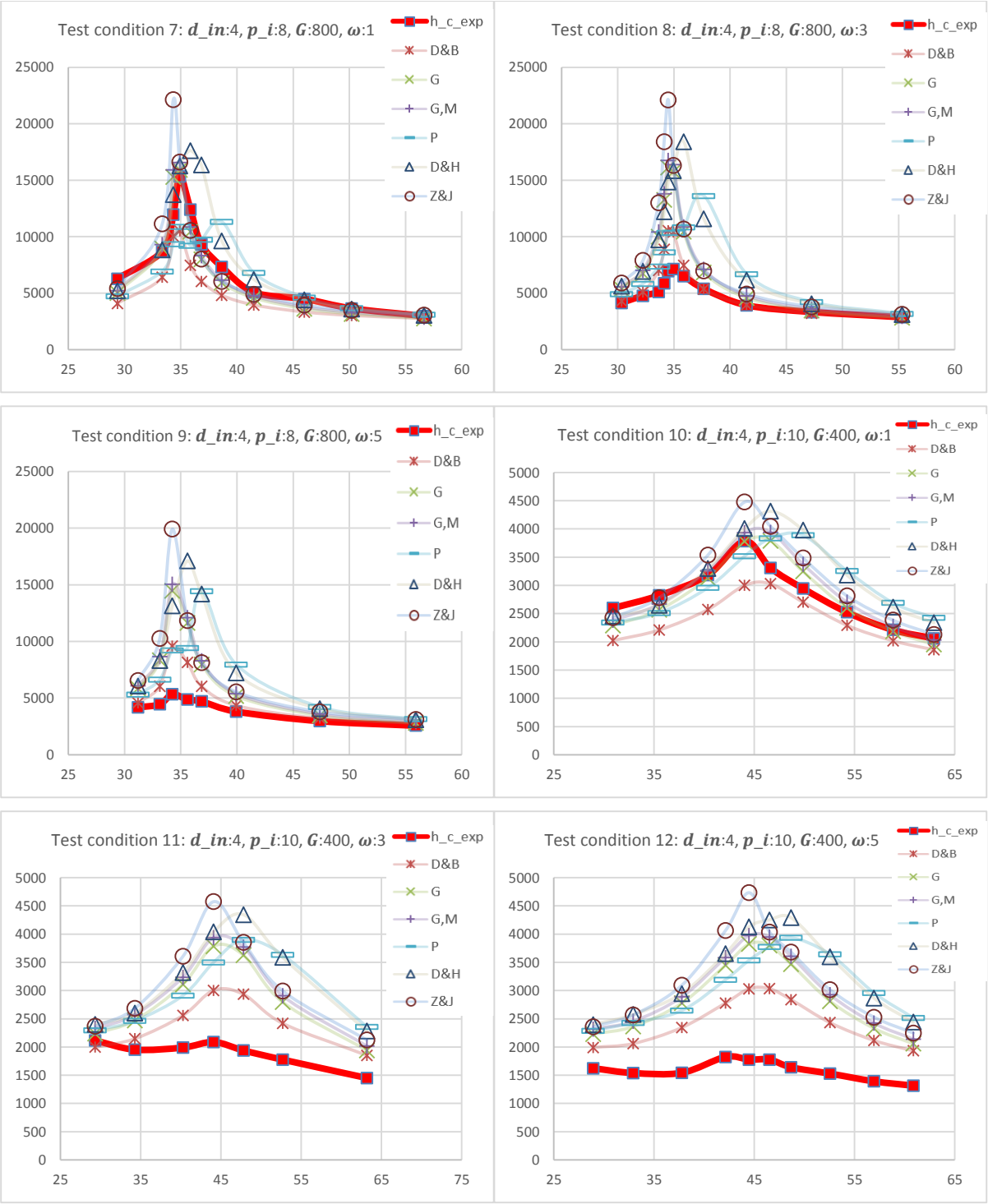
Test condition 7: d_in:4, p_i:8, G:800, ω:1
Test condition 8: d_in:4, p_i:8, G:800, ω:3
Test condition 9: d_in:4, p_i:8, G:800, ω:5
Test condition 10: d_in:4, p_i:10, G:400, ω:1
Test condition 11: d_in:4, p_i:10, G:400, ω:3
Test condition 12: d_in:4, p_i:10, G:400, ω:5
h_c_exp
D&B
G
G,M
P
D&H
Z&J

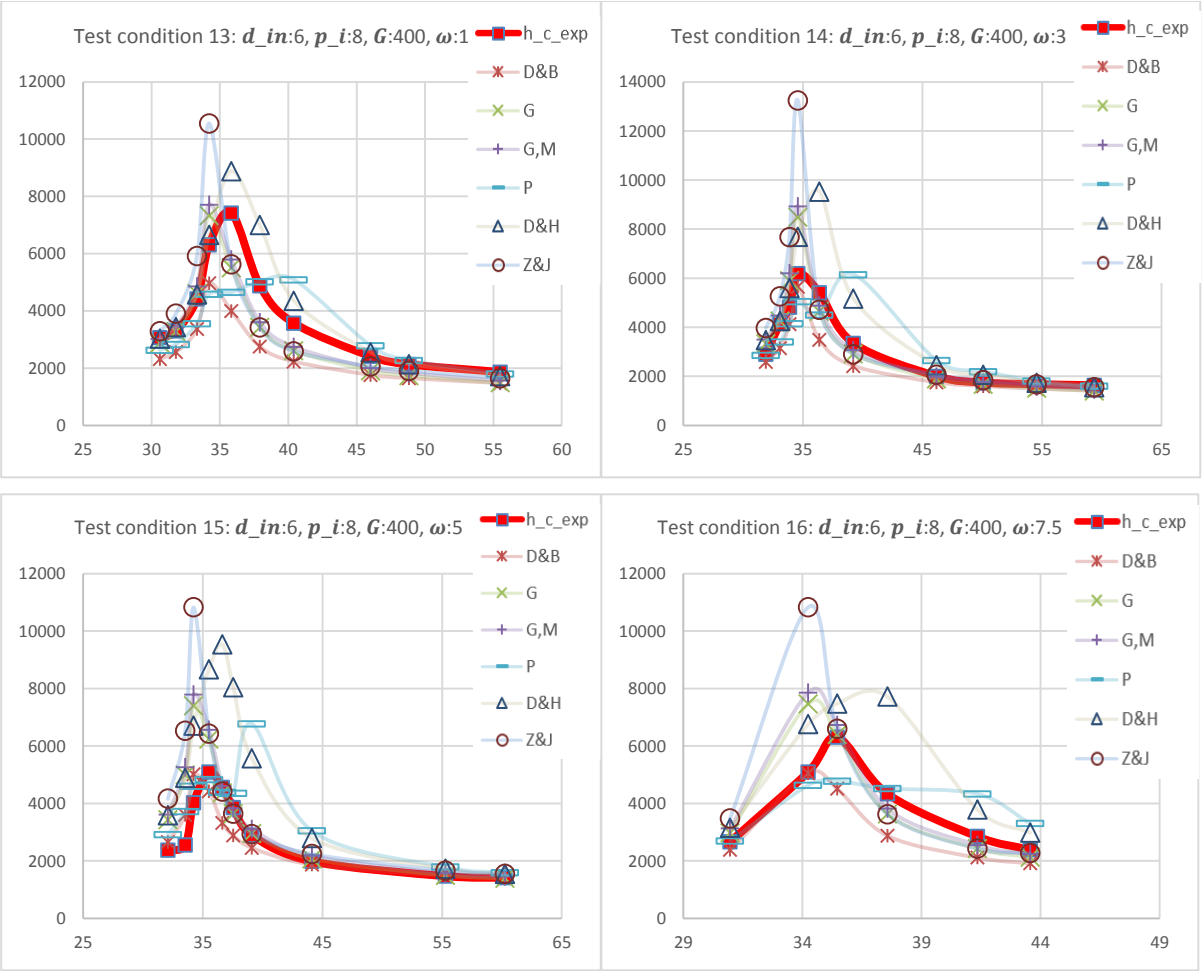
Test condition 13: d_in:6, p_i:8, G:400, ω:1
h_c_exp
D&B
G
G,M
P
D&H
Z&J
12000
10000
8000
6000
4000
2000
0
25
30
35
40
45
50
55
60
Test condition 14: d_in:6, p_i:8, G:400, ω:3
h_c_exp
D&B
G
G,M
P
D&H
Z&J
14000
12000
10000
8000
6000
4000
2000
0
25
35
45
55
65
Test condition 15: d_in:6, p_i:8, G:400, ω:5
h_c_exp
D&B
G
G,M
P
D&H
Z&J
12000
10000
8000
6000
4000
2000
0
25
35
45
55
65
Test condition 16: d_in:6, p_i:8, G:400, ω:7.5
h_c_exp
D&B
G
G,M
P
D&H
Z&J
12000
10000
8000
6000
4000
2000
0
29
34
39
44
49

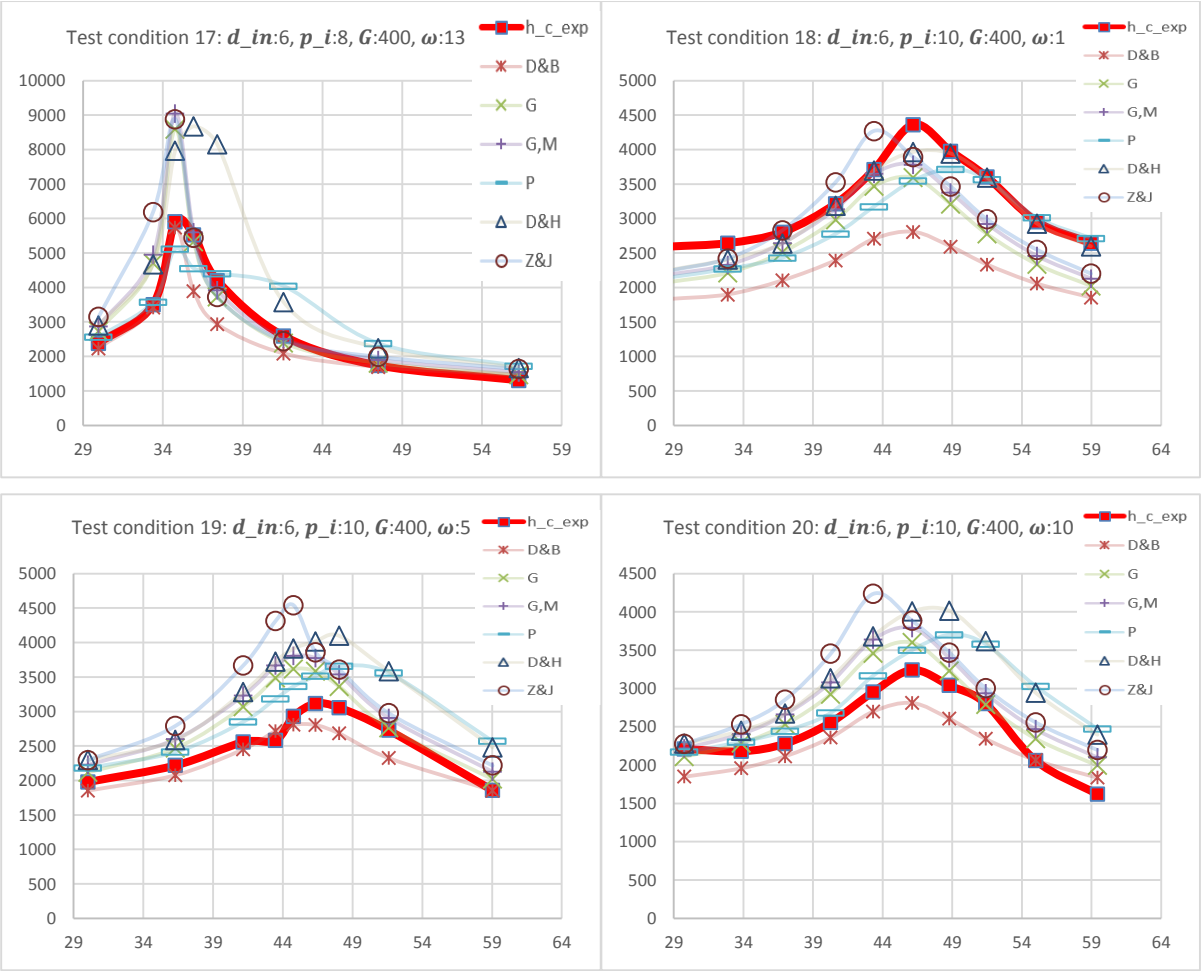

III. Graphical results on Zhao et al. (2011)'s data

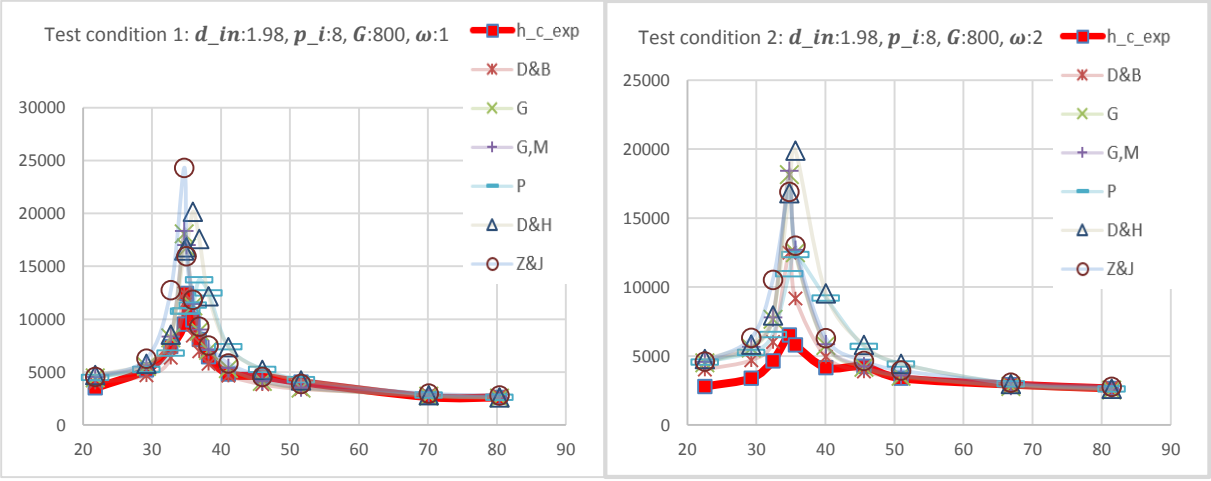

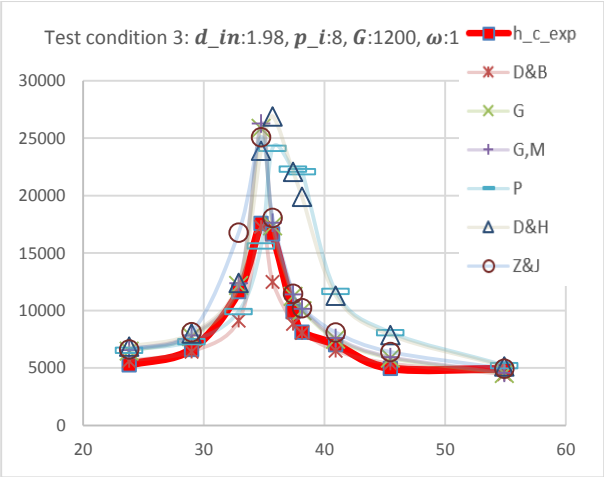
Test condition 3: d_in:1.98, p_i:8, G:1200, ω:1
h_c_exp
D&B
G
G,M
P
D&H
Z&J
30000
25000
20000
15000
10000
5000
0
20
30
40
50
60

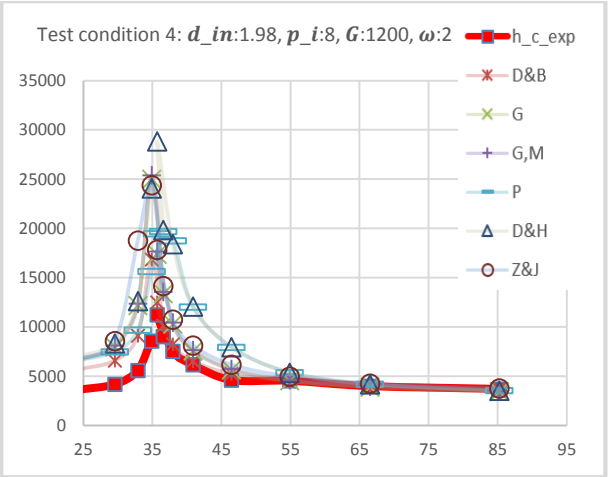
Test condition 4: d_in:1.98, p_i:8, G:1200, ω:2
h_c_exp
D&B
G
G,M
P
D&H
Z&J
35000
30000
25000
20000
15000
10000
5000
0
25
35
45
55
65
75
85
95

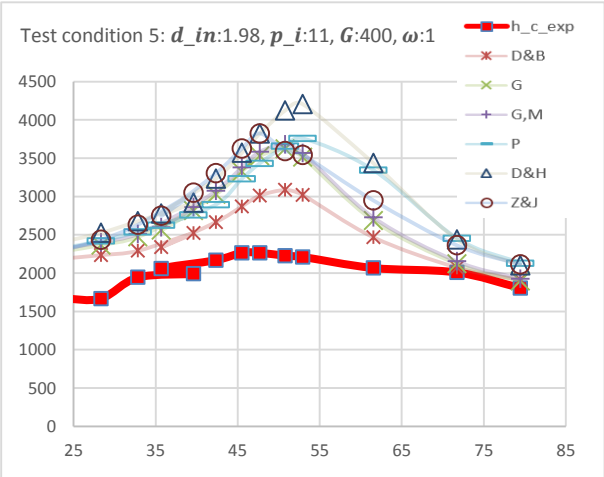
Test condition 5: d_in:1.98, p_i:11, G:400, ω:1
h_c_exp
D&B
G
G,M
P
D&H
Z&J
4500
4000
3500
3000
2500
2000
1500
1000
500
0
25
35
45
55
65
75
85

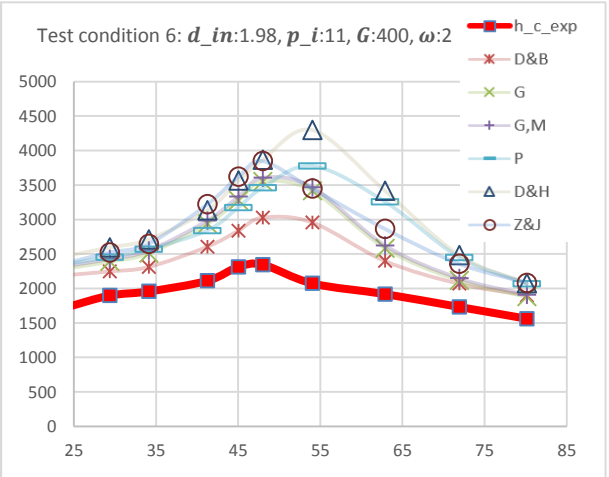
Test condition 6: d_in:1.98, p_i:11, G:400, ω:2
h_c_exp
D&B
G
G,M
P
D&H
Z&J
5000
4500
4000
3500
3000
2500
2000
1500
1000
500
0
25
35
45
55
65
75
85

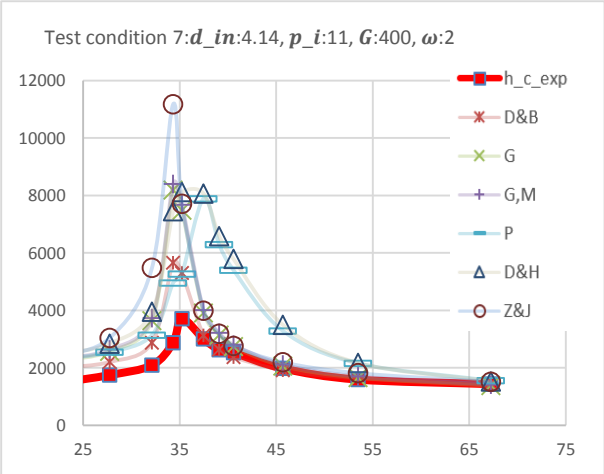
Test condition 7:d_in:4.14, p_i:11, G:400, ω:2
h_c_exp
D&B
G
G,M
P
D&H
Z&J
12000
10000
8000
6000
4000
2000
0
25
35
45
55
65
75

APPENDIX F: ALTERNATIVE CORRELATIONS WITH OIL COMPENSATION TESTED ON THE DATA OF DANG ET AL. (2007) AND ZHAO ET AL. (2011)

I. EES coding

```
"Engineering Equation Solver program"
"Oil-compensated alternative correlations tested on Dang et al. (2007)"
"Leander Kleyn"
"============================================================"
                              {Functions}
"============================================================"
Function convection(h_c_CO2,rho_oil,rho_b_CO2,omega,mu_oil,mu_b_CO2,T_ave,T_pc)

    If (T_ave<=T_pc) Then
        convection = h_c_CO2*(1.186*((rho_oil/rho_b_CO2)^(-0.236))*(omega*mu_oil/mu_b_CO2)^(-0.114))
    Else
        convection = h_c_CO2*(0.764*((rho_oil/rho_b_CO2)^(0.53))*(omega*mu_oil/mu_b_CO2)^(-0.227))
    Endif

End
"============================================================"
Function nusselt_Y(Re_b,Pr_b,T_ave,T_pc,rho_b_CO2,rho_pc_CO2)

    If (T_ave<=T_pc) Then
        nusselt_Y =  0.013*Re_b*(Pr_b^(-0.05))*(rho_pc_CO2/rho_b_CO2)^1.6
    Else
        nusselt_Y =  0.14*(Re_b^0.69)*(Pr_b^0.66)
    Endif

End
"============================================================"
Function c_vp_Z&J(T_ave,T_pc,Pr_w_Z&J,Pr_b,cp_ave_Z&J,cp_b_CO2,rho_w_CO2_Z&J,rho_b_CO2,T_w_Z&J,
T_ave_Kelvin)

     If (T_ave<=T_pc) Then
         c_vp_Z&J = 0.93*((Pr_w_Z&J/Pr_b)^(-
0.11))*((cp_ave_Z&J/cp_b_CO2)^(0.96))*(rho_w_CO2_Z&J/rho_b_CO2)^1.06
     Else
         c_vp_Z&J = 1.07*((T_w_Z&J/T_ave_Kelvin)^(-
0.45))*((cp_ave_Z&J/cp_b_CO2)^(0.61))*(rho_w_CO2_Z&J/rho_b_CO2)^(-0.18)
     Endif

End

"============================================================"
                            {Main program}
"============================================================"
"----------------------------------------GENERAL-----------------------------------------------"
"Input parameters"
d_input = 1 [mm]                          "Diameter of inner tube"
P_input = 8 [MPa]                          "Absolute static pressure"
G = 1200 [kg/m^2-s]                       "Mass flux of carbon dioxide"
T_pc = 34.7 [C]                           "Pseudocritical temperature"
omega_input = 5 [%]                        "Oil concentration"
T_i_input = 30.09 [C]                      "Inlet bulk temperature"
T_e_input = 28.644 [C]                    "Outlet bulk temperature"
h_c_exp = 8925 [W/m^2-K]                   "Convection heat transfer coefficient from test"
L = 0.5 [m]                                "Length of test section. Note: 1m for Zhao et al. (2011)'s data"

"SI Calculations"
d_in = d_input/1000                       "Diameter of inner tube"
```

```
P = P_input*10^6                                "Absolute static pressure"
omega = omega_input/100                         "Oil concentration"
T_i = T_i_input+273.15                          "Inlet bulk temperature"
T_e = T_e_input+273.15                          "Outlet bulk temperature"
T_ave = (T_i_input+T_e_input)/2                 "Average bulk temperature"
T_ave_Kelvin = T_ave+273.15                     "Average bulk temperature"
T_pc_Kelvin = T_pc+273.15


"Area calculations"
A_ff = pi*(d_in/2)^2                            "Free flow area of inner tube"
A_wall = pi*d_in*L                              "Inner wall area"

"Mass flow rate calculations"
m_dot_CO2 = G*A_ff                              "Mass flow rate of CO2"
omega = (m_dot_oil/(m_dot_oil+m_dot_CO2))       "Mass flow rate of oil"

"Heat transfer and real wall temperature"
Q_dot = m_dot_CO2*(h_i-h_e)
Q_dot_flux = Q_dot/A_wall
T_ave_Kelvin-T_wall = Q_dot*(1/(h_c_exp*A_wall) + F/A_wall)

"Fouling factor"
F=foulingfactor('CO2 vapor')


"----------------------------------------FLUID PROPERTIES----------------------------------------"
"Oil properties"
"Polyalkylene glycol: PAG100"

{Density calculation}
A = 0.6
T_ref = 15 [C]                                  "Reference temperature"
rho_oil_ref = 996 [kg/m^3]                      "Reference density. Use 957kg/m^3 for POE solest-68"

rho_oil = rho_oil_ref - A*(T_ave - T_ref)       "Oil density"

{Viscosity calculation}
mu_oil = (3.17343e-01) - (8.48149e-03)*T_ave + (1.01243e-04)*T_ave^2 - (6.21890e-07)*T_ave^3 + (1.59488e-
09)*T_ave^4                                     "Oil viscosity. Use equation 56 for POE solest-68"


"Carbon dioxide properties"

//At bulk temperature
rho_b_CO2 = density(CarbonDioxide,T=T_ave_Kelvin,P=P)       "Density of CO2"
mu_b_CO2 = viscosity(CarbonDioxide,T=T_ave_Kelvin,P=P)      "Viscosity"
k_b_CO2 = conductivity(CarbonDioxide,T=T_ave_Kelvin,P=P)    "Thermal conductivity"
cp_b_CO2 = cp(CarbonDioxide,T=T_ave_Kelvin,P=P)             "Specific heat"
h_b_CO2 = enthalpy(CarbonDioxide,T=T_ave_Kelvin,P=P)        "Enthalpy at average temperature"
h_i =  enthalpy(CarbonDioxide,T=T_i,P=P)                    "Enthalpy at inlet temperature"
h_e =  enthalpy(CarbonDioxide,T=T_e,P=P)                    "Enthalpy at outlet temperature"

//At pseudo-critical temperature
rho_pc_CO2 = density(CarbonDioxide,T=T_pc_Kelvin,P=P)

{Dimensionless parameters}
//At bulk temperature
Re_b = G*d_in/mu_b_CO2                          "Reynolds number"
Pr_b = cp_b_CO2*mu_b_CO2/k_b_CO2                "Prandtl number"


"----------------------------------------CORRELATIONS----------------------------------------"

"========================================================="
{Correlation by Dittus & Boelter - 1985}
```

```
Nusselt_D&B = 0.023*(Re_b^0.8)*(Pr_b^n_D&B)
n_D&B = 0.3


h_c_D&B = Nusselt_D&B*k_b_CO2/d_in
Error_D&B = (100*((h_c_D&B-h_c_exp)/h_c_exp))

//Compensated
h_c_D&B_comp = convection(h_c_D&B,rho_oil,rho_b_CO2,omega,mu_oil,mu_b_CO2,T_ave,T_pc)
Error_D&B_comp = (100*((h_c_D&B_comp-h_c_exp)/h_c_exp))


"========================================================="
"========================================================="
{Correlation 1 by Gnielinksi - 1975}

Nusselt_G = (f_fil_G/8)*(Re_b-1000)*Pr_b*(1.07+12.7*sqrt(f_fil_G/8)*(Pr_b^(2/3)-1))^(-1)
f_fil_G = (1.82*log10(Re_b)-1.64)^(-2)


h_c_G = Nusselt_G*k_b_CO2/d_in
Error_G = (100*((h_c_G-h_c_exp)/h_c_exp))

//Compensated
h_c_G_comp = convection(h_c_G,rho_oil,rho_b_CO2,omega,mu_oil,mu_b_CO2,T_ave,T_pc)
Error_G_comp = (100*((h_c_G_comp-h_c_exp)/h_c_exp))


"========================================================="
"========================================================="
{Modified correlation by Gnielinksi - 1975}

Nusselt_G_M = ((f_fil_G/8)*(Re_b-1000)*Pr_b*(1.07+12.7*sqrt(f_fil_G/8)*(Pr_b^(2/3)-1))^(-1))*(1+(d_in/L)^(2/3))

h_c_G_M = Nusselt_G_M*k_b_CO2/d_in
Error_G_M = (100*((h_c_G_M-h_c_exp)/h_c_exp))

//Compensated
h_c_G_M_comp = convection(h_c_G_M,rho_oil,rho_b_CO2,omega,mu_oil,mu_b_CO2,T_ave,T_pc)
Error_G_M_comp = (100*((h_c_G_M_comp-h_c_exp)/h_c_exp))


"========================================================="
"========================================================="
{Correlation by Yoon et al. - 2003}

Nusselt_Y = nusselt_Y(Re_b,Pr_b,T_ave,T_pc,rho_b_CO2,rho_pc_CO2)

h_c_Y = Nusselt_Y*k_b_CO2/d_in
Error_Y = (100*((h_c_Y-h_c_exp)/h_c_exp))

//Compensated
h_c_Y_comp = convection(h_c_Y,rho_oil,rho_b_CO2,omega,mu_oil,mu_b_CO2,T_ave,T_pc)
Error_Y_comp = (100*((h_c_Y_comp-h_c_exp)/h_c_exp))

"========================================================="
"========================================================="
{Correlation by Pitla et al. - 2002}

Nusselt_P = ((Nusselt_P_w+Nusselt_P_b)/2)*(k_w_CO2_P/k_b_CO2)
Nusselt_P_b = (f_fil_G/8)*(Re_b-1000)*Pr_b*(1.07+12.7*sqrt(f_fil_G/8)*(Pr_b^(2/3)-1))^(-1)
Nusselt_P_w = (f_fil_G_w_P/8)*(Re_w_P-1000)*Pr_w_P*(1.07+12.7*sqrt(f_fil_G_w_P/8)*(Pr_w_P^(2/3)-1))^(-1)
f_fil_G_w_P = (1.82*log10(Re_w_P)-1.64)^(-2)

"Dimensionless parameters"
//At wall temperature
Re_w_P = G*d_in/mu_w_CO2_P
```

```
Pr_w_P = cp_w_CO2_P*mu_w_CO2_P/k_w_CO2_P

"Carbon dioxide properties"
//At wall temperature
rho_w_CO2_P = density(CarbonDioxide,T=T_w_P,P=P)          "Density of CO2"
mu_w_CO2_P = viscosity(CarbonDioxide,T=T_w_P,P=P)          "Viscosity"
k_w_CO2_P = conductivity(CarbonDioxide,T=T_w_P,P=P)        "Thermal conductivity"
cp_w_CO2_P = cp(CarbonDioxide,T=T_w_P,P=P)                 "Specific heat"

T_ave_Kelvin-T_w_P = Q_dot*(1/(h_c_P_comp*A_wall) + F/A_wall)

h_c_P = Nusselt_P*k_b_CO2/d_in
Error_P = (100*((h_c_P-h_c_exp)/h_c_exp))

//Compensated
h_c_P_comp = convection(h_c_P,rho_oil,rho_b_CO2,omega,mu_oil,mu_b_CO2,T_ave,T_pc)
Error_P_comp = (100*((h_c_P_comp-h_c_exp)/h_c_exp))

"========================================================="
"========================================================="
{Correlation by Zhao & Jiang - 2011}

Nusselt_Z&J = ((f_fil_G/8)*(Re_b-1000)*Pr_b*(1.07+12.7*sqrt(f_fil_G/8)*(Pr_b^(2/3)-1))^(-
1))*(1+(d_in/L)^(2/3))*C_vp_Z&J

C_vp_Z&J =
c_vp_Z&J(T_ave,T_pc,Pr_w_Z&J,Pr_b,cp_ave_Z&J,cp_b_CO2,rho_w_CO2_Z&J,rho_b_CO2,T_w_Z&J,T_ave_Kelvi
n)

cp_ave_Z&J = (h_i-h_e)/(T_i-T_e)

T_ave_Kelvin-T_w_Z&J = Q_dot*(1/(h_c_Z&J_comp*A_wall) + F/A_wall)

"Dimensionless parameters"
//At wall temperature
Pr_w_Z&J = cp_w_CO2_Z&J*mu_w_CO2_Z&J/k_w_CO2_Z&J

"Carbon dioxide properties"
//At wall temperature
rho_w_CO2_Z&J = density(CarbonDioxide,T=T_w_Z&J,P=P)
mu_w_CO2_Z&J = viscosity(CarbonDioxide,T=T_w_Z&J,P=P)
k_w_CO2_Z&J = conductivity(CarbonDioxide,T=T_w_Z&J,P=P)
cp_w_CO2_Z&J = cp(CarbonDioxide,T=T_w_Z&J,P=P)

h_c_Z&J = Nusselt_Z&J*k_b_CO2/d_in
Error_Z&J = (100*((h_c_Z&J-h_c_exp)/h_c_exp))

//Compensated
h_c_Z&J_comp = convection(h_c_Z&J,rho_oil,rho_b_CO2,omega,mu_oil,mu_b_CO2,T_ave,T_pc)
Error_Z&J_comp = (100*((h_c_Z&J_comp-h_c_exp)/h_c_exp))

"========================================================="
"========================================================="
```

II. Graphical results on Dang et al. (2007)'s data

Note: The x-axis refers to the bulk temperature, T_b [°C], while the y-axis represents the convection heat transfer coefficients, h_c $\left[\frac{W}{m^2K}\right]$. Also, the results for Yoon et al. (2003) are not included in these graphs, because this correlation shows large errors relative to the other correlations used and then makes it difficult to see the other correlations' results.

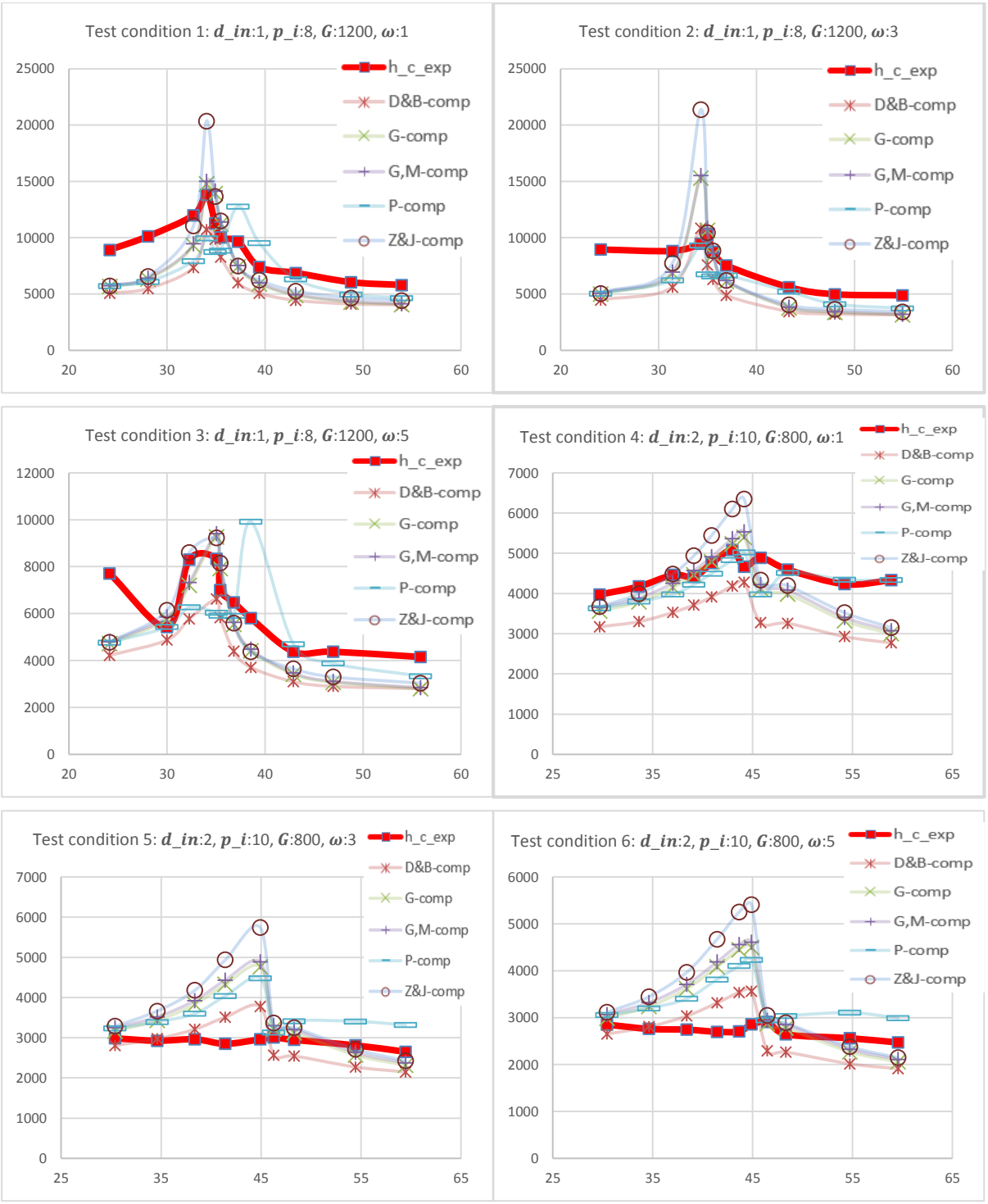
Test condition 1: d_in:1, p_i:8, G:1200, ω:1
Test condition 2: d_in:1, p_i:8, G:1200, ω:3
Test condition 3: d_in:1, p_i:8, G:1200, ω:5
Test condition 4: d_in:2, p_i:10, G:800, ω:1
Test condition 5: d_in:2, p_i:10, G:800, ω:3
Test condition 6: d_in:2, p_i:10, G:800, ω:5
h_c_exp
D&B-comp
G-comp
G,M-comp
P-comp
Z&J-comp

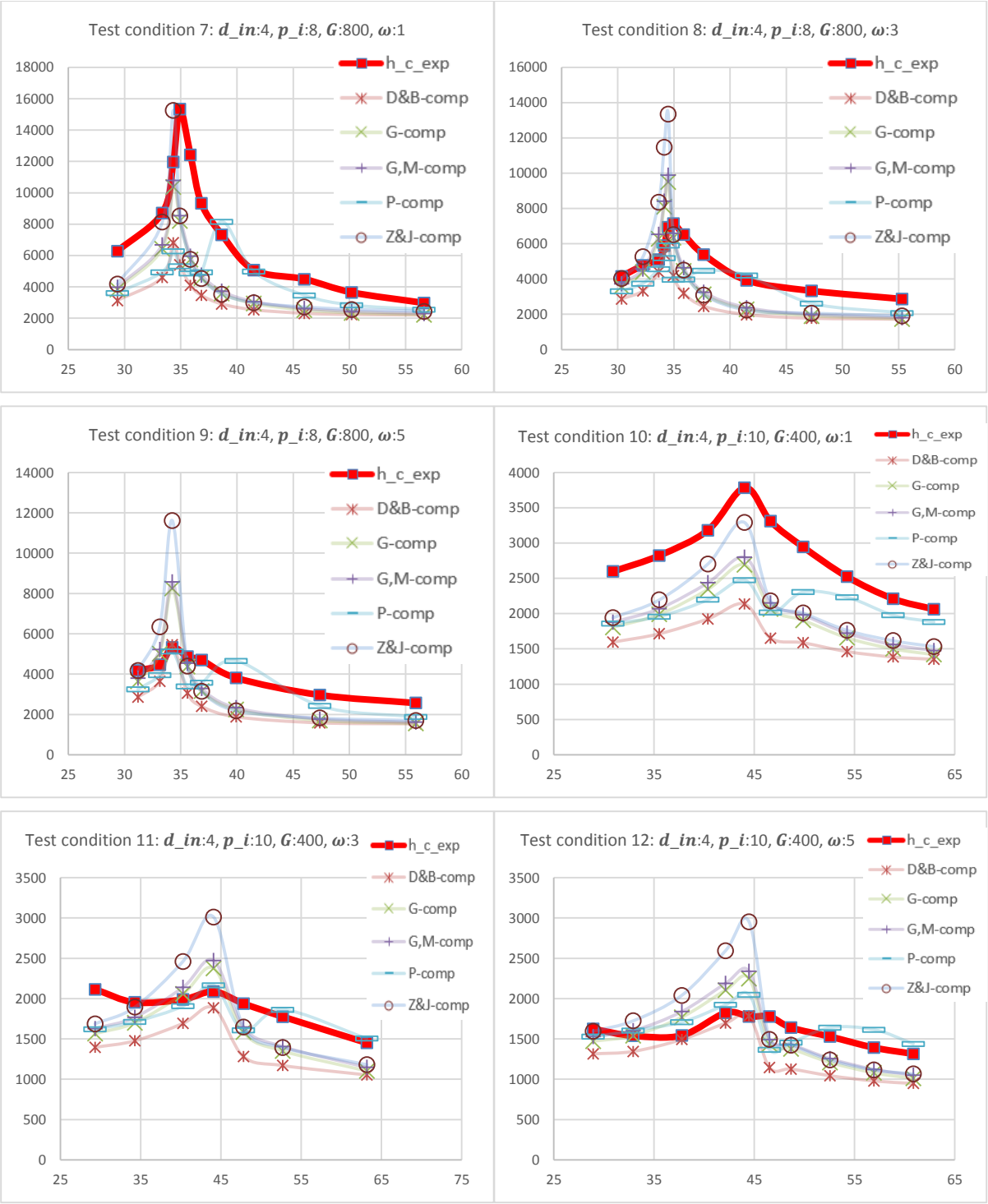
Test condition 7: d_in:4, p_i:8, G:800, ω:1
h_c_exp
D&B-comp
G-comp
G,M-comp
P-comp
Z&J-comp
Test condition 8: d_in:4, p_i:8, G:800, ω:3
Test condition 9: d_in:4, p_i:8, G:800, ω:5
Test condition 10: d_in:4, p_i:10, G:400, ω:1
Test condition 11: d_in:4, p_i:10, G:400, ω:3
Test condition 12: d_in:4, p_i:10, G:400, ω:5

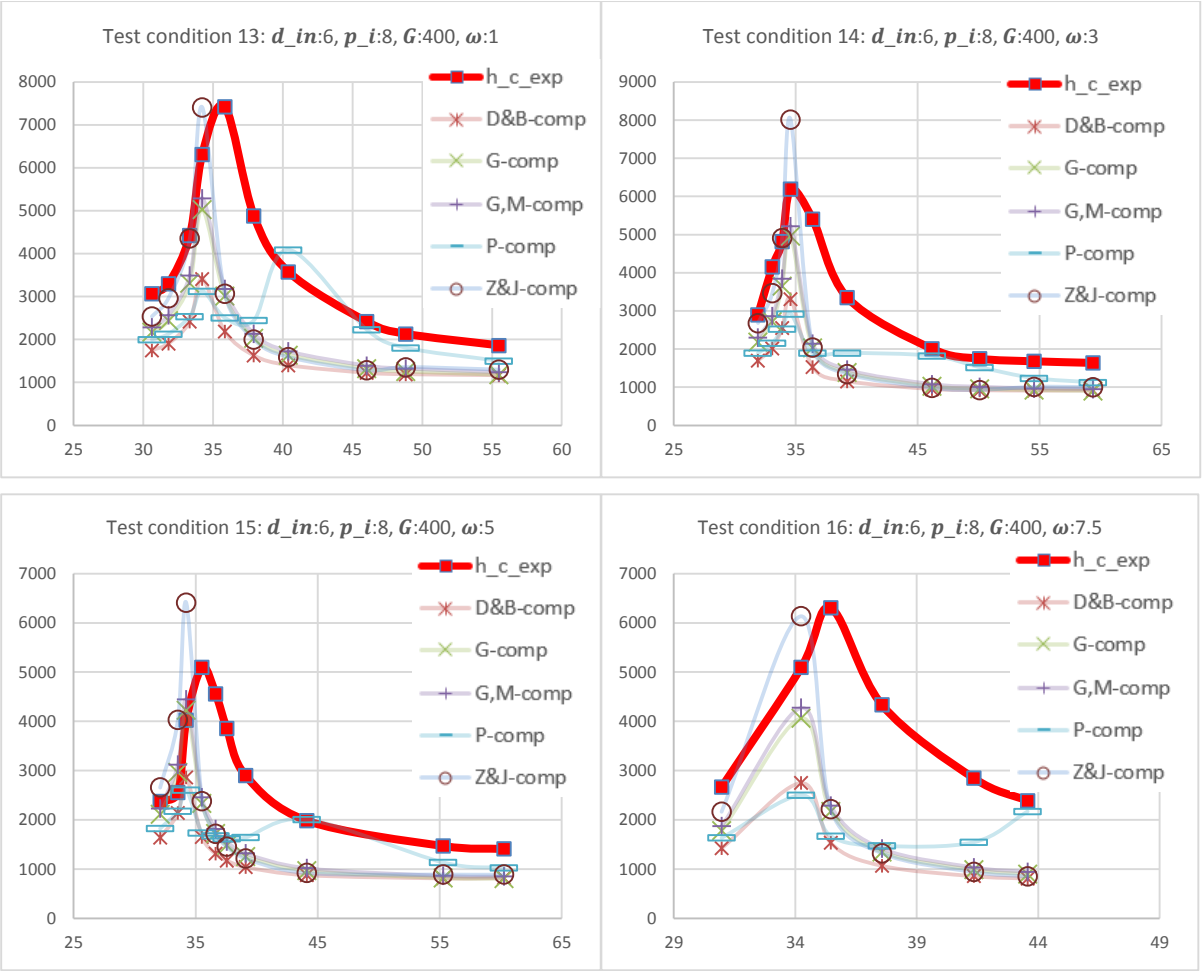
Test condition 13: d_in:6, p_i:8, G:400, ω:1
h_c_exp
D&B-comp
G-comp
G,M-comp
P-comp
Z&J-comp
Test condition 14: d_in:6, p_i:8, G:400, ω:3
h_c_exp
D&B-comp
G-comp
G,M-comp
P-comp
Z&J-comp
Test condition 15: d_in:6, p_i:8, G:400, ω:5
h_c_exp
D&B-comp
G-comp
G,M-comp
P-comp
Z&J-comp
Test condition 16: d_in:6, p_i:8, G:400, ω:7.5
h_c_exp
D&B-comp
G-comp
G,M-comp
P-comp
Z&J-comp

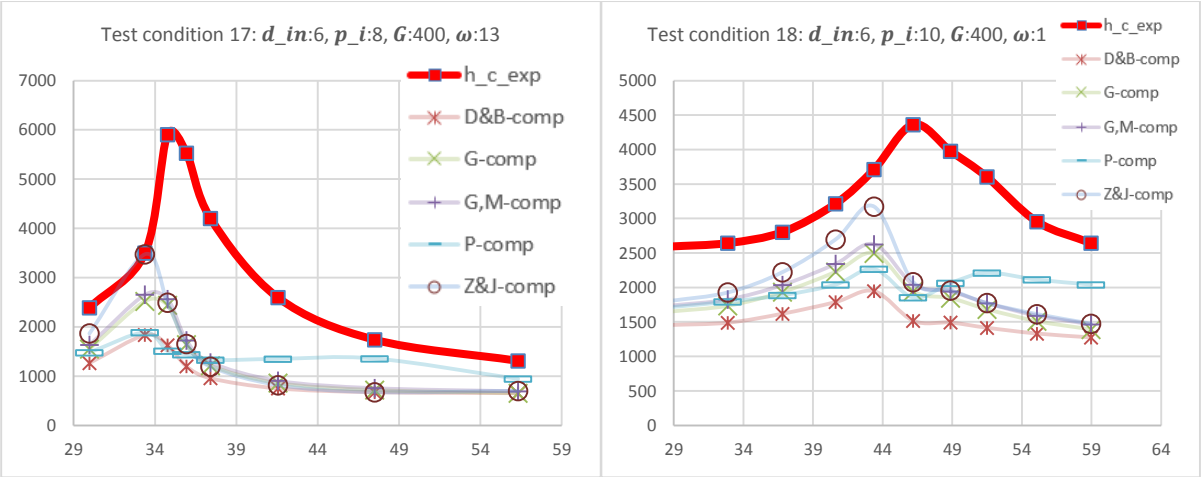

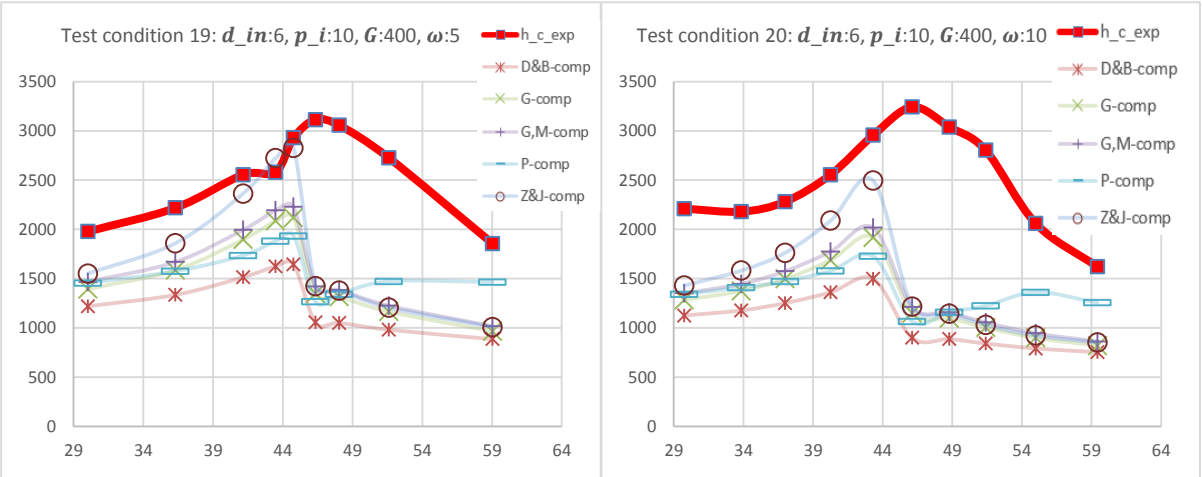

III. Graphical results on Zhao et al. (2011)'s data

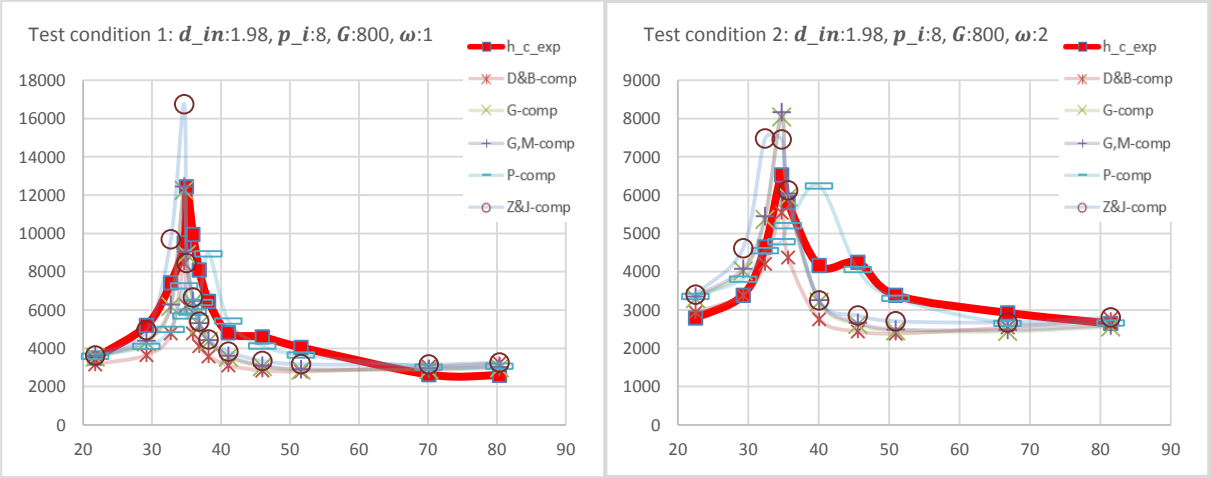

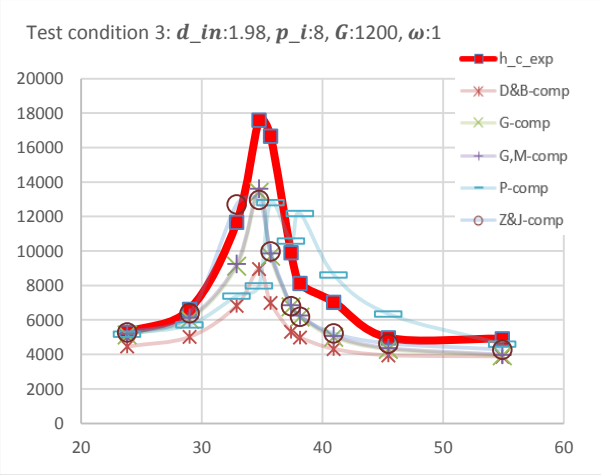
Test condition 3: d_in:1.98, p_i:8, G:1200, ω:1
h_c_exp
D&B-comp
G-comp
G,M-comp
P-comp
Z&J-comp
20000
18000
16000
14000
12000
10000
8000
6000
4000
2000
0
20
30
40
50
60

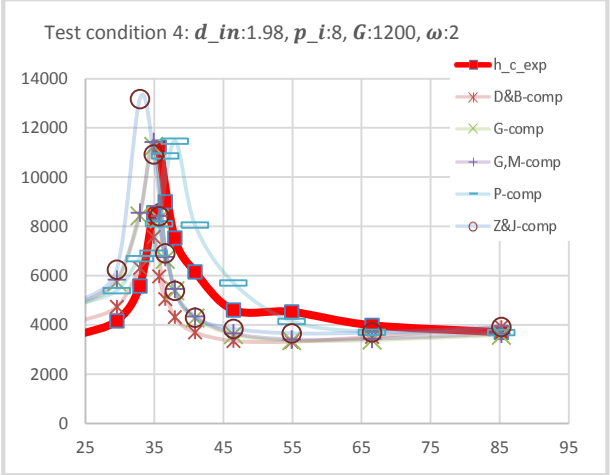
Test condition 4: d_in:1.98, p_i:8, G:1200, ω:2
h_c_exp
D&B-comp
G-comp
G,M-comp
P-comp
Z&J-comp
14000
12000
10000
8000
6000
4000
2000
0
25
35
45
55
65
75
85
95

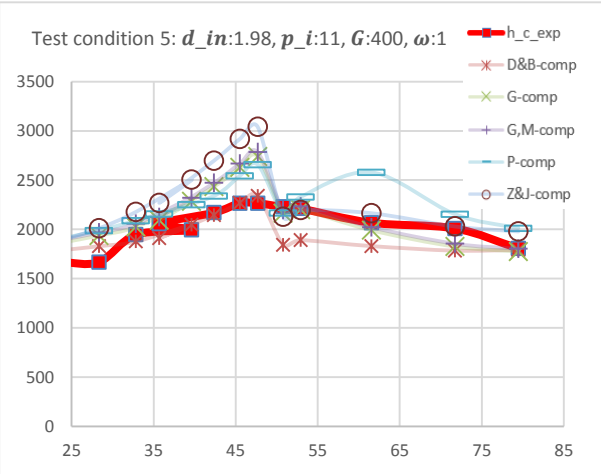
Test condition 5: d_in:1.98, p_i:11, G:400, ω:1
h_c_exp
D&B-comp
G-comp
G,M-comp
P-comp
Z&J-comp
3500
3000
2500
2000
1500
1000
500
0
25
35
45
55
65
75
85

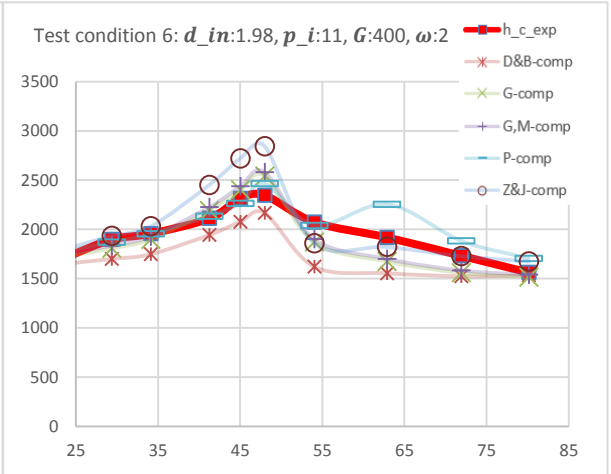
Test condition 6: d_in:1.98, p_i:11, G:400, ω:2
h_c_exp
D&B-comp
G-comp
G,M-comp
P-comp
Z&J-comp
3500
3000
2500
2000
1500
1000
500
0
25
35
45
55
65
75
85

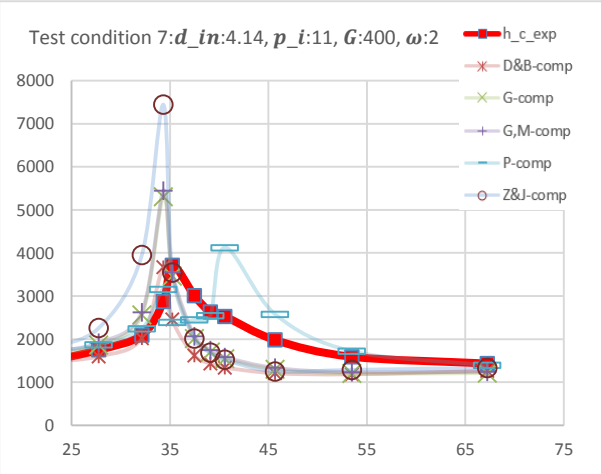
Test condition 7:d_in:4.14, p_i:11, G:400, ω:2
h_c_exp
D&B-comp
G-comp
G,M-comp
P-comp
Z&J-comp
8000
7000
6000
5000
4000
3000
2000
1000
0
25
35
45
55
65
75

APPENDIX G: NEW CORRELATION TESTED ON DANG ET AL. (2007)'S AND ZHAO ET AL. (2011)'S TEST DATA

I. Results of new correlation on Dang et al. (2007)'s experimental data

Numerical results:

Test condition 1		
d_{in}:1, p_i:8, G:1200, ω:1		
$h_{c,exp}$	h_c	$E_{\%}$
8925	5920	-33,67
10125	6292	-37,86
12000	8151	-32,07
13825	11610	-16,02
11275	13425	19,07
10025	11486	14,57
9650	8586	-11,03
7400	7412	0,1665
6875	6666	-3,046
6050	6362	5,151
5800	6380	10,01

Test condition 2		
d_{in}:1, p_i:8, G:1200, ω:3		
$h_{c,exp}$	h_c	$E_{\%}$
8950	6159	-31,19
8825	7442	-15,67
9475	13679	44,37
10250	10872	6,067
8750	9212	5,276
7550	7305	-3,239
5600	5447	-2,736
4975	5226	5,039
4875	5246	7,611

Test condition 3		
d_{in}:1, p_i:8, G:1200, ω:5		
$h_{c,exp}$	h_c	$E_{\%}$
7700	6388	-17,04
5425	7170	32,17
8300	8335	0,4224
8325	10296	23,68
7000	9182	31,17
6475	7116	9,904
5800	6126	5,62
4375	5290	20,92
4375	5064	15,74
4150	5079	22,38

Test condition 4		
d_{in}:2, p_i:10, G:800, ω:1		
$h_{c,exp}$	h_c	$E_{\%}$
3972	3638	-8,419
4175	3716	-11
4460	3902	-12,52
4415	4047	-8,316
4753	4205	-11,52
5084	4403	-13,38
4662	4441	-4,746
4888	4442	-9,123
4594	4539	-1,201
4232	4255	0,5555
4329	4134	-4,5

Test condition 5		
d_{in}:2, p_i:10, G:800, ω:3		
$h_{c,exp}$	h_c	$E_{\%}$
2986	3788	26,84
2925	3930	34,36
2962	4152	40,18
2849	4431	55,52
2961	4579	54,62
3006	3680	22,41
2946	3725	26,45
2810	3480	23,87
2651	3383	27,61

Test condition 6		
d_{in}:2, p_i:10, G:800, ω:5		
$h_{c,exp}$	h_c	$E_{\%}$
2851	3928	37,78
2760	4077	47,74
2744	4309	57,04
2698	4597	70,37
2706	4790	77,03
2856	4749	66,3
2908	3564	22,56
2645	3592	35,82
2561	3348	30,73
2470	3928	37,78

Test condition 7		
d_{in}:4, p_i:8, G:800, ω:1		
$h_{c,exp}$	h_c	$E_{\%}$
6278	3563	-43,25
8712	5061	-41,91
11975	7277	-39,23
15345	7364	-52,01
12419	5743	-53,76
9339	4930	-47,22
7332	4225	-42,38
5079	3779	-25,59
4495	3533	-21,42
3652	3478	-4,742
2975	3532	18,72

Test condition 8		
d_{in}:4, p_i:8, G:800, ω:3		
$h_{c,exp}$	h_c	$E_{\%}$
4148	3839	-7,449
4776	4386	-8,155
5112	5679	11,08
5894	6896	17,01
6950	7769	11,77
7149	6002	-16,04
6521	4707	-27,82
5387	3716	-31,01
3930	3101	-21,11
3331	2872	-13,76
2869	2879	0,3467

Test condition 9		
d_{in}:4, p_i:8, G:800, ω:5		
$h_{c,exp}$	h_c	$E_{\%}$
4179	4166	-0,3079
4454	5200	16,76
5327	7578	42,26
4867	4836	-0,6195
4698	3883	-17,34
3808	3140	-17,56
2963	2769	-6,561
2562	2783	8,633

Test condition 10		
d_{in}:4, p_i:10, G:400, ω:1		
$h_{c,exp}$	h_c	$E_{\%}$
2597	1821	-29,89
2823	1911	-32,3
3181	2078	-34,67
3782	2221	-41,27
3308	2261	-31,67
2945	2238	-24,03
2523	2127	-15,68
2211	2068	-6,473
2061	2057	-0,1834

Test condition 11		
d_{in}:4, p_i:10, G:400, ω:3		
$h_{c,exp}$	h_c	$E_{\%}$
2115	1892	-10,53
1953	1956	0,1867
1990	2157	8,355
2088	2311	10,68
1939	1866	-3,736
1776	1772	-0,2548
1451	1686	16,22

Test condition 12		
d_{in}:4, p_i:10, G:400, ω:5		
$h_{c,exp}$	h_c	$E_{\%}$
1624	1962	20,76
1539	1970	28,04
1543	2130	38,09
1824	2335	28,04
1777	2390	34,52
1777	1784	0,3954
1640	1791	9,238
1529	1711	11,93
1392	1648	18,42
1315	1627	23,76

Test condition 13		
d_{in}:6, p_i:8, G:400, ω:1		
$h_{c,exp}$	h_c	$E_{\%}$
3066	1979	-35,47
3301	2137	-35,26
4424	2663	-39,81
6309	3662	-41,96
7424	3064	-58,73
4884	2350	-51,88
3576	2068	-42,16
2418	1871	-22,65
2133	1846	-13,46
1864	1862	-0,1154

Test condition 14		
d_{in}:6, p_i:8, G:400, ω:3		
$h_{c,exp}$	h_c	$E_{\%}$
2898	2246	-22,52
4155	2628	-36,76
4817	3278	-31,97
6192	4118	-33,49
5404	2273	-57,94
3350	1779	-46,89
2008	1531	-23,72
1747	1510	-13,58
1679	1520	-9,476
1637	1556	-4,951

Test condition 15		
d_{in}:6, p_i:8, G:400, ω:5		
$h_{c,exp}$	h_c	$E_{\%}$
2370	2369	-0,0353
2554	3030	18,61
4021	3976	-1,117
5094	2610	-48,75
4557	2116	-53,58
3853	1916	-50,28
2897	1727	-40,4
1982	1507	-23,97
1469	1470	0,08173
1409	1509	7,047

Test condition 16		
d_{in}:6, p_i:8, G:400, ω:7.5		
$h_{c,exp}$	h_c	$E_{\%}$
2664	2274	-14,65
5094	4180	-17,94
6301	2701	-57,14
4331	1948	-55,01
2847	1619	-43,11
2385	1548	-35,08

Test condition 17		
d_{in}:6, p_i:8, G:400, ω:13		
$h_{c,exp}$	h_c	$E_{\%}$
2387	2387	-0,0214
3502	3345	-4,48
5907	3641	-38,37
5530	2776	-49,79
4205	2269	-46,05
2595	1848	-28,8
1739	1714	-1,449
1310	1727	31,79

Test condition 18		
d_{in}:6, p_i:10, G:400, ω:1		
$h_{c,exp}$	h_c	$E_{\%}$
2593	1676	-35,35
2643	1684	-36,3
2803	1794	-36,01
3215	1927	-40,07
3712	2042	-44,99
4364	2067	-52,63
3977	2086	-47,56
3603	2022	-43,88
2955	1947	-34,1
2643	1906	-27,9

Test condition 19		
d_{in}:6, p_i:10, G:400, ω:5		
$h_{c,exp}$	h_c	$E_{\%}$
1978	1810	-8,48
2218	1921	-13,38
2555	2105	-17,6
2580	2206	-14,51
2929	2195	-25,06
3114	1639	-47,37
3056	1659	-45,72
2727	1596	-41,48
1856	1506	-18,86

Test condition 20		
d_{in}:6, p_i:10, G:400, ω:10		
$h_{c,exp}$	h_c	$E_{\%}$
2210	1975	-10,62
2180	2027	-7,038
2281	2118	-7,167
2555	2251	-11,9
2955	2402	-18,69
3241	1751	-45,95
3039	1772	-41,69
2803	1718	-38,71
2058	1654	-19,64
1620	1616	-0,299

Graphical results:

Note: The x-axis refers to the bulk temperature, T_b [°C], while the y-axis represents the convection heat transfer coefficients, h_c $\left[\frac{W}{m^2K}\right]$.

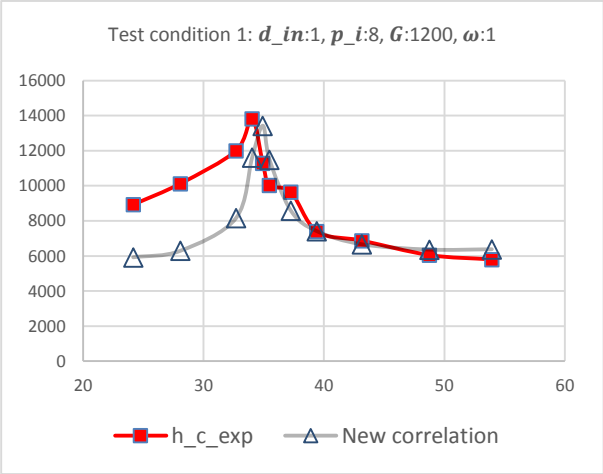

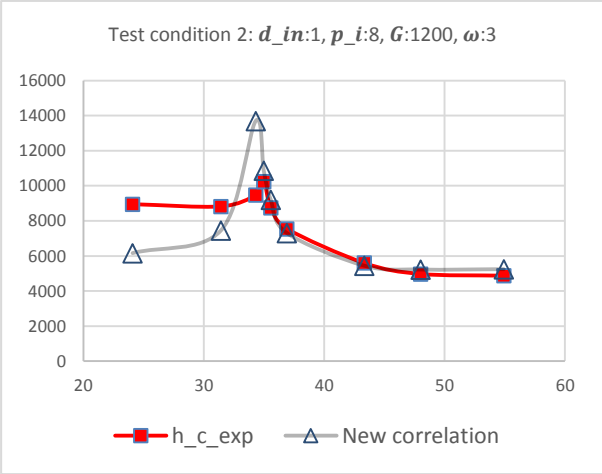

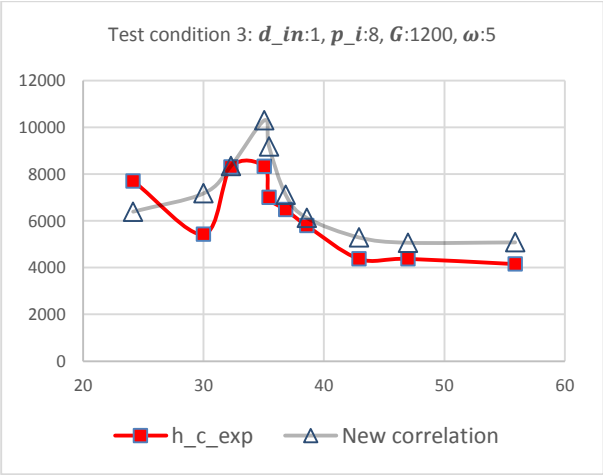

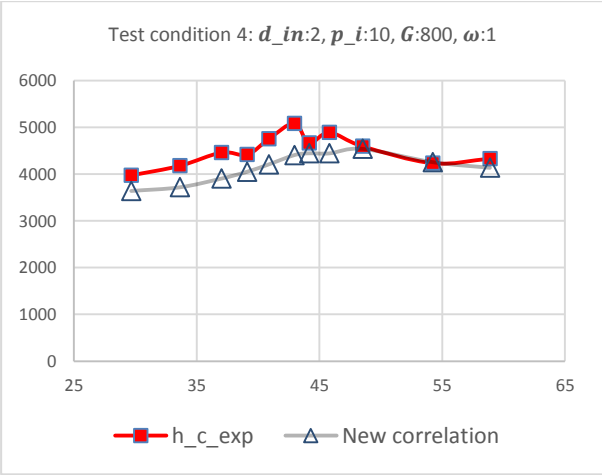

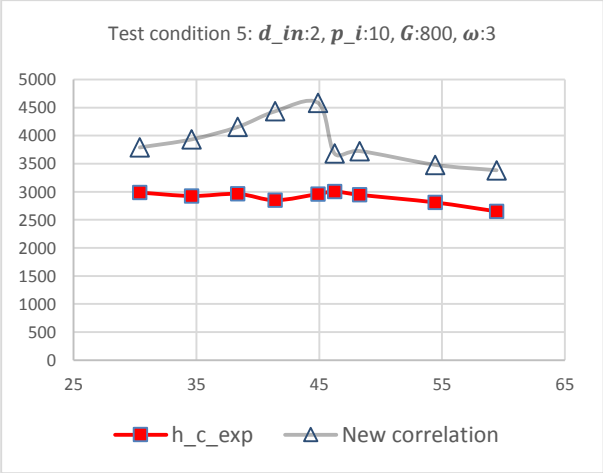

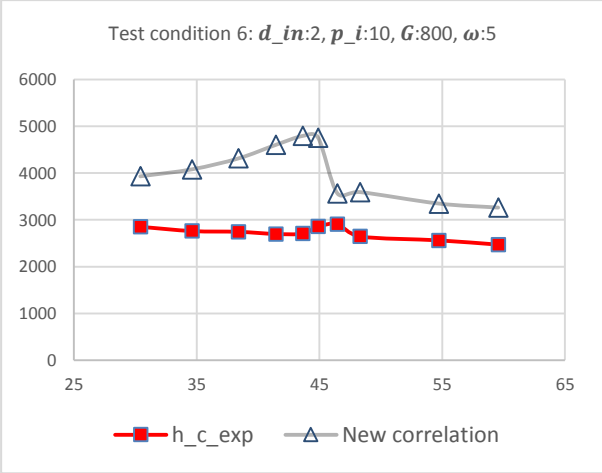

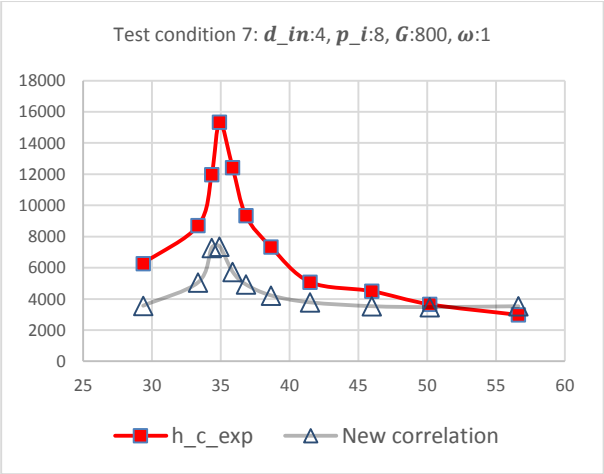
Test condition 7: d_in:4, p_i:8, G:800, ω:1
18000
16000
14000
12000
10000
8000
6000
4000
2000
0
25
30
35
40
45
50
55
60
h_c_exp
New correlation

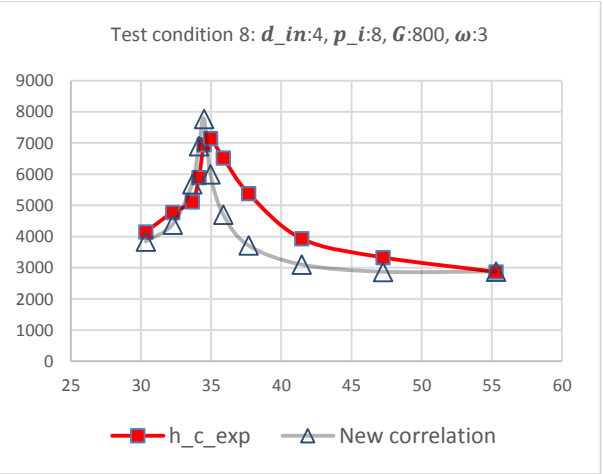
Test condition 8: d_in:4, p_i:8, G:800, ω:3
9000
8000
7000
6000
5000
4000
3000
2000
1000
0
25
30
35
40
45
50
55
60
h_c_exp
New correlation

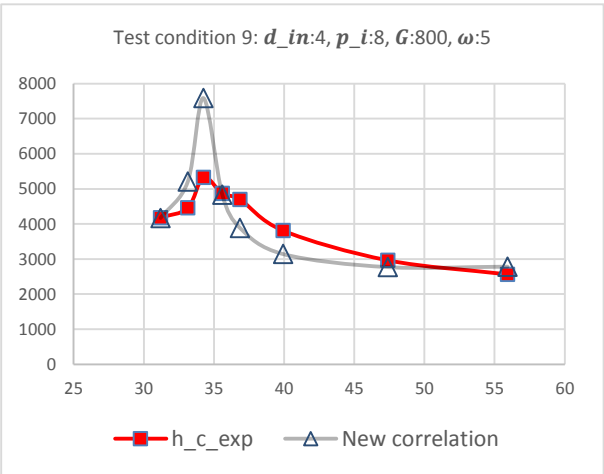
Test condition 9: d_in:4, p_i:8, G:800, ω:5
8000
7000
6000
5000
4000
3000
2000
1000
0
25
30
35
40
45
50
55
60
h_c_exp
New correlation

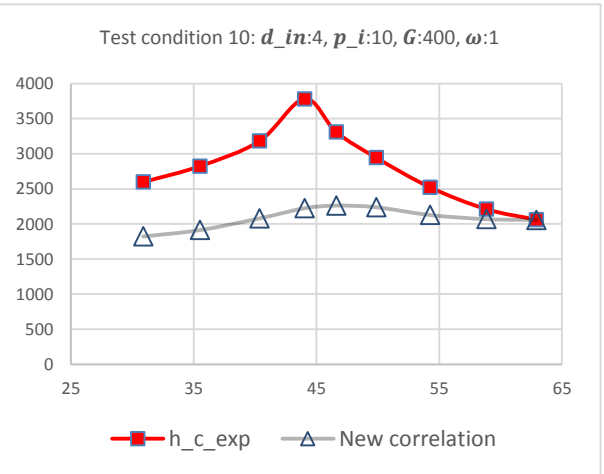
Test condition 10: d_in:4, p_i:10, G:400, ω:1
4000
3500
3000
2500
2000
1500
1000
500
0
25
35
45
55
65
h_c_exp
New correlation

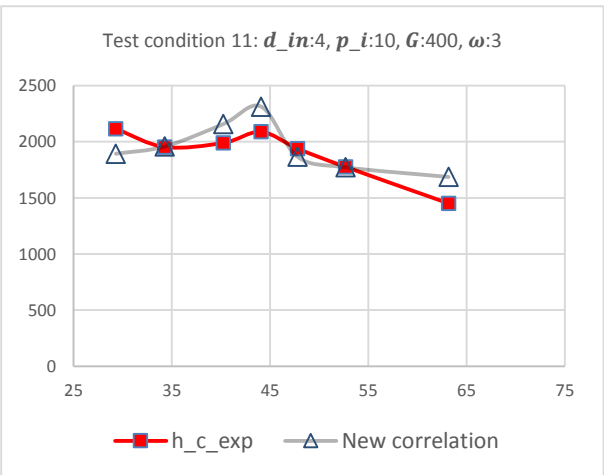
Test condition 11: d_in:4, p_i:10, G:400, ω:3
2500
2000
1500
1000
500
0
25
35
45
55
65
75
h_c_exp
New correlation

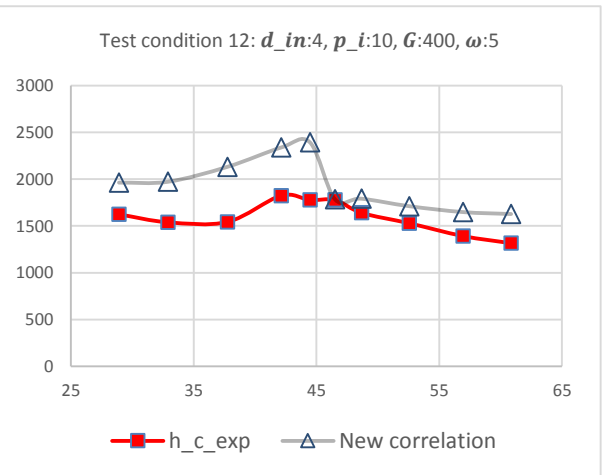
Test condition 12: d_in:4, p_i:10, G:400, ω:5
3000
2500
2000
1500
1000
500
0
25
35
45
55
65
h_c_exp
New correlation

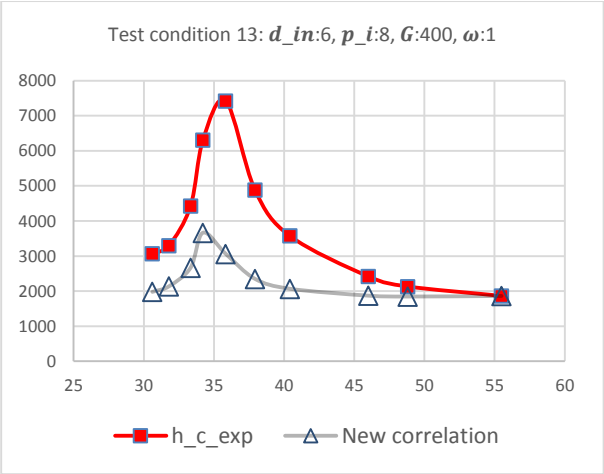
Test condition 13: d_in:6, p_i:8, G:400, ω:1
8000
7000
6000
5000
4000
3000
2000
1000
0
25
30
35
40
45
50
55
60
h_c_exp
New correlation

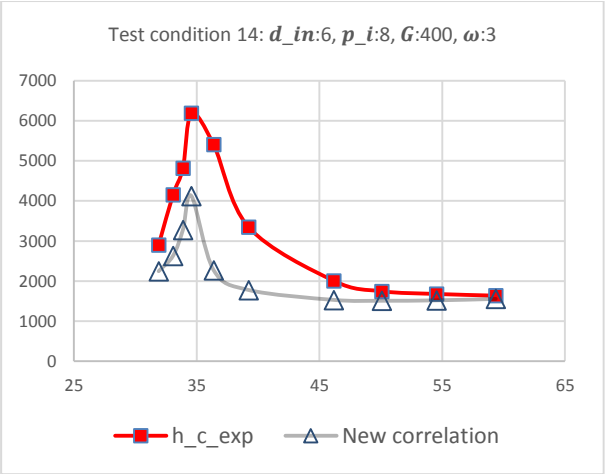
Test condition 14: d_in:6, p_i:8, G:400, ω:3
7000
6000
5000
4000
3000
2000
1000
0
25
35
45
55
65
h_c_exp
New correlation

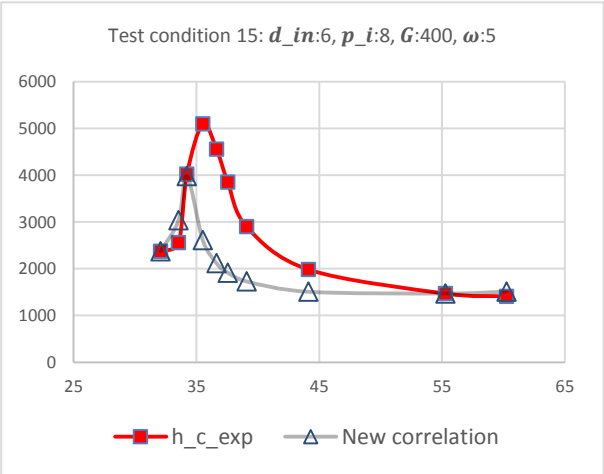
Test condition 15: d_in:6, p_i:8, G:400, ω:5
6000
5000
4000
3000
2000
1000
0
25
35
45
55
65
h_c_exp
New correlation

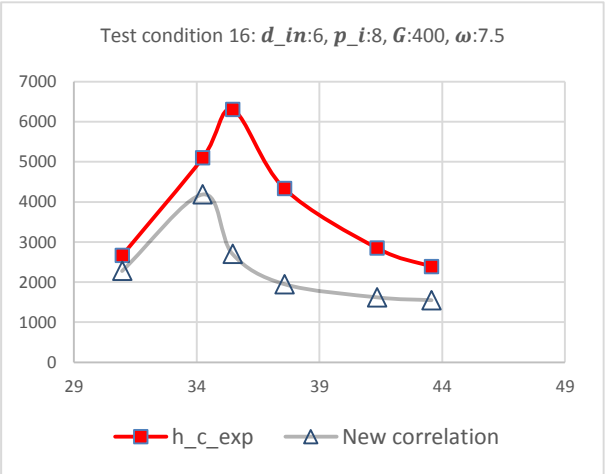
Test condition 16: d_in:6, p_i:8, G:400, ω:7.5
7000
6000
5000
4000
3000
2000
1000
0
29
34
39
44
49
h_c_exp
New correlation

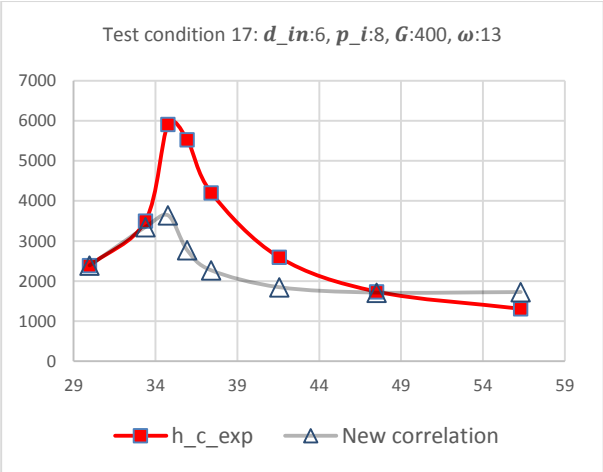

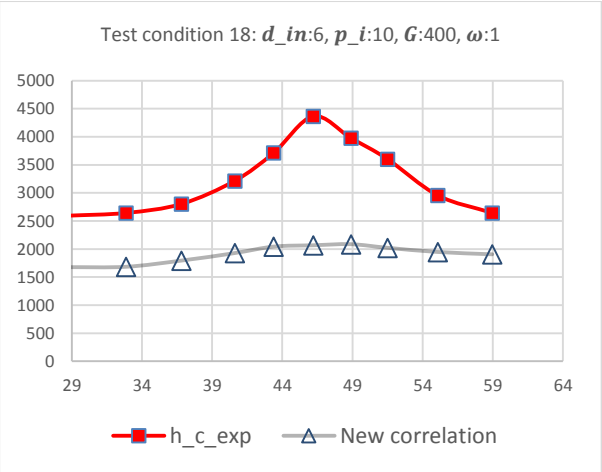

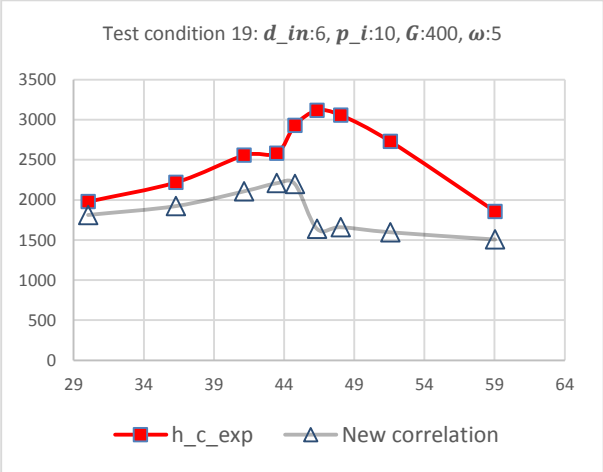

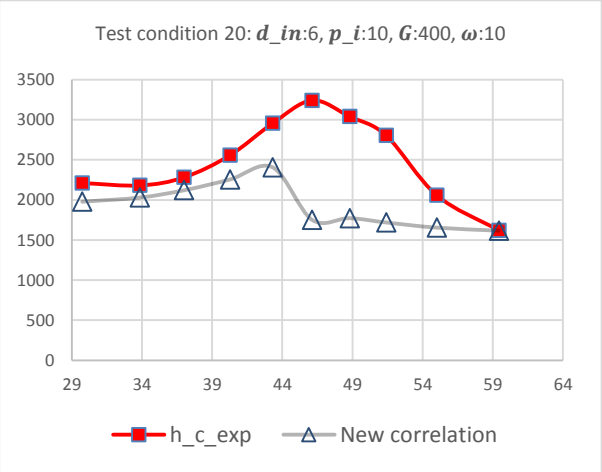

II. Results of new correlation on Zhao et al. (2007)'s experimental data

Test condition 1		
d_{in}:1.98, p_i:8, G:800, ω:1		
$h_{c,exp}$	h_c	$E_{\%}$
3501,27	3789	8,234
5194,66	4166	-19,81
7419,85	5274	-28,93
9519,08	8759	-7,983
12444,02	8505	-31,65
9938,93	6709	-32,5
8091,60	5861	-27,57
6454,20	5210	-19,28
4816,79	4645	-3,561
4592,88	4395	-4,305
4047,07	4442	9,762
2633,59	5212	97,87
2591,60	5682	119,2

Test condition 2		
d_{in}:1.98, p_i:8, G:800, ω:2		
$h_{c,exp}$	h_c	$E_{\%}$
2787,53	3876	39,01
3389,31	4263	25,79
4648,85	5143	10,62
6524,17	7615	16,72
5810,43	6208	6,848
4159,03	4158	-0,02203
4243,00	3829	-9,76
3389,31	3851	13,65
2927,48	4398	50,25
2647,58	4985	88,26

Test condition 3		
d_{in}:1.98, p_i:8, G:1200, ω:1		
$h_{c,exp}$	h_c	$E_{\%}$
5279,11	5271	-0,1598
6624,77	5731	-13,5
11670,98	7501	-35,73
17597,04	12107	-31,2
16665,43	9757	-41,45
9911,28	7661	-22,7
8125,69	7238	-10,92
7038,82	6447	-8,416
4968,58	6090	22,57
4916,82	6279	27,71

Test condition 4		
d_{in}:1.98, p_i:8, G:1200, ω:2		
$h_{c,exp}$	h_c	$E_{\%}$
3597,04	5385	49,71
4166,36	5947	42,76
5589,65	7659	37,01
8565,62	10487	22,43
9005,55	7304	-18,9
11231,05	8488	-24,42
7530,50	6379	-15,29
6158,96	5617	-8,807
4606,28	5283	14,69
4528,65	5461	20,58
3985,21	6064	52,17
3700,55	7109	92,09

Test condition 5		
d_{in}:1.98, p_i:11, G:400, ω:1		
$h_{c,exp}$	h_c	$E_{\%}$
1667,85	2122	27,22
1667,85	2117	26,93
1944,94	2113	8,633
1992,90	2200	10,4
2056,84	2112	2,653
2168,74	2252	3,841
2264,65	2313	2,111
2264,65	2331	2,895
2227,35	2548	14,41
2211,37	2660	20,29
2067,50	2732	32,19
2008,88	2795	39,14
1806,39	2883	59,66

Test condition 6		
d_{in}:1.98, p_i:11, G:400, ω:2		
$h_{c,exp}$	h_c	$E_{\%}$
1726,47	2166	25,5
1896,98	2161	13,89
1955,60	2156	10,25
2110,12	2278	7,954
2312,61	2353	1,726
2344,58	2377	1,382
2072,82	2342	12,95
1918,29	2380	24,09
1731,79	2433	40,49
1561,28	2516	61,19

Test condition 7		
d_{in}:4.14, p_i:11, G:400, ω:2		
$h_{c,exp}$	h_c	$E_{\%}$
1467,11	1920	30,85
1750,00	2036	16,37
2092,11	2477	18,39
2875,00	4289	49,2
3710,53	3444	-7,183
3006,58	2371	-21,15
2631,58	2140	-18,69
2526,32	2029	-19,69
1980,26	1897	-4,208
1592,11	1937	21,67
1434,21	2187	52,54